INPUT FILTER COMPENSATION FOR SWITCHING REGULATORS

by

Shriram S Kelkar

Dissertation submitted to the Faculty of the

Virginia Polytechnic Institute and State University

in partial fulfillment of the requirements for the degree of

DOCTOR OF PHILOSOPHY

in

Electrical Engineering

APPROVED:

Dr.F.C.Lee,Chairman

Dr.D.Y.Chen

Dr.L.L.Grigsby

Dr.C.E.Nunnally

Dr.R.D.Riess

October, 1982

Blacksburg, Virginia

INPUT FILTER COMPENSATION FOR
SWITCHING REGULATORS

by

Shriram S. Kelkar

(ABSTRACT)

An input filter is often required between a switching regulator and its power source due to the need of preventing the regulator switching current from being reflected back into the source. The presence of the input filter often results in various performance difficulties such as loop instability, degradation of transient response, audiosusceptibility and output impedance characteristics. These problems are caused mainly by the interaction between the peaking of the output impedance of the input filter and the regulator control loop. Conventional single-stage and two-stage input filters can be designed to minimize the peaking effect, however this often resuts in a penalty of weight or loss increase in the input filter.

A novel input filter compensation scheme for a buck regulator that eliminates the interaction between the input filter output impedance and the regulator control loop is presented. The scheme is implemented using a feedforward

loop that senses the input filter state variables and uses this information to modulate the duty cycle signal. The feedforward design process presented is seen to be straightforward and the feedforward easy to implement. Extensive experimental data supported by analytical results show that significant performance improvement is achieved with the use of feedforward in the following performance categories: loop stability, audiosusceptibility, output impedance and transient response.

The use of feedforward results in isolating the switching regulator from its power source thus eliminating all interaction between the regulator and equipment upstream. In addition the use of feedforward removes some of the input filter design constraints and makes the input filter design process simpler thus making it possible to optimize the input filter. The concept of feedforward compensation can also be extended to other types of switching regulators.

## ACKNOWLEDGEMENTS

I would like to acknowledge, at the outset, my gratitude to all who gave of their time and knowledge to help me in my research.

In particular I would like to thank and gratefully acknowledge the help and guidance of Dr. F.C.Lee. It was a real pleasure working with him and discovering the intricacies of switching regulators; his guidance and advice were very helpful and invaluable in the two years of the research project.

I am also sincerely grateful to Dr. L.L.Grigsby who has always evinced a keen interest in my work and guided me during the earlier days of my stay at Virginia Tech. My grateful thanks also to Dr. D.Y.Chen, Dr. C.E.Nunnally and Dr. R.D.Riess for providing support.

My work at V.P.I.& S.U. was supported by NASA under contracts NAG3-81 and NAS3-220 and I gratefully acknowledge the financial support that was provided.

The support provided by my wife Shashi was very important to me during our stay at V.P.I. and I express my sincere thanks to her.

CONTENTS

## LIST OF TABLES

LIST OF FIGURES

# Chapter I

# INTRODUCTION

Switching-mode dc-dc regulators are coming into increasing use as power supplies because of the significant reduction of weight, size and increase in equipment efficiency that can be attained. The dissipative regulators used earlier had the advantage of design simplicity, but suffer from low efficiency and higher weight due to the large transformer and filter needed to achieve the required voltage/current regulation.

Since the late sixties, the rapid expansion of the computer and communication industries and increasing complexity and sophistication of various systems necessitated the development of higher performance switched mode power supplies. The incentive for performance improvement prompted the initial development of multiple loop control schemes, such as the standardized control module (SCM) for dc-dc converters [2,7,8] and the current-injected control scheme [9]. The ever continuing search for performance improvement forms the underlying theme of this dissertation.

The work presented in this dissertation is mainly concerned with developing a control scheme to alleviate the problem brought about due to the use of an input filter in switching regulators. The switching regulator input current has a substantial ripple component at the switching frequency and this necessitates the use of an input filter to smooth the pulsating current drawn from the supply. Furthermore the input filter also serves to attenuate noise present in the supply voltage from being propagated through the regulator to the payload downstream. The presence of the input filter, however, often results in various performance difficulties such as loop instability, degradation of transient response, audiosusceptibility (closed loop input-to-output gain) and output impedance characteristics [3,4,5,6,10]. These problems are caused mainly by the interaction between the resonant peaking of the output impedance of the input filter and the regulator control loop. Conventional single-stage and two-stage input filters can be designed such that the peaking effect is minimized, however such a design is often accompanied with a penalty of weight and loss in the input filter [3,4,5,6,10]. This dissertation presents a different approach via a feedforward control scheme to mitigate the undesirable interaction between the input filter and the regulator control loop.

The concept of pole-zero cancellation is used, in this dissertation, to develop a novel feedforward control loop that senses the input filter state variables and processes this information in a manner designed to cancel the detrimental effect of peaking of the output impedance of the input filter. The feedforward loop working in conjunction with the feedback loops developed earlier [2,7,8] constitute a total state control scheme that eliminates the interaction between the input filter and the regulator control loop. Employing the novel feedforward compensation scheme presented in this dissertation, a high performance converter together with an effective input filter design (minimum weight and loss) can be accomplished concurrently. A buck regulator employing a feedforward control loop working in conjunction with the feedback loops was used to obtain measurements that showed significant improvement in the following performance categories:

1. Loop stability (open loop gain and phase margins);
2. Audiosusceptibility;
3. Output impedance; and
4. Transient response.

In this dissertation the problem caused by input filter interaction and conventional input filter design techniques are discussed in Chapter 2 followed in Chapter 3 by the concept of pole-zero cancellation developed earlier [2,7,8]. Chapters 4 and 5 present the modeling of the power stage with input filter and the implementation of the feedforward for a buck regulator respectively. Measurements of open loop gain and phase that confirm the analytical prediction of performance improvement using the feedforward scheme developed, are discussed in Chapter 6 along with other measurements of audiosusceptibility, output impedance and transient response. Chapter 7 presents experimental and analytical results pertaining to transient response while Chapter 8 discusses the use of the feedforward loop in stabilizing a regulator system made unstable due to input filter interaction. Chapter 9 is concerned with extending the concept of feedforward compensation to other types of control and to other types of regulators i.e. the buck-boost regulators. Finally, Chapter 10 presents the conclusions and suggestions for future work.

# Chapter II

# INPUT FILTER RELATED PROBLEMS AND CONVENTIONAL DESIGN TECHNIQUES

## 2.1 INPUT FILTER RELATED PROBLEMS

An input filter is often required between a switching regulator and its power source. A buck type switching regulator with a single-stage input filter is shown in Figure 1 . The regulator input current has a substantial pulsating current component at the switching frequency as a result of the opening and closing of the switch and this component should be prevented from being reflected back into the source ; an input filter is required to provide high attenuation at switching frequency and thus smooth the current drawn from the source. The input filter also serves to isolate source voltage disturbances from being propagated to the switching regulator payload downstream.

A presumably well-designed input filter, satisfying the above mentioned requirements, when used with a switching regulator can often cause significant performance degradations [3,4,5,6,10]. This is due primarily to the complex interaction between the switching regulator control loop, the input filter and the regulator output filter [3,4,5,6,10].

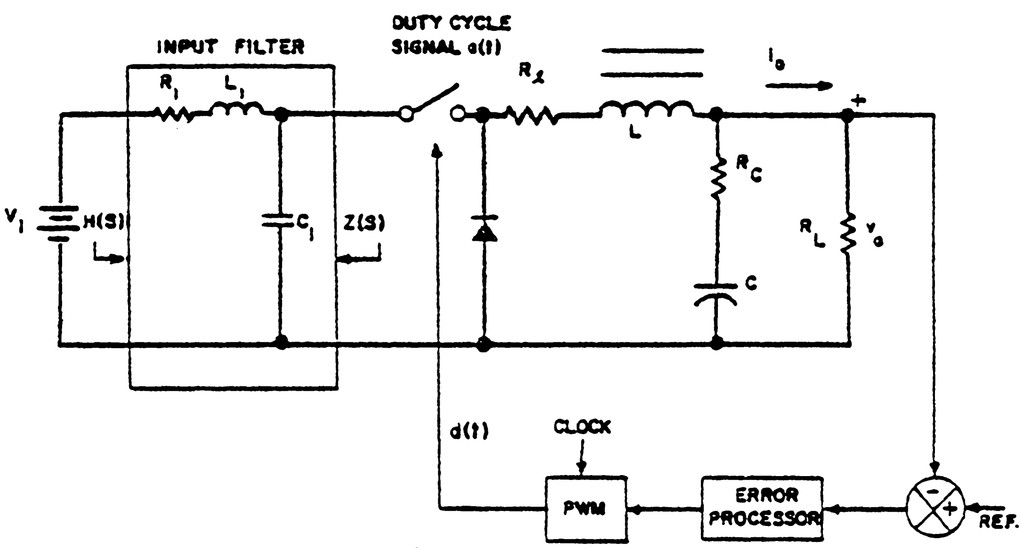


Figure 1: Buck Converter with an Input Filter

$V_I$ =12v  $V_o$ =5v  $R_L$=0.86 ohm  L=200 microH
$R_\ell$=20mohm  C=1540microF  $R_c$=7mohm  $T_p$=50microsecs
$L_1$=77 microH  $R_1$ =39.6 mohm  $C_1$ =412 microF

The interaction between the control loop and the input filter is illustrated in Figure 2 . The switching regulator has been shown to have a nonlinear negative resistance, as illustrated in the figure,[3]. The input current $i_r$ to the switching regulator is related nonlinearly to the input voltage $e_r$ and the input resistance $\frac{di_r}{de_r} = -\frac{1}{r}$ . Under certain conditions the input filter-switching regulator combination can become a negative resistance oscillator, producing large amplitude voltage excursions across capacitor C. When this happens serious degradation of regulator performance could occur, [3], including loss of stability.

The effect of the input filter is more clearly seen using a small signal model.

The averaging technique [1] is used to relate the low frequency modulation component of the source voltage and control signal to the corresponding frequency components of the converter output voltage. Using the continuous inductor current buck regulator with input filter of Figure 1 , as an example, a small signal model using the dual-input describing function can be developed, as shown in Figure 3 , [6]. In this model the effect of the input filter is characterized by the following two parameters: the forward transfer characteristic of the input filter H(s) and the output impedance of the input filter Z(s).

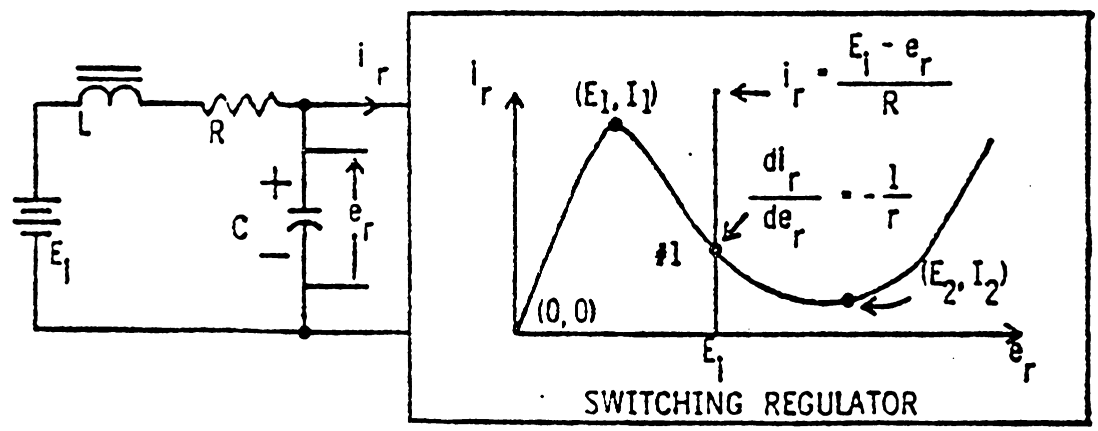


Figure 2: Negative resistance oscillation.

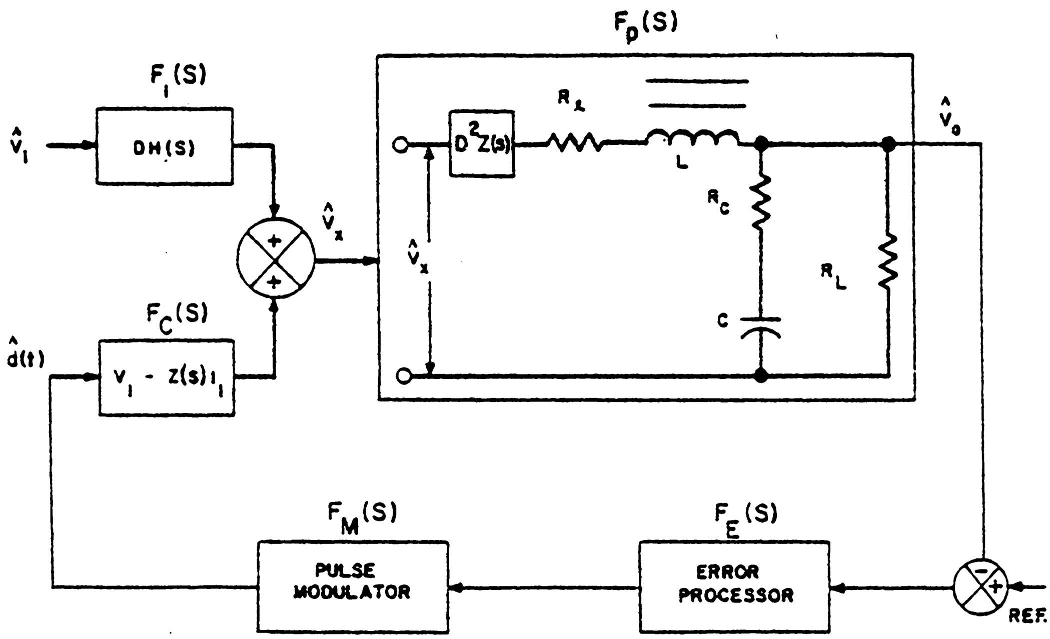


Figure 3: Small-signal model using the dual-input describing function.

In Figure 1 the output filter is made up of $R_\ell$, L, $R_C$ and C, $R_L$ is the load resistance, D is the steady state duty cycle ratio $D = T_{on}/T$, $V_I$ and $I_I$ are the steady state regulator input voltage and current respectively, and the lower case letters with a caret above them denote modulation signals.

The small signal model of Figure 3 is used to illustrate briefly the complex interaction between the input filter, output filter and the control loop and the problems caused by the interaction. For detailed analysis please refer to [6].

### 2.1.1 Input Filter Interaction -- Loop Stability and Transient Response

The stability of a switching regulator can be examined by the open loop gain $G_T(s)$:

$$G_T(s) = F_C(s)F_P(s)F_E(s)F_M(s) \tag{2-1}$$

where $F_C(s)F_P(s)$ is the duty cycle-to-output describing function $\hat{v}_o/\hat{d}$ , and $F_E(s)$, $F_M(s)$ are the transfer functions of the error processor and the pulse modulator respectively. The peaking of the output impedance of the input filter Z(s) has the following effects:

(1) The duty-cycle power stage gain $F_C(s)$ includes the output impedance Z(s) --

$$F_C(s) = V_I - Z(s)I_I \text{ or} \tag{2-2}$$

$$F_C(s) = I_I\left[\frac{V_I}{I_I} - Z(s)\right] \qquad (2\text{-}3)$$

The first term in the brackets $\frac{V_I}{I_I}$ is the negative input impedance of the regulator. At the input filter resonant frequency, Z(s) reaches a peak value and if this value is large enough the result could be a reduction in loop gain or even worse a negative duty cycle power stage gain $F_C(s)$. Reduction in loop gain could lead to loop instability, whereas a negative $F_C(s)$ together with the negative feedback loop will result in a positive feedback unstable system.

(2) The power stage transfer function $F_p(s)$ includes the output impedance Z(s) --

$$F_p(s) = \frac{[R_C + 1/sC]//R_L}{D^2 Z(s) + Z_i(s)} \quad \text{where} \qquad (2\text{-}4)$$

$$Z_i(s) = R_\ell + sL + [R_C + 1/sC]//R_L \qquad (2\text{-}5)$$

= input impedance of the regulator.

Excessive Z(s) at the input filter resonant frequency can significantly reduce $F_p(s)$, and thus the loop gain.

Figures 4 [6], illustrate the effect of peaking of Z(s) on the duty cycle-to-output transfer function $F_C(s)F_p(s)$ if an improperly designed input filter is employed.

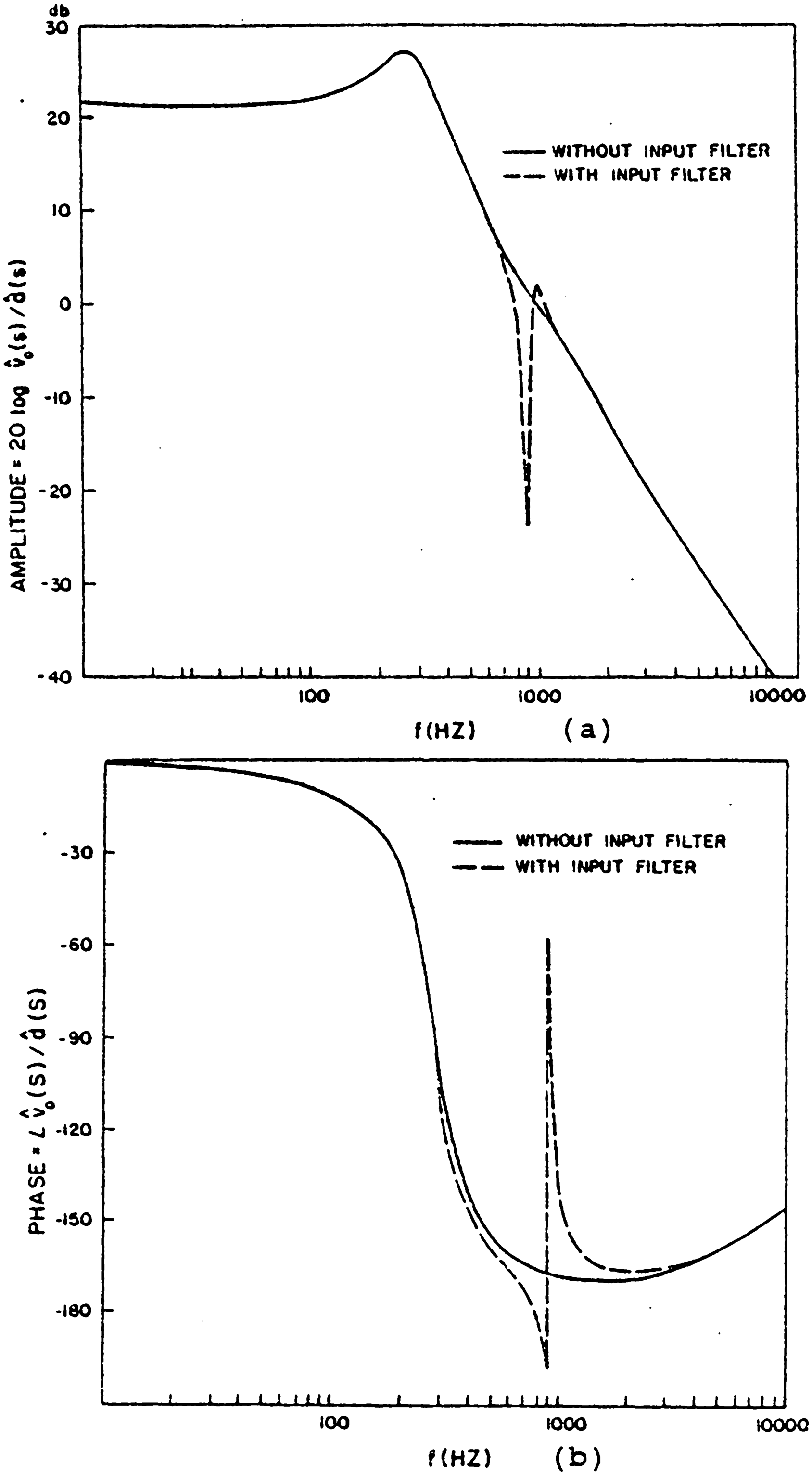


Figure 4: Duty cycle-to-output voltage characteristic with and without input filter (a) gain (b) phase. (parameter values are as shown in Fig.1)

At the input filter resonant frequency the peaking of the output impedance Z(s) causes a sharp change in the gain and phase of the duty cycle-to-output transfer function. This could result in loop instability and degradation of transient response from a presumably well damped system to an oscillatory one; control of the peaking effect of the output impedance Z(s) is necessary to avoid these problems.

### 2.1.2 Input Filter Interaction--Audiosusceptibility and Output Impedance

The audiosusceptibility refers to the switching regulator's ability to attenuate small signal sinusoidal disturbances present at the input so as not to affect the regulated output voltage. The audiosusceptibility performance is of considerable importance, as the regulator generally shares the input bus with other on-line equipment. The operation of this equipment generates noise voltages on the input line which must be attenuated by the closed-loop regulator so that operation of the various payloads at the regulator output will not be adversely affected. The audiosusceptibility is expressed in terms of the closed loop input-to-output transfer function $G_A(s)$:

$$G_A(s) = \frac{v_O(s)}{v_I(s)} = \frac{F_I(s)F_p(s)}{1+F_C(s)F_p(s)F_E(s)F_M(s)} = \frac{F_I(s)F_p(s)}{1 + G_T(s)} \quad (2\text{-}6)$$

where $F_I(s) = DH(s)$ = input voltage gain of the power stage. $G_A(s)$ and thus the audiosusceptibility are affected by the resonant peaking of the output impedance $Z(s)$ and of the forward transfer function of the input filter with the regulator disconnected $H(s)$, because $F_I(s)$ is a function of $H(s)$ whereas $F_C(s)$ and $F_p(s)$ are functions of $Z(s)$. The reduction of loop gain at the resonant frequency can thus severely degrade the audiosusceptibility. Figure 5 , [6], illustrates the audiosusceptibility of the buck regulator with and without an input filter.

The output impedance of the regulator should be small so that the regulator behaves like an ideal voltage source, however the output impedance is increased by the peaking of the output impedance of the input filter.

$$Z_o(s) = \frac{Z_p(s)}{1 + G_T(s)} \qquad (2\text{-}7)$$

where $Z_p(s)$ is the output impedance of the power stage with the control loop open.

At the resonant frequency the output impedance of the regulator $Z_O(s)$ is increased. This is a consequence of the loss of loop gain $G_T(s)$ as a result of peaking.

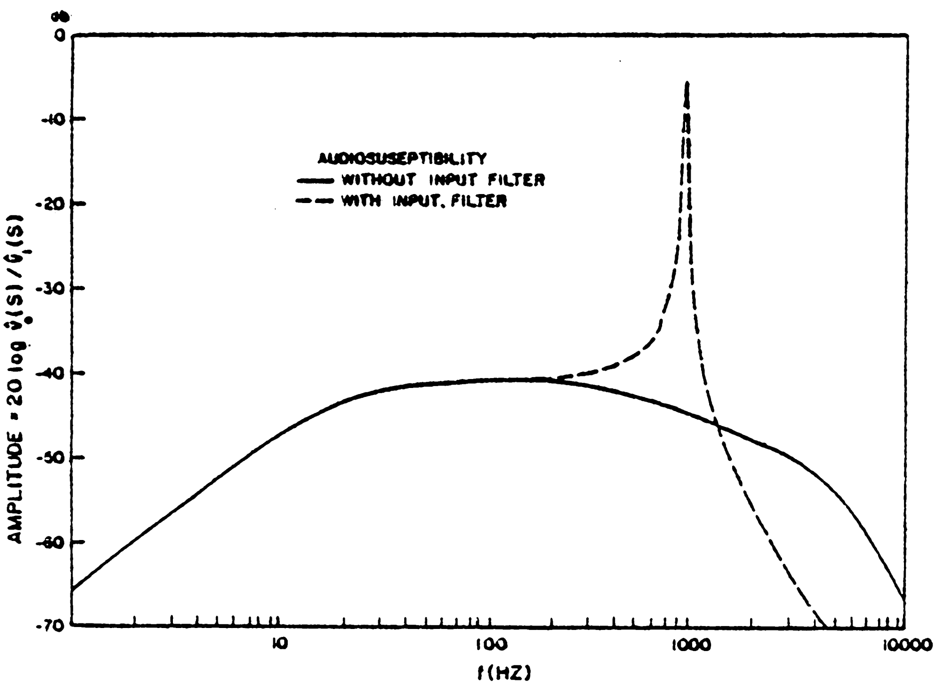


Figure 5: Audiosusceptibility with and without input filter.

(parameters values are as shown in Fig.1)

The peaking of H(s) and Z(s) of the input filter thus results in a reduction in the loop gain, this in turn affects stability, transient response, audiosusceptibility and the output impedance of the regulator.

A buck type switching regulator with a two stage input filter is shown in Figure 6 . Figure 7 , [6], shows the measured values of open loop gain and phase as a function of the frequency. ( The input filter damping resistance $R_D$ is not employed to purposely illustrate the effect of input filter interaction with the regulator control loop.) Significant changes in the open loop gain and phase characteristics at the resonant frequencies of both the first stage and the second stage of the input filter are observed, [6]. Thus it is seen that the peaking of the output impedance at resonant frequency of the two stage input filter can also cause serious performance degradation.

## 2.2 INPUT FILTER DESIGN CONSIDERATIONS

The design of the input filter is made more complicated by the necessity of satisfying the following constraints, which result from the interaction between the input filter and the regulator control loop discussed in section 2.1 :

1. The amount of regulator switching current reflected back into the source should be limited (conducted interference requirement).

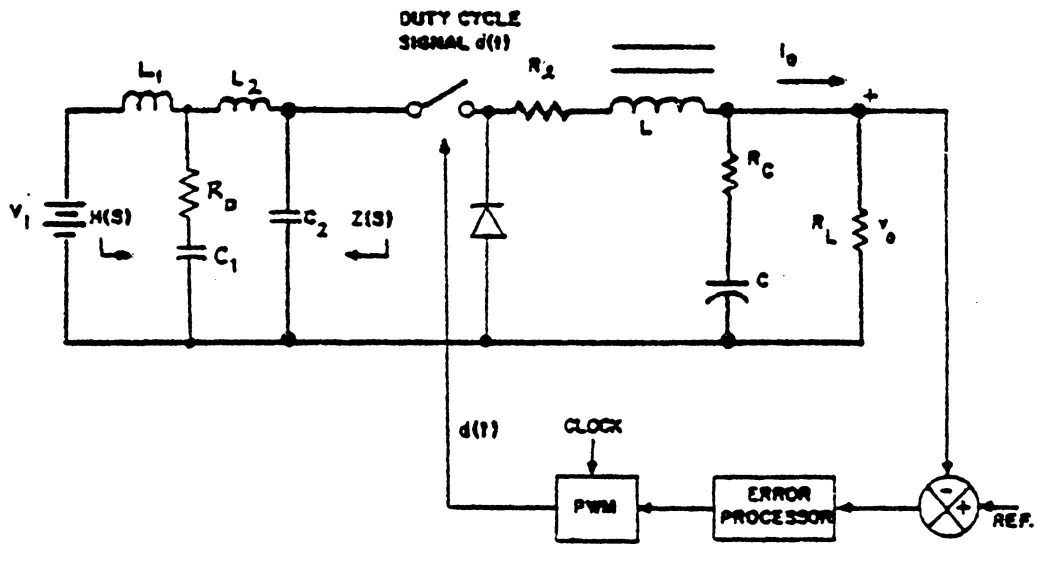


Figure 6: Buck type switching regulator with a two stage input filter.

$V_I$ =40v $V_o$ =20v $R_L$=7 ohm $R_\ell$ =0.05 ohm
L=1 mH C=455microF $R_c$=0.068ohm $T_p$=50microsecs
$L_1$ =1.1 mH $R_1$ =0.05 mohm $L_2$=0.27 mH
$R_2$=0.02 ohm $C_1$ =225 microF $C_2$=20 microF

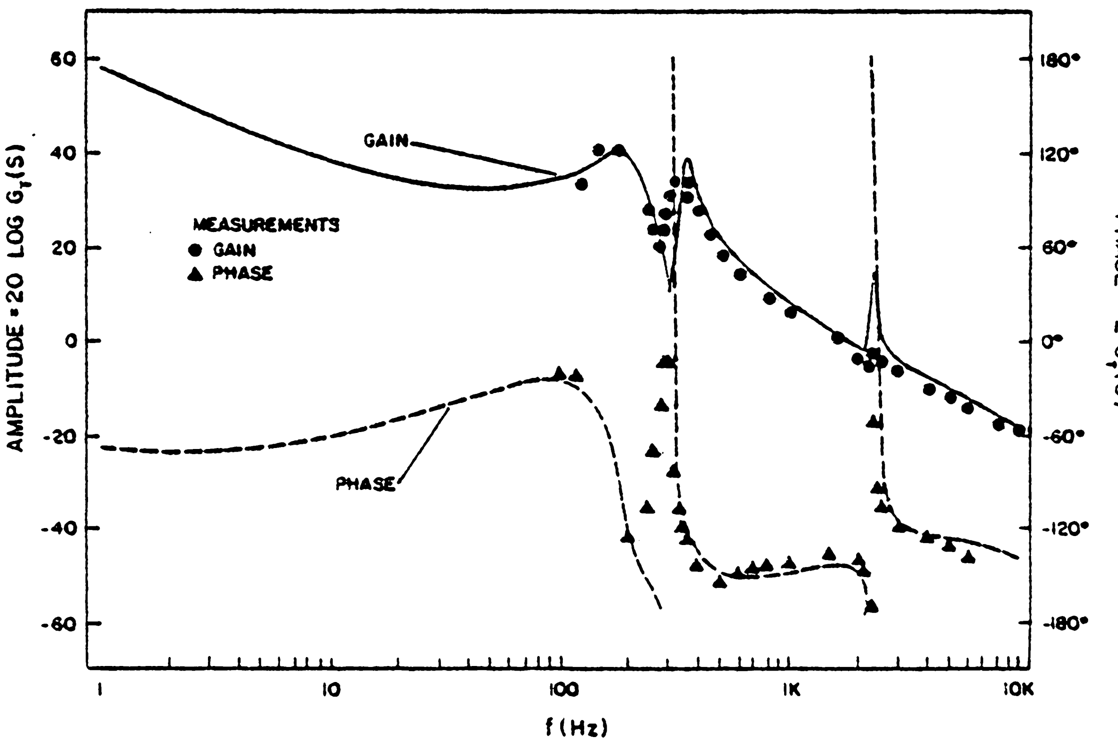


Figure 7: Open loop gain and phase characteristics without the input filter damping resistance $R_D$.

(parameter values used are as shown in Fig.6)

2. The peaking of the output impedance of the input filter Z(s) should be limited to a safe value to avoid significant loop gain reduction.
3. The peaking of the transfer function of the input filter H(s) should be limited to achieve a satisfactory rejection rate of audio signals propagating from input to output.
4. The input filter weight and energy loss should be limited to low values.
5. The Nyquist stability criterion has to be satisfied; thus the closed loop poles should be in the left half plane for stable operation -

$$|1 + F_C(s)F_p(s)F_E(s)F_M(s)| > 0$$

6. The closed-loop input-to-output transfer characteristic (audiosusceptibility) and transient response due to a sudden line/load change should not be degraded by a noticeable amount.

An input filter design that satisfies one constraint may often result in violating some other constraint. For example, an input filter design that limits performance degradation (degradation of stability, transient response and audiosusceptibility) often results in higher weight and increased losses in the input filter. A satisactory input filter design trades off one or more of the performance degradations for size, weight and loss. A near-to- optimal design thus requires many trial and error design attempts. Some of the conventional input filter design techniques are presented next.

### 2.2.1 Conventional Input Filter Design Techniques

A single stage input filter as shown in Figure 8(a) can be designed to avoid performance degradation -- but this would result in larger filter $L_1$ and $C_1$ thus resulting in weight and size increase. The filter is simple and commonly used but it cannot often satisfy the stringent requirement on audiosusceptibility without size/weight penalty. Resonant peaking of the filter of Figure 8(b), [3], is lowered by adding resistance R, but this lowers efficiency because the pulse current flowing through $C_1$ increases losses. Another design uses a resistance R in parallel across $C_1$, [4], but this results in a large $C_1$.

The optimal design of a single stage input filter thus is rather difficult without tradeoff between performance degradations and the weight and loss limitations.

The degradation of the power stage transfer function $F_p(s)$ due to peaking of $Z(s)$ can be avoided if there is sufficient separation of the input filter resonance frequency $\omega_1 = \frac{1}{\sqrt{L_1 C_1}}$ and the output filter resonant frequency

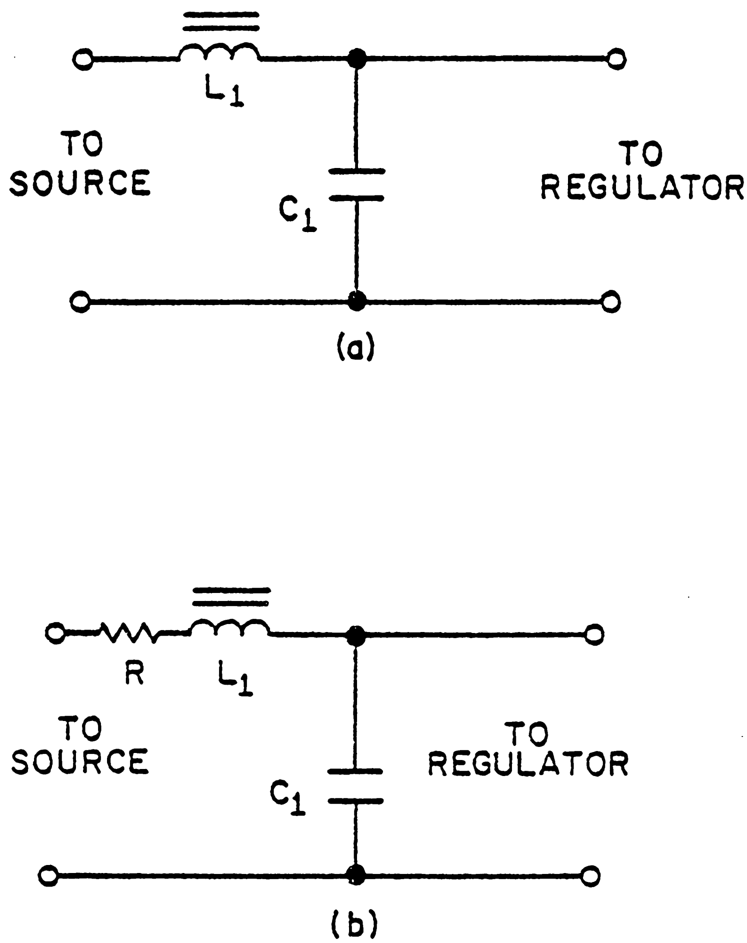


Figure 8: Single-stage input filters

$\omega_0 = \frac{1}{\sqrt{LC}}$ , [4,5,10]. Figure 9 , [4,5,10], shows three possible combinations of $\omega_0$ and $\omega_1$. $F_p(s)$ is related to both Z(s) and the input impedance of the regulator $Z_i(s)$ thus

$$F_p(s) = \frac{[R_C + 1/sC]//R_L}{D^2 Z(s) + Z_i(s)} \qquad (2\text{-}8)$$

where $\quad Z_i(s) = R_\ell + sL + [R_C + 1/sC]//R_L$

= input impedance of the regulator.

Z(s) and $Z_i(s)$ peak at the frequencies $\omega_0$ and $\omega_1$ respectively. If the two resonance frequencies are the same as in Figure 9 then both Z(s) and $Z_i(s)$ peak at the same frequency and thus at that frequency the transfer function $F_p(s)$ would be affected, i.e. reduced, to the maximum possible extent. Shifting the two frequencies $\omega_0$ and $\omega_1$ apart as shown in Figure 9 will result in reducing the effect of peaking on $F_p(s)$. Reducing $\omega_1$ would result in increasing the size and weight of the input filter. A high value of $\omega_1$ is desirable from the point of view of weight and size reduction but this can result in severe performance degradation -- from Figure 4 it is clear that the gain of the duty cycle-to-output transfer function $F_C(s)F_p(s)$ decreases with increasing frequency and thus the effect of peaking of Z(s) on the gain of $F_C(s)F_p(s)$ would be more pronounced if Z(s) peaks at a higher $\omega_1$.

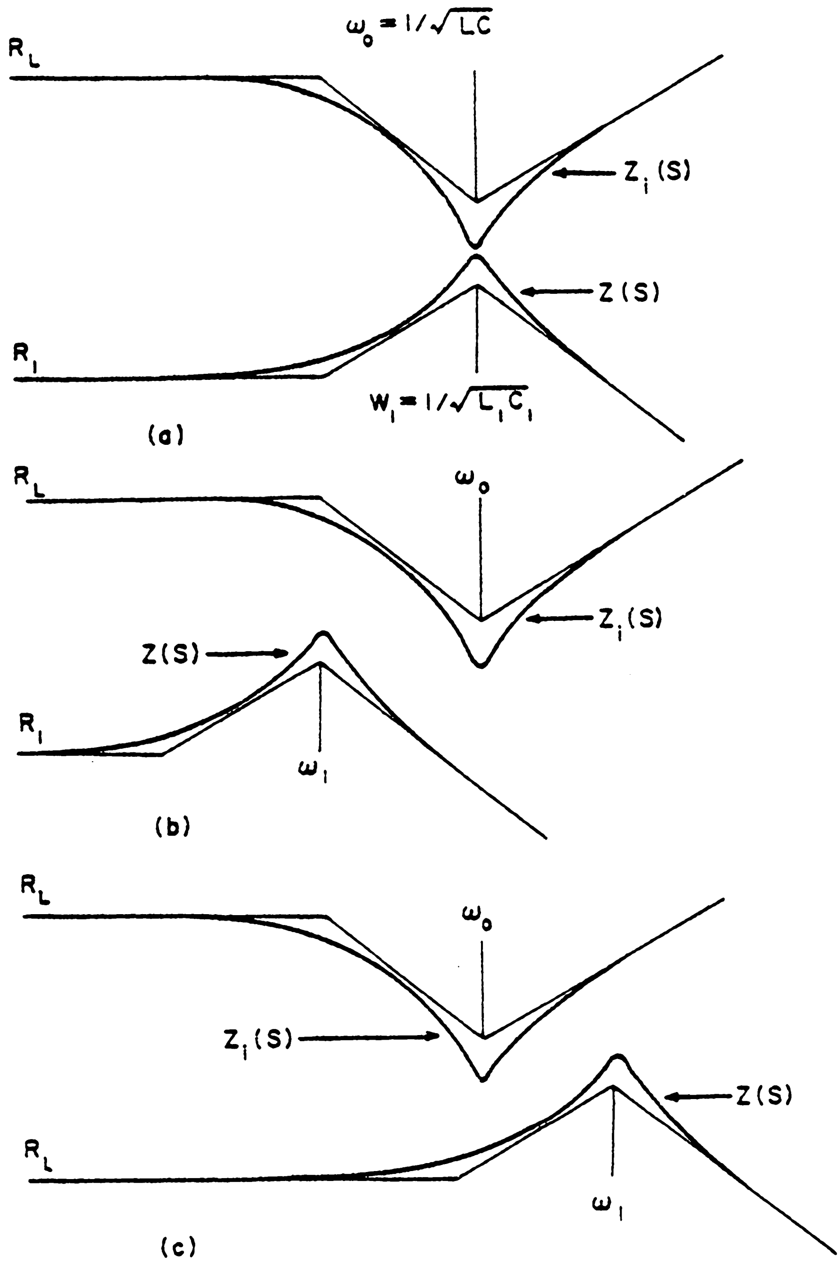


Figure 9: Interaction between output impedance Z(s) of input filter and input impedance Z (s) of regulator.

The reduction of the loop gain at higher input filter resonant frequency $\omega_1$ often results in poor audiosusceptibility, oscillatory transient response or even an unstable system. The choice of $\omega_1$ thus involves a trade off between meeting performance specifications and size/weight.

### 2.2.2 An Optimal Configuration

A two-stage input filter configuration has been described, [3,6] and is shown in Figure 10 . The first stage consisting of $L_1, C_1, R_3$ and $R_1$ controls the resonant peaking of the filter. The second stage consisting of $L_2$, $C_2$ supplies most of the pulse current required by the regulator. As shown in the literature, [6], the two-stage input filter is capable of reducing H(s) and Z(s) at resonant frequency without significantly increasing weight and loss, unlike the single-stage input filter. Computer optimization techniques have been utilized to optimally design the two-stage filter[6]. It has been shown that the two-stage filter is much lighter than its single-stage counterpart under identical design constraints. Also it has been shown that for the same filter weight the single stage filter has a significantly higher peaking of H(s) and Z(s). Figure 11 shows the gain and phase of the duty cycle-to-output describing function of a power stage with a two stage input filter, [6].

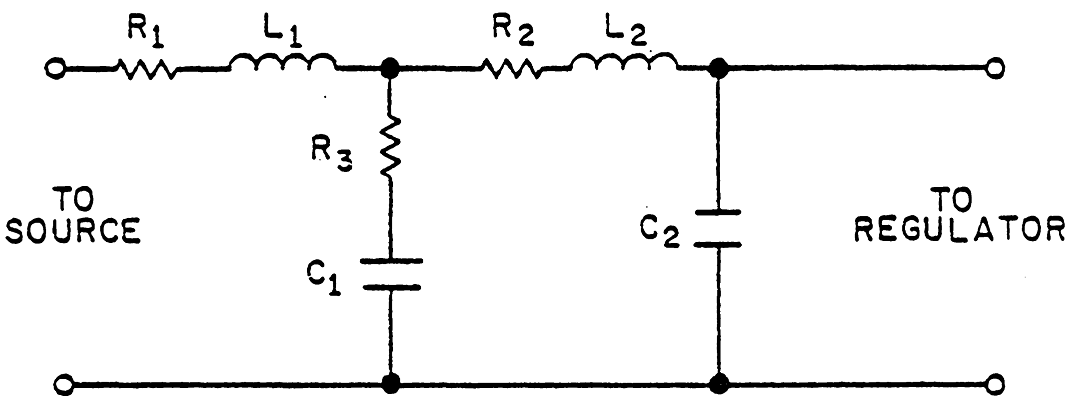


Figure 10: Two-stage input filter.

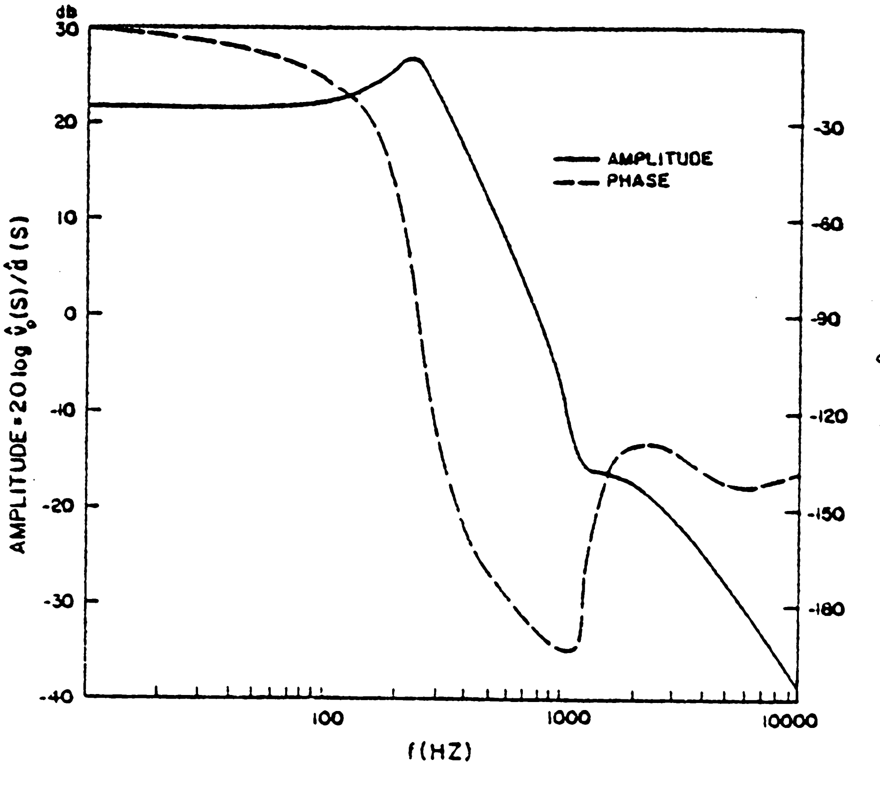


Figure 11: Duty cycle-to-output describing function of power stage with two-stage input filter.

(parameter values used are as shown in Fig.1 with the following two-stage input filter parameters --
$L_1$=232 microH $R_1$=0.0276 ohm $L_2$=77 microH
$R_2$=0.0119 ohm $C_1$=100 microF $R_3$=1.73 ohm
$C_2$=30 microF )

Figure 4 shows the gain and phase of the duty cycle-to-output describing function of a power stage with a single-stage input filter, and the two-stage filter of Figure 11 was designed to have the same weight as the single-stage input filter of Figure 4 . Comparing the two figures the improvement in performance regarding the duty cycle-to-output transfer function is dramatic.

It can therefore be concluded that the two-stage filter provides the best compromise among the conflicting requirements of an input filter.

### 2.2.3 Input Filter Compensation Via a Feedforward Loop

Limiting interaction between the input filter and the regulator control loop is possible with the addition of a feedforward control loop. At this point it is important to emphasize that such a scheme is designed to eliminate the effect of peaking of the output impedance of the input filter Z(s), since the peaking of Z(s) interacts with the control loop. The forward transfer function H(s) does not interact with the regulator control loop, as is evident from Figure 3 and therefore the peaking of H(s) cannot be controlled in any way by adding a feedforward loop. The peaking of H(s) can only be controlled by proper filter design. In this dissertation a feedforward loop is implemented for a switching buck regulator employing multiple control loops. The feedforward loop will be designed to cancel the detrimental effect of input filter interaction and thus improve the regulator performance and stability. The use of the feedforward control loop thus removes some of the conflicting design constraints mentioned above and makes an optimal input filter design more easily attainable.

### 2.2.4 Objectives of Feedforward Loop Design

The proposed feedforward loop will be designed such that :

1. It will eliminate input filter interaction with the regulator loop. This will result in improvement in stability margins, audiosusceptibility, output impedance and transient response of the regulator.
2. It will allow the input filter to be optimized. Some of the design constraints that make an optimal filter design difficult to attain are removed with the addition of feedforward.
3. It will eliminate equipment interaction. Figure 12 shows a switching regulator and its preregulator which may be a rectifier and a filter. The dynamic output impedance of the preregulator will interact with the switching regulator and may cause problems like loop instability, degradation of audiosuscepti-

bility, output impedance and transient response. The addition of a feedforward loop will eliminate such interaction, thus isolating the switching regulator from equipment upstream.

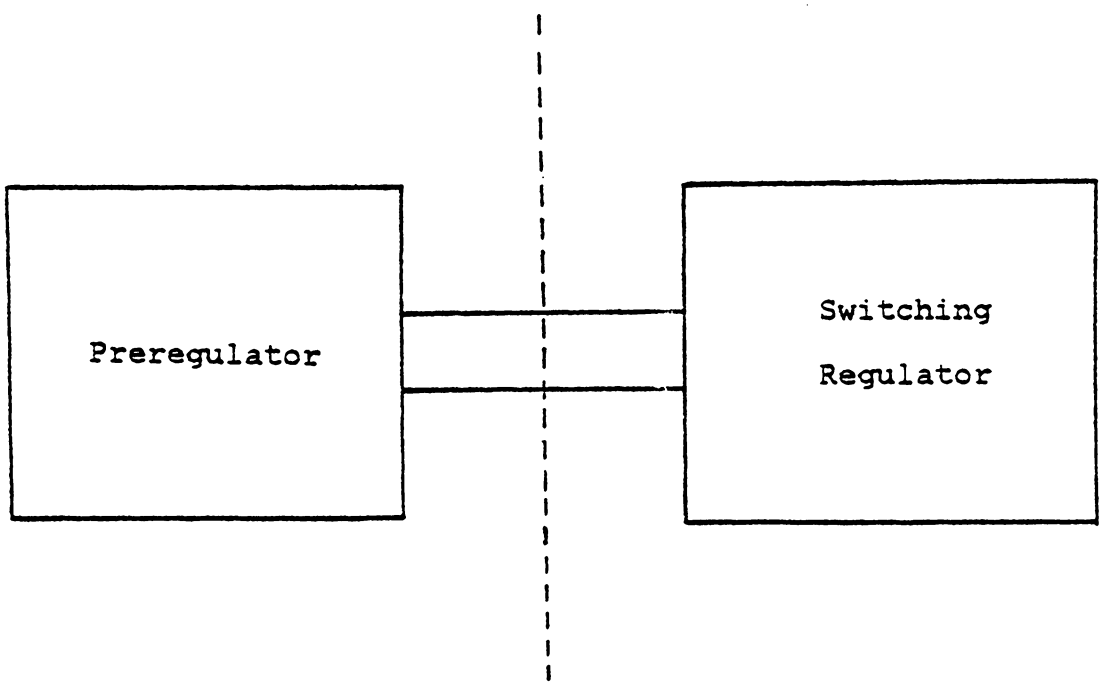


Figure 12: Interaction between the switching regulator and its preregulator.

# Chapter III

# CONCEPT OF POLE-ZERO CANCELLATION USED IN TOTAL STATE CONTROL

## 3.1 CONCEPT OF POLE-ZERO CANCELLATION.

The concept of pole-zero cancellation that was developed earlier [2,7,8] was implemented by feedback loops that sense the regulator output filter state variables and process this information to achieve better performance, and a control adaptive to filter parameter and load changes.

Figure 13 [2], shows a two-loop controlled switching buck regulator. The dc loop senses the converter output voltage and compares it with the referance voltage to generate a dc error signal for voltage regulation. The ac loop senses the ac voltage across the output filter inductor to generate an ac signal. Both ac and dc signals are processed through an operational amplifier summing junction to provide a total error signal at the output of the operational amplifier integrator. It is apparent that the error signal at the output of the integrator contains information regarding the output filter state variables -- the inductor current and the capacitor voltage.

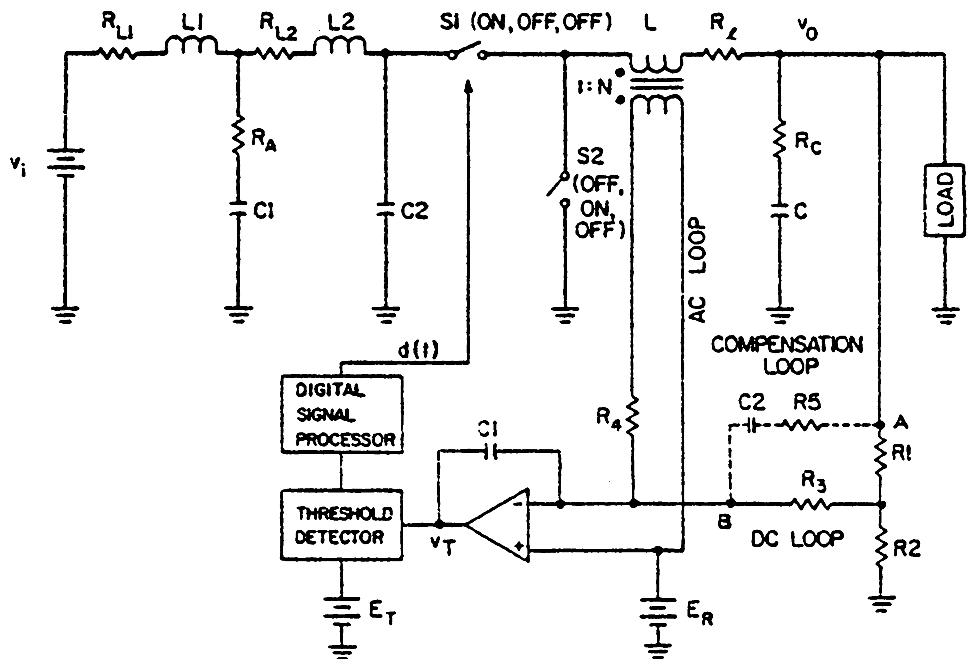


Figure 13: Two loop controlled switching buck regulator.

It was shown, [2], that the feedback control loops when properly designed can provide complex zeros to cancel completely the complex poles presented by the low-pass output filter of the power stage. It was also shown that the feedback control loop has the ability to sense filter parameter changes and automatically provide pole-zero cancellation. To examine the adaptive nature of the control loops the open loop regulator transfer function $G_T(s)$ is used

$$G_T(s) = \frac{KZ(j\omega)}{sP(j\omega)} \tag{3-1}$$

where K is a constant determined by the power stage and control loop parameters and

$$Z(j\omega) = 1 + j2\zeta_1\ \omega/\omega_{n1} - \omega^2/\omega^2_{n1} \tag{3-2}$$

$$P(j\omega) = 1 + j2\zeta_2\ \omega/\omega_{n2} - \omega^2/\omega^2_{n2} \tag{3-3}$$

$P(j\omega)$ has complex poles corresponding to the output filter and $Z(j\omega)$ has complex zeros produced by the two loop feedback control.

$$\omega_{n1} = \sqrt{\frac{\alpha}{LC}} \tag{3-4}$$

$$\omega_{n2} = \frac{1}{\sqrt{LC}} \tag{3-5}$$

$$\zeta_1 = \frac{\omega_{n1}}{2}\tau_z \tag{3-6}$$

$$\zeta_2 = \frac{\omega_{n2}}{2}\left(\frac{L}{R_L} + R_C C + R_\ell C\right) \tag{3-7}$$

$$\alpha \quad = \frac{R_4}{NR_Y} \tag{3-8}$$

$$\tau_z \quad = (R_Y + R_5)C_2 + \frac{L}{\alpha R_L} \tag{3-9}$$

$$R_Y = \left[(R_1/R_2) + R_3\right]\frac{(R_1 + R_2)}{R_2} \tag{3-10}$$

L, C, $R_\ell$ and $R_C$ form the output filter as in Figure 13 . The control parameters can be chosen such that

$$\omega_{n1} = \omega_{n2} \tag{3-11}$$

$$\zeta_1 = \zeta_2 \tag{3-12}$$

thus resulting in

$$P(j\omega) = Z(j\omega) \tag{3-13}$$

and

$$G_T(s) = \frac{K}{s} \tag{3-14}$$

The open loop transfer function is of first order and is completely independent of output filter parameters. The adaptive nature of the control loop is apparent from the fact that the complex zeros imitate the change in the complex poles due to component tolerance, aging or temperature variations, thus preserving the pole-zero cancellation.

### 3.2 TOTAL STATE CONTROL

The concept of pole-zero cancellation of the output filter characteristics led to the idea of using similar means to control the effect of peaking of the output impedance of the input filter. The objective of the work reported in this dissertation is thus to develop a feedforward loop that senses the input filter state variables and uses the information contained therein to eliminate the interaction between the input filter and the regulator control loop. Such a feedforward loop working in conjunction with existing feedback loops forms a total state control scheme, which is illustrated in Figure 14 . The feedforward loop senses the input filter state variables and feeds this information to the error processor.

The other inputs to the error processor are the ac voltage across the output filter inductor and the output voltage - as shown in section 3.1 these contain information regarding the output filter state variables.

The pulse modulator thus has as its input information regarding the state variables of the output filter and also the input filter. The duty cycle signal d(t), which controls the switch in the power stage, is thus also affected by the input filter state variables. It is shown later in this dissertation, in Chapters 4 and 5, that the feedforward loop

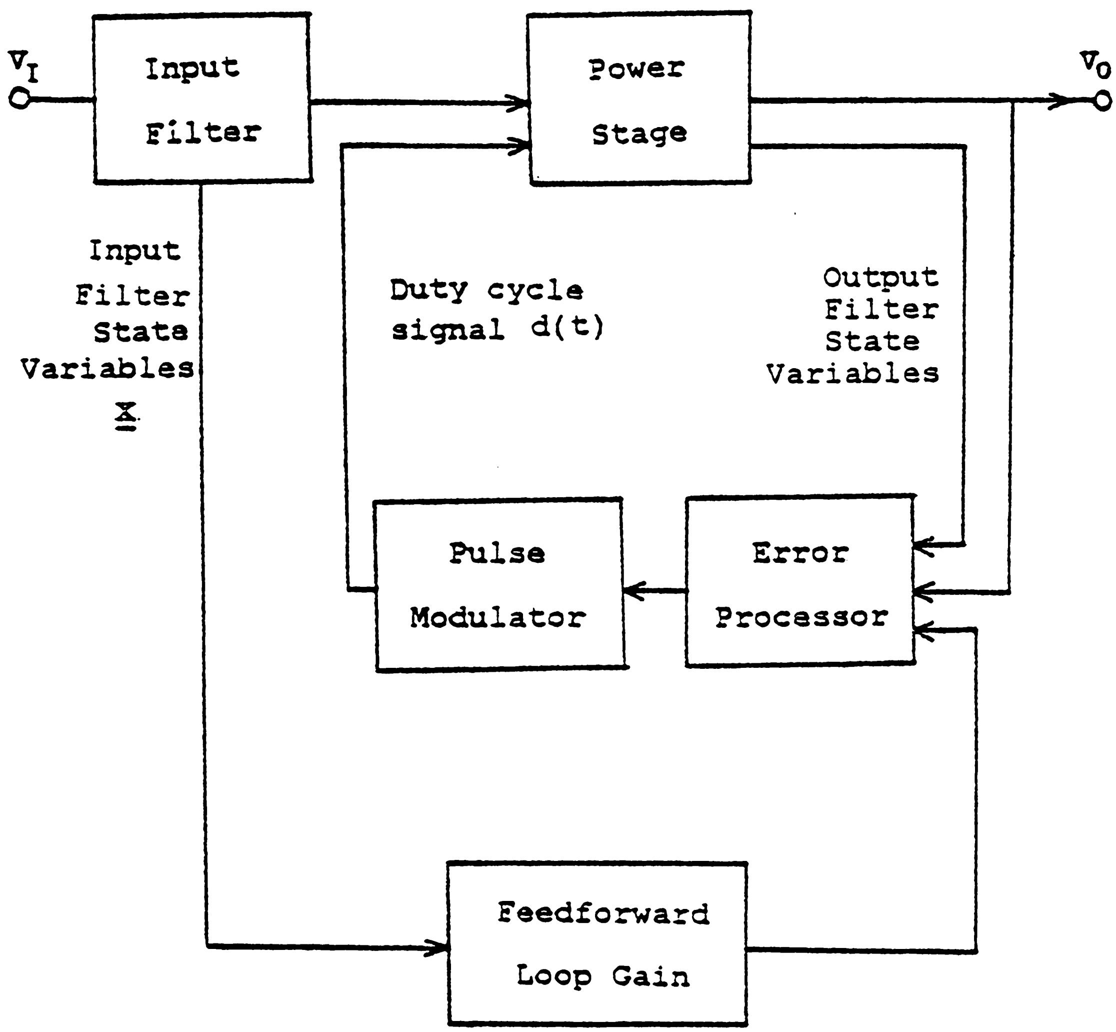


Figure 14: Total State Control.

can be designed such that interaction between the input filter and the regulator is eliminated.

# Chapter IV

## MODELING OF THE POWER STAGE WITH INPUT FILTER

The first step in the design and analysis of the feed-forward loop is to develop the small signal model of the power stage with input filter for the buck-boost, buck and boost type of switching regulators, using the averaging technique, [1]. The modeling is carried out in the continuous conduction operating mode, in which the inductor current is always nonzero. This mode is the prevalent operating mode for most dc-dc converters. The discontinuous conduction operating mode in which the inductor current is zero for some time during the cycle occurs at light loads and is seldom used as the intended design at full load.

The modeling is carried out in the following steps --

1. State space equation formulation during $T_{ON}$ and $T_{OFF}$.
2. State space averaging and perturbation.
3. Linearization and derivation of the small signal equations and the small signal equivalent circuit and state space model.

## 4.1 BUCK-BOOST CONVERTER SMALL SIGNAL MODEL DERIVATION

The buck-boost converter is shown in Figure 15 . In the buck-boost converter shown the input filter is composed of $R_{L1}$, L1, $R_{C1}$ and C1. The load is represented by $R_L$ while $V_I$ and $V_0$ are the input and output voltages respectively. During $T_{ON}$, the switch S is on and the circuit as shown in Figure 16 (a).

The equations describing the circuit are

$$i_p = \frac{N_p}{L_p}\phi \qquad \phi = \text{flux in core} \tag{4-1}$$

$$\frac{di_{L1}}{dt} = \frac{i_{L1}}{L1}(-R_{L1} - R_{C1}) + \frac{R_{C1}}{L1}\frac{N_p}{L_p}\phi - \frac{v_{C1}}{L1} + \frac{v_I}{L1} \tag{4-2}$$

$$\frac{d\phi}{dt} = \frac{v_{C1}}{N_p} + \frac{R_{C1}}{N_p} i_{L1} - \frac{\phi}{L_p}(R_{C1} + R_p) \tag{4-3}$$

$$\frac{dv_{C1}}{dt} = \frac{i_{L1}}{C1} - \frac{N_p}{C1L_p}\phi \tag{4-4}$$

$$\frac{dv_C}{dt} = \frac{-v_C}{C(R_L+R_C)} \tag{4-5}$$

$$v_0 = \frac{R_L v_C}{R_C+R_L} \tag{4-6}$$

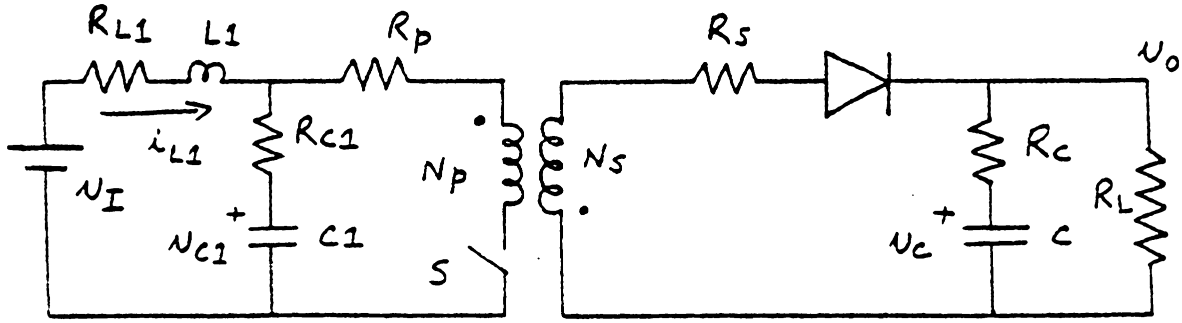


Figure 15: Buck-boost converter power stage.

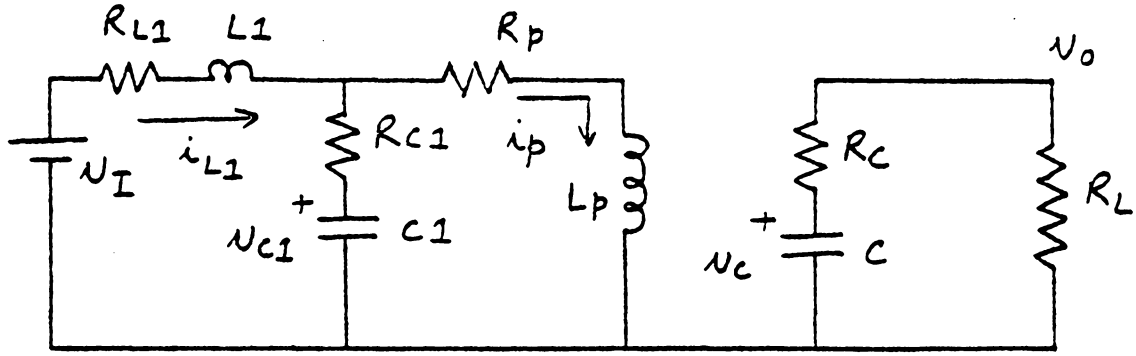


(a)

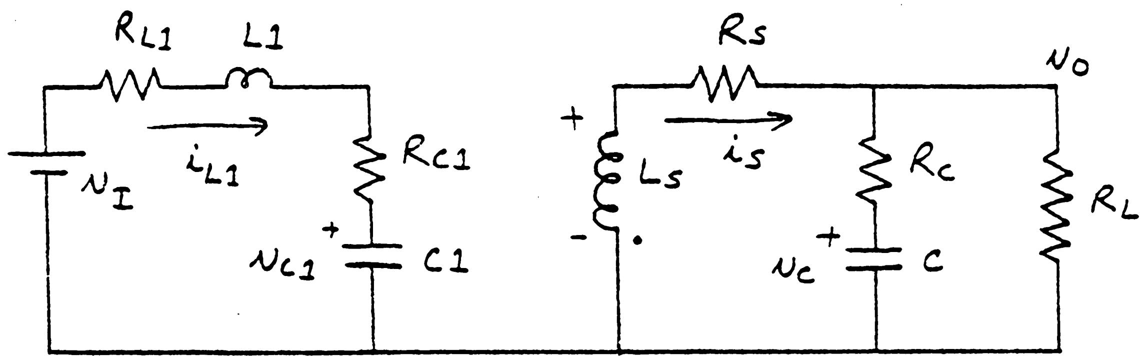


(b)

Figure 16: Buck-boost converter power stage model: (a) during $T_{ON}$ and (b) during $T_{OFF}$.

During $T_{OFF}$ the switch S is off and the circuit is as shown in Figure 16 (b).

The equations describing the circuit are

$$i_S = \frac{N_S}{L_S}\phi \tag{4-7}$$

$$\frac{di_{L1}}{dt} = \frac{i_{L1}}{L1}(-R_{L1} - R_{C1}) - \frac{v_{C1}}{L1} + \frac{v_I}{L1} \tag{4-8}$$

$$\frac{d\phi}{dt} = \frac{-(R_S R_C + R_S R_L + R_C R_L)\phi}{L_S(R_C + R_L)} - \frac{R_L v_C}{N_S(R_C + R_L)} \tag{4-9}$$

$$\frac{dv_{C1}}{C1} = \frac{i_{L1}}{C1} \tag{4-10}$$

$$\frac{dv_C}{dt} = \frac{N_S R_L \phi}{CL_S(R_C + R_L)} - \frac{v_C}{C(R_C + R_L)} \tag{4-11}$$

$$v_0 = \frac{R_L v_C}{R_C + R_L} + \frac{R_C R_L N_S \phi}{L_S(R_C + R_L)} \tag{4-12}$$

The following vectors are defined

$$\underline{x} = \begin{bmatrix} i_{L1} \\ \phi \\ v_{C1} \\ v_C \end{bmatrix} \qquad \underline{u} = [v_I] \qquad \underline{y} = [v_0] \tag{4-13}$$

resulting in the following state space equations

$$\underline{T_{ON}} \qquad\qquad \underline{T_{OFF}}$$

$$\dot{\underline{x}} = A_1\,\underline{x} + B_1\,\underline{u} \qquad \dot{\underline{x}} = A_2\,\underline{x} + B_2\,\underline{u} \tag{4-14}$$

$$\underline{y} = C_1\,\underline{x} \qquad \underline{y} = C_2\,\underline{x}$$

where

$$A_1 = \begin{bmatrix} -\dfrac{(R_{L1}+R_{C1})}{L1} & \dfrac{R_{C1}N_P}{L1L_P} & \dfrac{-1}{L1} & 0 \\ \dfrac{R_{C1}}{N_P} & \dfrac{-(R_{C1}+R_P)}{L_P} & \dfrac{1}{N_P} & 0 \\ \dfrac{1}{C1} & \dfrac{-N_P}{C1L_P} & 0 & 0 \\ 0 & 0 & 0 & \dfrac{-1}{C(R_L+R_C)} \end{bmatrix} \tag{4-15}$$

$$A_2 = \begin{bmatrix} -\dfrac{(R_{L1}+R_{C1})}{L1} & 0 & \dfrac{-1}{L1} & 0 \\ 0 & \dfrac{-R_1}{L_S} & 0 & \dfrac{-R_L}{N_S(R_C+R_L)} \\ \dfrac{1}{C1} & 0 & 0 & 0 \\ 0 & \dfrac{N_S R_L}{CL_S(R_C+R_L)} & 0 & \dfrac{-1}{C(R_C+R_L)} \end{bmatrix} \tag{4-16}$$

$$B_1 = [\,\frac{1}{L1} \quad 0 \quad 0 \quad 0\,]^T \tag{4-17}$$

$$B_2 = B_1 \tag{4-18}$$

$$C_1 = \begin{bmatrix} 0 & 0 & 0 & \dfrac{R_L}{R_C+R_L} \end{bmatrix} \tag{4-19}$$

$$C_2 = \begin{bmatrix} 0 & \frac{R_C R_L N_S}{L_S(R_C + R_L)} & 0 & \frac{R_L}{R_C + R_L} \end{bmatrix} \tag{4-20}$$

$$R_1 = \frac{R_S R_C + R_S R_L + R_C R_L}{R_C + R_L} \tag{4-21}$$

The state space averaged model over the entire period T is

$$\begin{aligned} \dot{\underline{x}} &= [dA_1 + d'A_2]\, \underline{x} + [dB_1 + d'B_2]\, \underline{u} \\ \underline{y} &= [dC_1 + d'C_2]\, \underline{x} \end{aligned} \tag{4-22}$$

where $d$ = duty cycle ratio = $T_{ON}/(T_{ON}+T_{OFF})$

$$d' = 1-d \tag{4-23}$$

$$T = T_{ON} + T_{OFF}$$

The state space averaged model is perturbed thus -

$$\begin{aligned} d &= D + \hat{d} \\ d' &= D' - \hat{d} \\ \underline{u} &= \underline{U} + \hat{\underline{u}} \\ \underline{y} &= \underline{Y} + \hat{\underline{y}} \\ \underline{x} &= \underline{X} + \hat{\underline{x}} \end{aligned} \tag{4-24}$$

Assuming that the perturbation is small

$\frac{\hat{d}}{D} << 1, \frac{\hat{\underline{x}}}{\underline{X}} << 1$ etc. leads to the following small

signal linearized model

$$\underline{0} = [DA_1 + D'A_2]\ \underline{X} + [DB_1 + D'B_2]\ V_I$$

$$V_0 = [DC_1 + D'C_2]\ \underline{X}$$

$$\dot{\hat{\underline{x}}} = [DA_1 + D'A_2]\ \hat{\underline{x}} + [DB_1 + D'B_2]\ \hat{v}_I \qquad (4\text{-}25)$$

$$+ [A_1 - A_2)\ \underline{X} + (B_1 - B_2\ V_I]\ \hat{d}$$

$$\hat{v_0} = [C_1 - C_2]\ \underline{X}\ \hat{d} + [DC_1 + D'C_2]\ \hat{\underline{x}}$$

Defining

$$A = DA_1 + D'A_2$$

$$B = DB_1 + D'B_2 \qquad (4\text{-}26)$$

$$C = DC_1 + D'C_2$$

results in

$$\dot{\hat{\underline{x}}} = A\ \hat{\underline{x}} + B\ \hat{v}_I$$

$$+ [A_1 - A_2)\ \underline{X} + (B_1 - B_2)\ V_I]\ \hat{d} \qquad (4\text{-}27)$$

$$\hat{v_0} = [C_1 - C_2]\ \underline{X}\ \hat{d} + C\ \hat{\underline{x}}$$

Using Laplace transforms results in

$$\hat{\underline{x}}(s) = [SI - A]^{-1}B\ \hat{v_I}(s)$$

$$+ [SI - A]^{-1}[(A_1 - A_2)\ \underline{X} + (B_1 - B_2)\ V_I]\ \hat{d}(s) \qquad (4\text{-}28)$$

$$\hat{v}_0(s) = [C_1 - C_2]\ \underline{X}\ \hat{d}(s) + C\ \hat{\underline{x}}(s)$$

The state space model is derived from the two equations above, and is shown in Figure 17 .

To derive the small signal equivalent circuit, it is first necessary to use the equation for $\hat{v}_0$ to substitute for $\hat{v}_C$ in terms of $\hat{v}_0$, in the small signal equations described above. Simplifying, the four equations are obtained

$$\hat{v}_I = (R_{C1} + R_{L1})\hat{i}_{L1} - \frac{R_{C1}N_P D}{L_P}\hat{\phi} + L1\frac{d\hat{i}_{L1}}{dt} \tag{4-29}$$

$$+ \hat{v}_{C1} - \frac{R_{C1}N_P}{L_P}\phi\,\hat{d}$$

$$C1\frac{d\hat{v}_{C1}}{dt} = \hat{i}_{L1} - \frac{DN_P}{L_P}\hat{\phi} - \frac{N_P}{L_P}\phi\,\hat{d} \tag{4-30}$$

$$C\frac{d\hat{v}_C}{dt} = \frac{D'N_S}{L_S}\hat{\phi} - \frac{\hat{v}_0}{R_L} - \frac{N_S}{L_S}\phi\,\hat{d} \tag{4-31}$$

$$D\frac{\hat{v}_{C1}N_S}{N_P} = \frac{N_S d\hat{\phi}}{dt} - \frac{R_{C1}N_S D}{N_P}\hat{i}_{L1} + \frac{DR_{C1}N_S}{L_P}\hat{\phi} \tag{4-32}$$

$$+ \frac{R_S N_S}{L_s}\hat{\phi} + \frac{DD'R_C R_L N_S}{L_S(R_C + R_L)}\hat{\phi} + D'\hat{v}_0$$

$$- \frac{R_{C1}I_{L1}N_S}{N_P}\hat{d} + \frac{R_{C1}\hat{d}\phi N_S}{L_P} - \hat{d}\,V_0$$

$$- \frac{R_C R_L N_S \phi\hat{d}(D - D')}{L_S(R_C + R_L)} - \frac{V_{C1}N_S}{N_P}\hat{d}$$

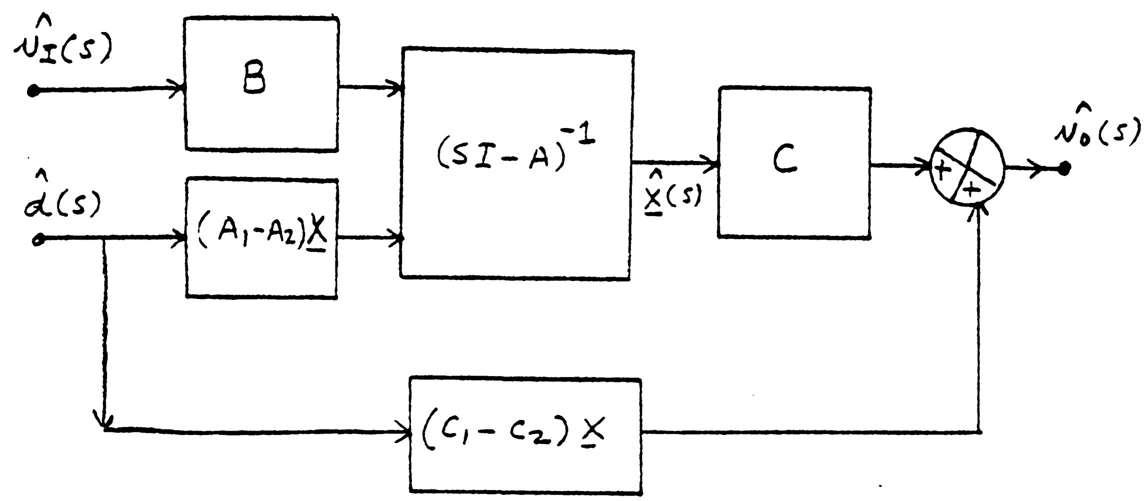


Figure 17: Buck-boost converter power stage small signal state space model

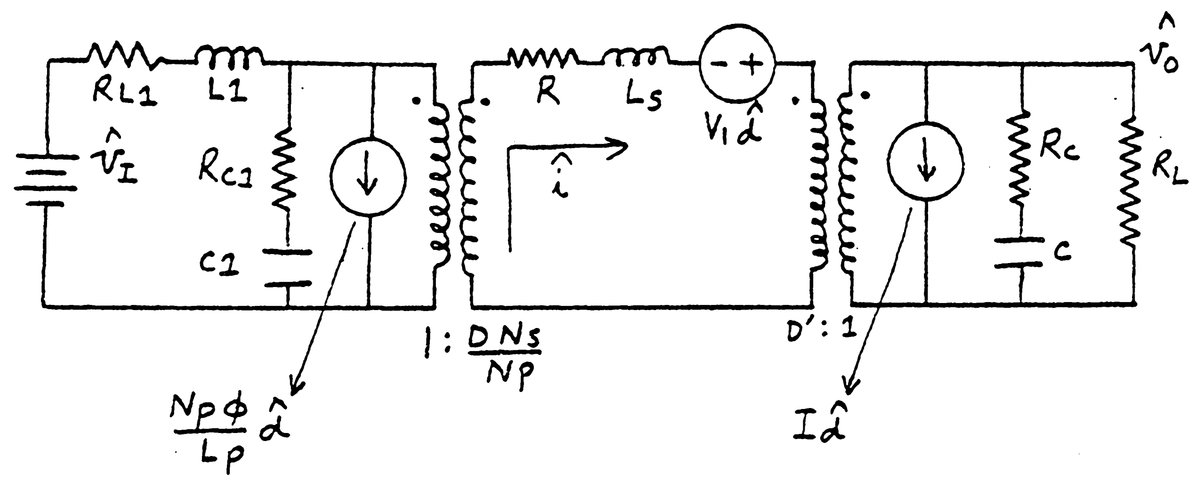


$$R = \frac{DD'R_{C1}L_S}{L_P} + \frac{DD'R_C R_L}{R_C + R_L} + R_S$$

$$V_1 = \left[ \frac{R_{C1}I_{L1}N_S}{N_P} - \frac{R_{C1}IL_S}{L_P} + \frac{R_C R_L I(D - D')}{(R_C + R_L)} + \frac{V_{C1}N_S}{N_P} + V_O \right]$$

Figure 18: Buck-boost converter power stage small signal equivalent circuit

Using a fictitious current i described by

$$L_S i = N_S \phi \qquad (4\text{-}33)$$

an equivalent circuit can be made up that is described by the four equations given above. This circuit will use the current i flowing through $L_S$ and it is thus the small signal equivalent circuit for the buck-boost converter, as shown in Figure 18.

## 4.2 BUCK CONVERTER SMALL SIGNAL MODEL DERIVATION

The procedure used in deriving the small signal model for the buck converter is exactly similar to that used for the buck-boost converter. The buck converter is shown in Figure 19 .

During $T_{ON}$ the switch S is on and the circuit is as shown in Figure 20 (a).

The equations describing the circuit are

$$\frac{di_{L1}}{dt} = \frac{-(R_{L1} + R_{C1})}{L1} i_{L1} + \frac{R_{C1}}{L1} i_L - \frac{v_{C1}}{L1} + \frac{v_I}{L1} \qquad (4\text{-}34)$$

$$\frac{di_L}{dt} = \frac{R_{C1}}{L} i_{L1} - \frac{R_1}{L} i_L + \frac{v_{C1}}{L} - \frac{R_L v_C}{L(R_C + R_L)} \qquad (4\text{-}35)$$

$$\frac{dv_{C1}}{dt} = \frac{i_{L1}}{C1} - \frac{i_L}{C1} \qquad (4\text{-}36)$$

$$\frac{dv_C}{dt} = \frac{R_L i_L}{C(R_C + R_L)} - \frac{v_C}{C(R_C + R_L)} \qquad (4\text{-}37)$$

$$v_0 = \frac{R_L R_C i_L}{R_L + R_C} + \frac{R_L v_C}{R_L + R_C} \tag{4-38}$$

During $T_{OFF}$, the switch S is off, and the circuit is shown in Figure 20 (b). The equations describing the circuit are

$$\frac{di_{L1}}{dt} = \frac{-(R_{L1} + R_{C1})}{L1} i_{L1} - \frac{v_{C1}}{L1} + \frac{v_I}{L1} \tag{4-39}$$

$$\frac{di_L}{dt} = \frac{-R_2 i_L}{L} - \frac{R_L v_C}{L(R_L + R_C)} \tag{4-40}$$

$$\frac{dv_{C1}}{dt} = \frac{i_{L1}}{C1} \tag{4-41}$$

$$\frac{dv_C}{dt} = \frac{R_L i_L}{C(R_L + R_C)} - \frac{v_C}{C(R_L + R_C)} \tag{4-42}$$

$$v_0 = \frac{R_L R_C i_L}{R_L + R_C} + \frac{R_L v_C}{R_L + R_C} \tag{4-43}$$

$$R_2 = R_\ell + \frac{R_C R_L}{R_C + R_L} \tag{4-44}$$

$$R_1 = R_{C1} + R_\ell + \frac{R_C R_L}{R_C + R_L} \tag{4-45}$$

The following vectors are defined

$$\underline{u} = [v_I] \qquad \underline{x} = \begin{bmatrix} i_{L1} \\ i_L \\ v_{C1} \\ v_C \end{bmatrix} \qquad \underline{y} = [v_0] \tag{4-46}$$

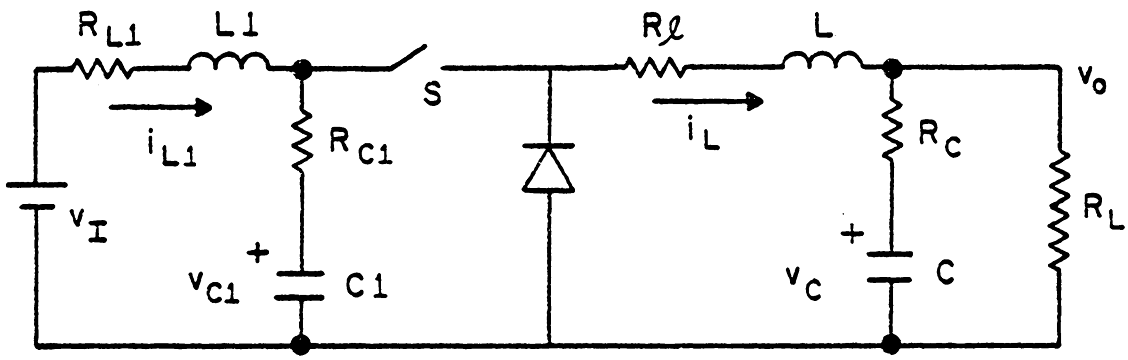


Figure 19: Buck converter power stage.

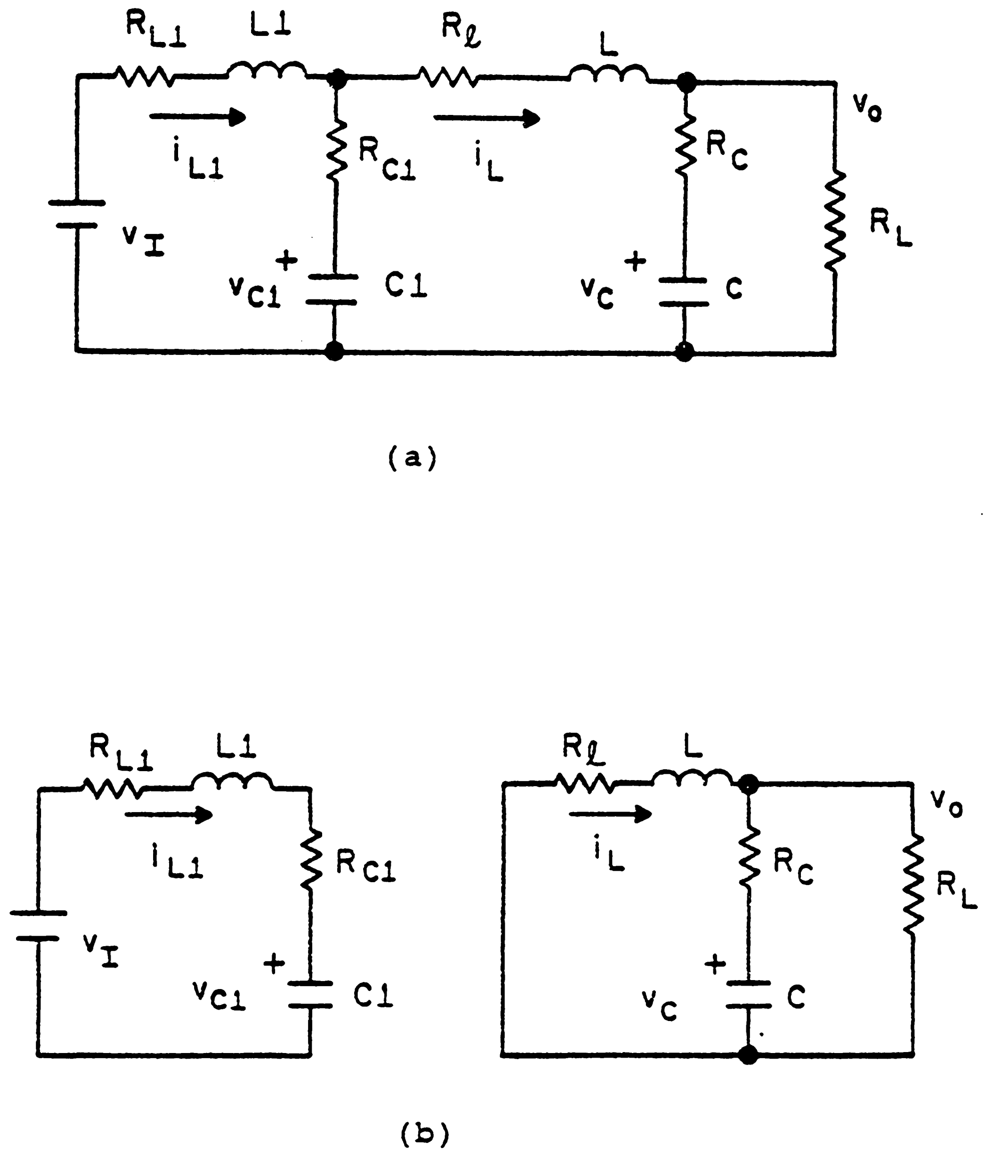


Figure 20: Buck converter power stage model during: (a) $T_{ON}$ and (b) $T_{OFF}$.

resulting in the following state space equation

$$\begin{array}{ll} \underline{T_{ON}} & \underline{T_{OFF}} \\ \underline{\dot{x}} = A_1 \underline{x} + B_1 \underline{u} & \underline{\dot{x}} = A_2 \underline{x} + B_2 \underline{u} \\ \underline{y} = C_1 \underline{x} & \underline{y} = C_2 \underline{x} \end{array} \tag{4-47}$$

where

$$A_1 = \begin{bmatrix} \frac{-(R_{L1}+R_{C1})}{L1} & \frac{R_{C1}}{L1} & \frac{-1}{L1} & 0 \\ \frac{R_{C1}}{L} & \frac{-R_1}{L} & \frac{1}{L} & \frac{-R_L}{L(R_C+R_L)} \\ \frac{1}{C1} & \frac{-1}{C1} & 0 & 0 \\ 0 & \frac{R_L}{C(R_L+R_C)} & 0 & \frac{-1}{C(R_L+R_C)} \end{bmatrix} \tag{4-48}$$

$$A_2 = \begin{bmatrix} \frac{-(R_{L1}+R_{C1})}{L1} & 0 & \frac{-1}{L1} & 0 \\ 0 & \frac{-R_2}{L} & 0 & \frac{-R_L}{L(R_C+R_L)} \\ \frac{1}{C1} & 0 & 0 & 0 \\ 0 & \frac{R_L}{C(R_L+R_C)} & 0 & \frac{-1}{C(R_L+R_C)} \end{bmatrix} \tag{4-49}$$

$$B_1 = \begin{bmatrix} \frac{1}{L1} & 0 & 0 & 0 \end{bmatrix}^T \quad (4\text{-}50)$$

$$B_2 = B_1 \quad (4\text{-}51)$$

$$C_1 = \begin{bmatrix} 0 & \frac{R_L R_C}{R_L + R_C} & 0 & \frac{R_L}{R_L + R_C} \end{bmatrix} \quad (4\text{-}52)$$

$$C_2 = C_1 \quad (4\text{-}53)$$

The state space averaged model over the entire period T is

$$\dot{\underline{x}} = [dA_1 + d'A_2]\underline{x} + [dB_1 + d'B_2]\underline{u} \quad (4\text{-}54)$$
$$\underline{y} = [dC_1 + d'C_2]\underline{x}$$

where $\quad d$ = duty cycle ratio $= T_{ON}/(T_{ON}+T_{OFF})$

$$d' = 1 - d \quad (4\text{-}55)$$
$$T = T_{ON} + T_{OFF}$$

The state space averaged model is perturbed and linearized in exactly the same way as for the buck-boost converter. The resulting small signal linearized model is

$$\underline{0} = [DA_1 + D'A_2]\underline{X} + [DB_1 + D'B_2]V_I$$
$$\dot{\hat{\underline{x}}} = [DA_1 + D'A_2]\hat{\underline{x}} + [DB_1 + D'B_2]\hat{v}_I$$
$$+ [(A_1 - A_2)\underline{X} + (B_1 - B_2)V_I]\hat{d} \quad (4\text{-}56)$$
$$V_0 = [DC_1 + D'C_2]\underline{X}$$
$$\hat{v}_0 = [C_1 - C_2]\underline{X}\hat{d} + [DC_1 + D'C_2]\hat{\underline{x}}$$

Defining

$$A = DA_1 + D'A_2$$
$$B = DB_1 + D'B_2 \qquad (4\text{-}57)$$
$$C = DC_1 + D'C_2$$

results in

$$\dot{\hat{\underline{x}}} = A\hat{\underline{x}} + B\hat{v}_1$$
$$+ [(A_1 - A_2)\underline{X} + (B_1 - B_2)V_I]\hat{d} \qquad (4\text{-}58)$$
$$\hat{v}_0 = [C_1 - C_2]\underline{X}\hat{d} + C\hat{\underline{x}}$$

Using Laplace transforms gives

$$\hat{\underline{x}}(s) = [SI - A]^{-1}B\ \hat{v}_I(s)$$
$$+ [SI - A]^{-1}[(A_1 - A_2)\underline{X} + (B_1 - B_2)V_I]\hat{d}(s) \qquad (4\text{-}59)$$
$$v_0(s) = [C_1 - C_2]\underline{X}\ \hat{d}(s) + C\ \hat{\underline{x}}(s)$$

The state space model is derived from the above two equations and is shown in Figure 21 .

The procedure for deriving the small signal equivalent circuit is exactly similar to the one used for the buck-boost converter. The four equations that result are

$$\hat{v}_I = (R_{L1} + R_{C1})\hat{i}_{L1} - DR_{C1}\ \hat{i}_L + L1\frac{d\hat{i}_{L1}}{dt} \qquad (4\text{-}60)$$
$$+ \hat{v}_{C1} - R_{C1}I_L\hat{d}$$

$$D\hat{v}_{C1} = (DR_{C1} + R_\ell)\hat{i}_L - DR_{C1}\hat{i}_{L1} + \hat{v}_0 \qquad (4\text{-}61)$$
$$+ L\frac{d\hat{i}_L}{dt} - (R_{C1}I_{L1} - R_{C1}I_L + V_{C1})\hat{d}$$

$$C1\frac{d\hat{v}_{C1}}{dt} = \hat{i}_{L1} - D\hat{i}_L - \hat{d}I_L \qquad (4\text{-}62)$$

$$C\frac{d\hat{v}_C}{dt} = \hat{i}_L - \frac{\hat{v}_O}{R_L} \qquad (4\text{-}63)$$

The small signal equivalent circuit is described by the four equations above, as in the buck-boost converter, and is shown in Figure 22 .

## 4.3 BOOST CONVERTER SMALL SIGNAL MODEL DERIVATION

The procedure used in deriving the small signal model for the boost converter is exactly similar to that used for the buck-boost converter. The boost converter is shown in Figure 23 .

During $T_{ON}$, the switch S is on, and the resulting circuit is shown in Figure 24 (a).

The equations describing the circuit are

$$\frac{di_{L1}}{dt} = \frac{-(R_{L1} + R_{C1})}{L1} i_{L1} + \frac{R_{C1}}{L1} i_L - \frac{v_{C1}}{L1} + \frac{v_I}{L1} \qquad (4\text{-}64)$$

$$\frac{dv_{C1}}{dt} = \frac{i_{L1}}{C1} - \frac{i_L}{C1} \qquad (4\text{-}65)$$

$$\frac{di_L}{dt} = \frac{R_{C1}}{L} i_{L1} - \frac{(R_{C1} + R_\ell)}{L} i_L + \frac{v_{C1}}{L} \qquad (4\text{-}66)$$

$$\frac{dv_C}{dt} = \frac{-v_C}{C(R_C + R_L)} \qquad (4\text{-}67)$$

$$v_O = \frac{v_C R_L}{R_C + R_L} \qquad (4\text{-}68)$$

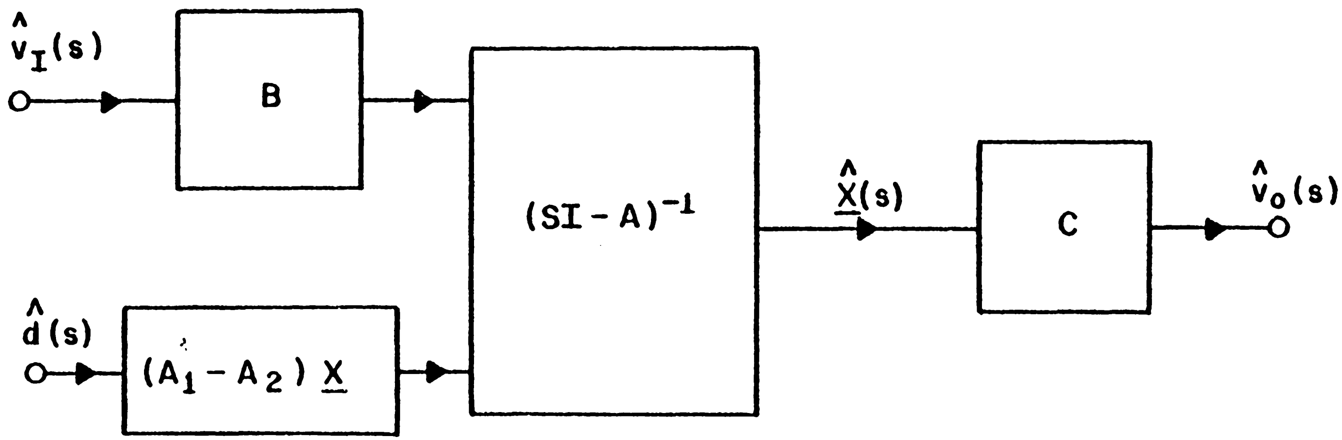


Figure 21: Buck converter power stage small signal state space model.

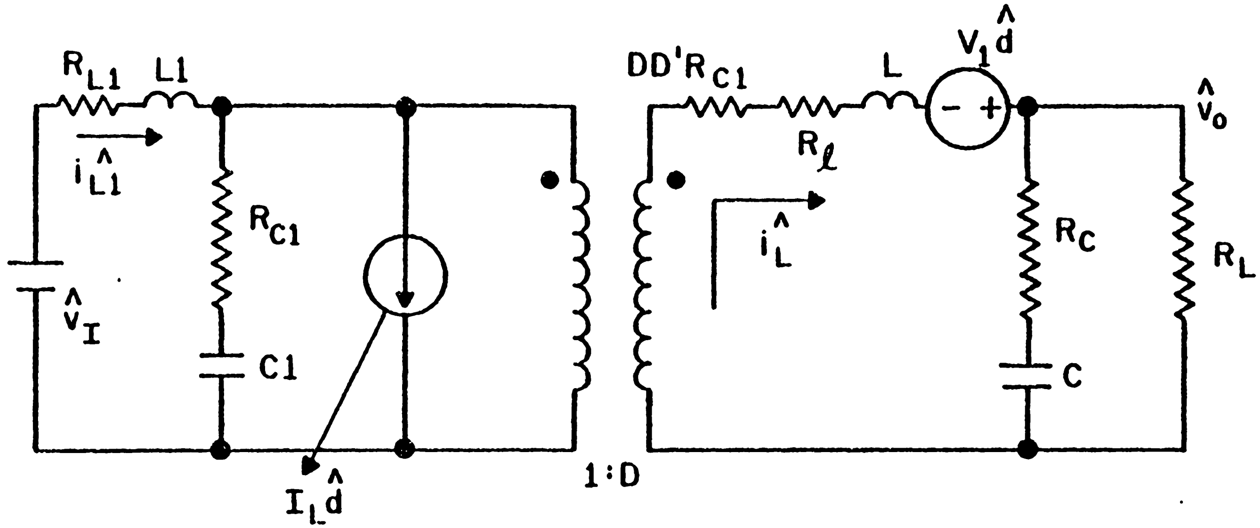


$$V_1 = V_{C1} - D'R_{C1}I_L + R_{C1}I_{L1}$$

Figure 22: Buck converter power stage small signal equivalent circuit.

During $T_{OFF}$ the switch S is off and the resulting circuit is shown in Figure 24 (b).

The equations describing the circuit are

$$\frac{di_{L1}}{dt} = \frac{-(R_{L1} + R_{C1})}{L1} i_{L1} + \frac{R_{C1}}{L1} i_L - \frac{v_{C1}}{L1} + \frac{V_I}{L1} \quad (4\text{-}69)$$

$$\frac{dv_{C1}}{dt} = \frac{i_{L1}}{C1} - \frac{i_L}{C1} \quad (4\text{-}70)$$

$$\frac{di_L}{dt} = \frac{R_{C1}}{L} i_{L1} - \frac{i_L}{L} \left(R_{C1} + R_\ell + \frac{R_C R_L}{R_C + R_L}\right) - \frac{R_L v_C}{L(R_C + R_L)} + \frac{v_{C1}}{L} \quad (4\text{-}71)$$

$$\frac{dv_C}{dt} = \frac{R_L i_L}{C(R_C + R_L)} - \frac{v_C}{C(R_C + R_L)} \quad (4\text{-}72)$$

$$v_O = \frac{R_C R_L}{R_C + R_L} i_L + \frac{R_L v_C}{R_C + R_L} \quad (4\text{-}73)$$

The following vectors are defined

$$\underline{x} = \begin{bmatrix} i_{L1} \\ i_L \\ v_{C1} \\ v_C \end{bmatrix} \qquad \underline{u} = [v_I] \qquad \underline{y} = [v_O] \quad (4\text{-}74)$$

resulting in the following state space equations.

$$\begin{array}{ll} \underline{T_{ON}} & \underline{T_{OFF}} \\ \dot{\underline{x}} = A_1\underline{x} + B_1\underline{u} & \dot{\underline{x}} = A_2\underline{x} + B_2\underline{u} \\ \underline{y} = C_1\underline{x} & \underline{y} = C_2\underline{x} \end{array} \quad (4\text{-}75)$$

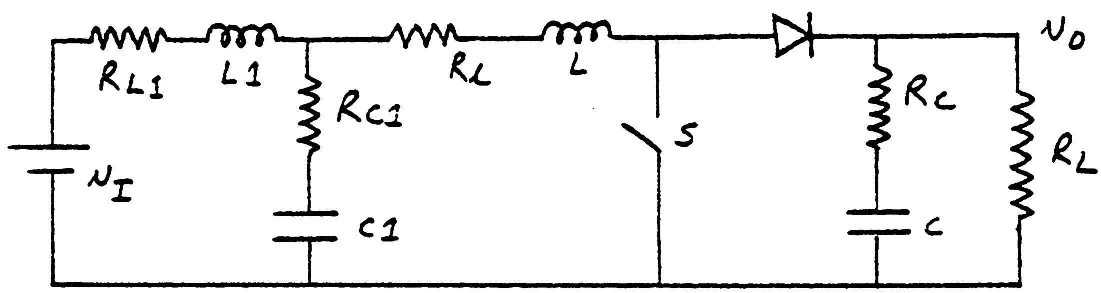


Figure 23:  Boost converter power stage

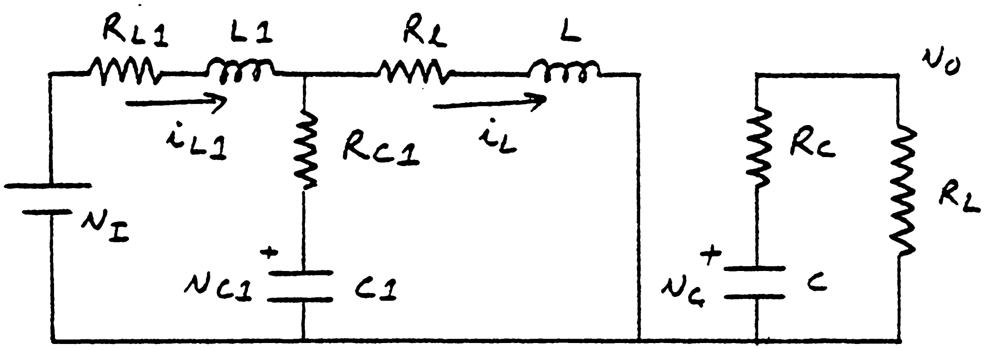


(a)

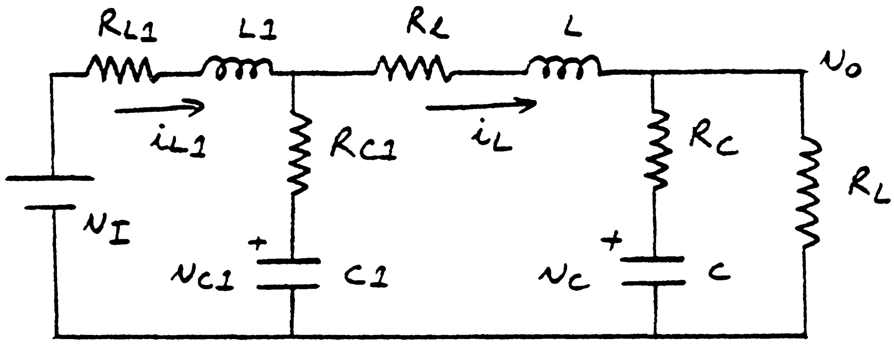


(b)

Figure 24: Boost converter power stage models during : (a) $T_{ON}$ and (b) $T_{OFF}$.

where

$$A_1 = \begin{bmatrix} \frac{-(R_{L1}+R_{C1})}{L1} & \frac{R_{C1}}{L1} & \frac{-1}{L1} & 0 \\ \frac{R_{C1}}{L} & \frac{-(R_{C1}+R_{\ell})}{L} & \frac{1}{L} & 0 \\ \frac{1}{C1} & \frac{-1}{C1} & 0 & 0 \\ 0 & 0 & 0 & \frac{-1}{C(R_C+R_L)} \end{bmatrix} \tag{4-76}$$

$$A_2 = \begin{bmatrix} \frac{-(R_{L1}+R_{C1})}{L1} & \frac{R_{C1}}{L1} & \frac{-1}{L1} & 0 \\ \frac{R_{C1}}{L} & \frac{-R_1}{L} & \frac{1}{L} & \frac{-R_L}{L(R_C+R_L)} \\ \frac{1}{C1} & \frac{-1}{C1} & 0 & 0 \\ 0 & \frac{R_L}{C(R_C+R_L)} & 0 & \frac{-1}{C(R_C+R_L)} \end{bmatrix} \tag{4-77}$$

$$R_1 = R_{C1} + R_{\ell} + \frac{R_C R_L}{R_C + R_L} \tag{4-78}$$

$$B_1 = \begin{bmatrix} \frac{1}{L1} & 0 & 0 & 0 \end{bmatrix}^T \tag{4-79}$$

$$B_2 = B_1 \tag{4-80}$$

$$C_1 = \begin{bmatrix} 0 & 0 & 0 & \frac{R_L}{R_C + R_L} \end{bmatrix} \tag{4-81}$$

$$C_2 = \begin{bmatrix} 0 & \frac{R_L R_C}{R_L + R_C} & 0 & \frac{R_L}{R_C + R_L} \end{bmatrix} \tag{4-82}$$

The state space averaged model over the entire period T is

$$\begin{aligned} \underline{\dot{x}} &= [dA_1 + d'A_2]\underline{x} + [dB_1 + d'B_2]\underline{u} \\ \underline{y} &= [dC_1 + d'C_2]\underline{x} \end{aligned} \tag{4-83}$$

where

$$\begin{aligned} d &= \text{duty cycle ratio} = T_{ON}/(T_{ON}+T_{OFF}) \\ d' &= 1 - d \\ T &= T_{ON} + T_{OFF} \end{aligned} \tag{4-84}$$

The state space averaged model is perturbed and linearized in exactly the same way as for the buck-boost converter. The resulting small signal linearized model is

$$\begin{aligned} \underline{0} &= A\,\underline{X} + B\,V_I \\ \underline{\dot{\hat{x}}} &= A\,\underline{\hat{x}} + B\,\hat{v}_I \\ &\quad + [(A_1 - A_2)\,\underline{X} + (B_1 - B_2)V_I]\hat{d} \end{aligned} \tag{4-85}$$

$$V_0 = C\,\underline{X} \tag{4-86}$$

$$\hat{v}_0 = [C_1 - C_2]\,\underline{X}\,\hat{d} + C\,\underline{\hat{x}} \tag{4-87}$$

where

$$\begin{aligned} A &= DA_1 + D'A_2 \\ B &= DB_1 + D'B_2 \\ C &= DC_1 + D'C_2 \end{aligned} \tag{4-88}$$

Using Laplace transforms gives

$$\underline{\hat{x}(s)} = [SI - A]^{-1} B \hat{v}_I(s) + [SI - A]^{-1}[(A_1 - A_2)\underline{X} + (B_1 - B_2)V_I]\hat{d}(s) \qquad (4\text{-}89)$$

$$\hat{v}_0(s) = [C_1 - C_2]\underline{X}\, \hat{d}(s) + C\underline{\hat{x}(s)}$$

The state space model is derived from the above two equations and is shown in Figure 25 .

The procedure for deriving the small signal equivalent circuit is exactly similar to the one used for the buck-boost converter. The four equations that result are --

$$L1\frac{d\hat{i}_{L1}}{dt} = -(R_{L1} + R_{C1})\hat{i}_{L1} + R_{C1}\hat{i}_L - \hat{v}_{C1} + \hat{v}_I \qquad (4\text{-}90)$$

$$L\frac{d\hat{i}_L}{dt} = R_{C1}\hat{i}_{L1} - (R_{C1} + R_\ell)\hat{i}_L - DD'\frac{R_C R_L}{R_C + R_L}\hat{i}_L + \hat{v}_{C1} - D'\hat{v}_0 + \frac{R_C R_L I_L \hat{d}(D - D')}{R_C + R_L} + V_0\hat{d} \qquad (4\text{-}91)$$

$$C_1\frac{d\hat{v}_{C1}}{dt} = \hat{i}_{L1} - \hat{i}_L \qquad (4\text{-}92)$$

$$C\frac{d\hat{v}_C}{dt} = D'\hat{i}_L - \frac{\hat{v}_0}{R_L} - I_L\hat{d} \qquad (4\text{-}93)$$

The small signal equivalent circuit is described by the four equations above as in the buck-boost converter, and is shown in Figure 26 .

The power stage small signal models developed include the input filter state variables, whereas earlier models [3,4,5,6] had treated the input filter only in terms of its output impedance and transfer function. The models developed in this chapter are used to analyze and design a feedforward loop that includes the input filter state variables.

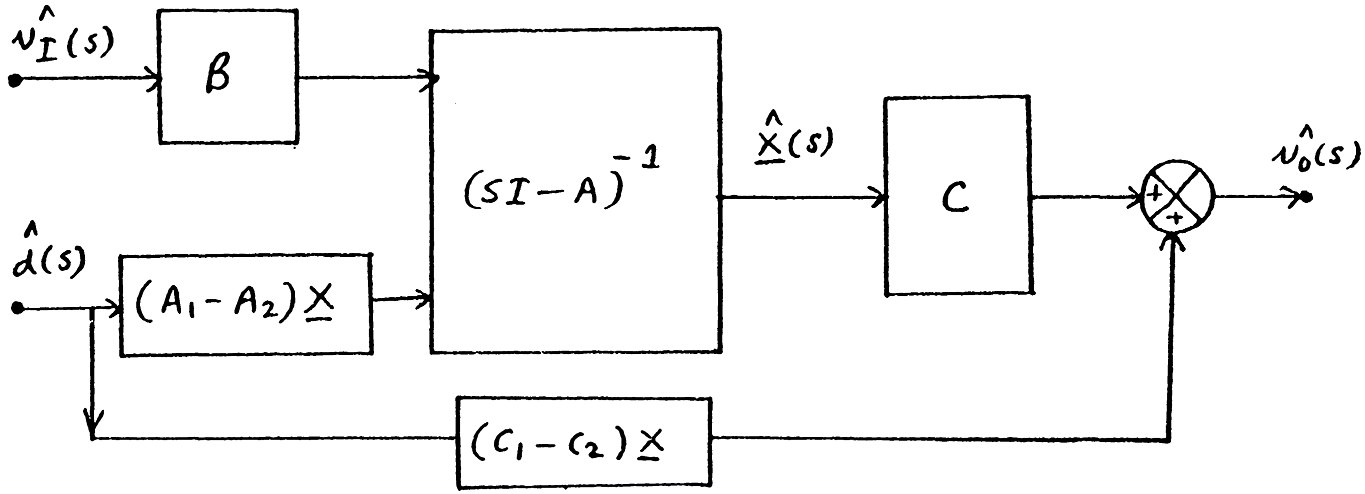


Figure 25: Boost converter power stage small signal state space model.

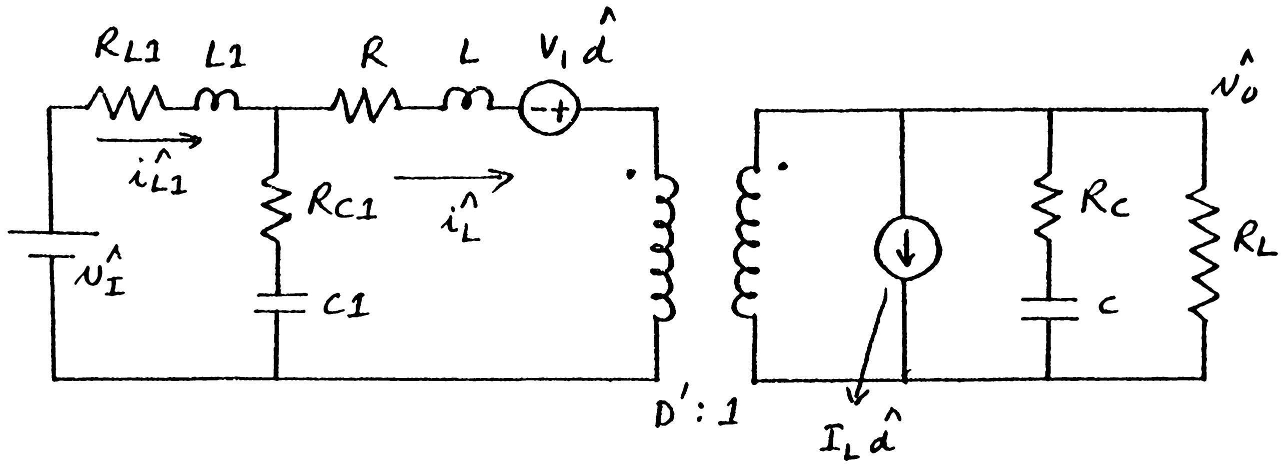


$$R = R_\ell + \frac{DD'R_C R_L}{R_C + R_L}$$

$$V_1 = V_0 + \frac{R_C R_L I_L (D - D')}{R_C + R_L}$$

Figure 26: Boost converter power stage small signal equivalent circuit.

## Chapter V

# IMPLEMENTATION OF THE FEEDFORWARD LOOP FOR A BUCK REGULATOR

This chapter first presents an analysis that leads to a design of the feedforward loops for a buck regulator. A small signal model that includes a general form of the feedforward loops is developed first. Analysis of the small signal model leads to a design of the feedforward loop. Implementation of the design is next discussed and two feedforward circuits are presented. The buck regulator alone is treated in this chapter, however the analysis and design procedure would be similar for the boost and the buck-boost regulators.

## 5.1 STATE SPACE MODEL OF BUCK REGULATOR

The state space model of the buck regulator is shown in Figure 27 . In the figure the feedforward loop has as its input the input filter state variables $\hat{i}_{L1}$ and $\hat{v}_{C1}$ (the input filter inductor current and capacitor voltage respectively). These two inputs are multiplied by the transfer functions $c_2(s)$ and $c_3(s)$ whose properties are yet to be determined. The feedback loop has as its inputs the output voltage and the output filter inductor current. The feedback control in this case is the two loop control (the standardized control module or SCM) developed earlier [2,7,8] and discussed in Chapter 3. The error processor in Figure 27 is thus composed of the blocks labelled $c_2$, $c_3$ and the feedback, and has as its input information regarding the output filter and input filter state variables. The pulse modulator is represented by its transfer function $F_M$ [2,8]. The rest of Figure 27 is the state space model of the buck power stage developed in Chapter 4.

The feedforward and feedback signals are added and fed to the pulse modulator. In physical terms this means sensing the small signal variations in input filter inductor current and capacitor voltage, processing these variations (as represented by the blocks $c_2(s)$ and $c_3(s)$ in Figure 27) and adding the processed variations to the feedback signal. The total state feedforward/feedback error signal is then used to modulate the duty cycle of the switch for loop gain correction.

The transfer function $\hat{v}_0(s)/\hat{v}_x(s)$, Figure 27, is used to design the feedforward because it expresses clearly what the feedforward does; also the resulting design is independent of the feedback loop parameters. The generalized small signal model for the buck regulator is developed next and used to write the transfer function $\hat{v}_0(s)/\hat{v}_x(s)$.

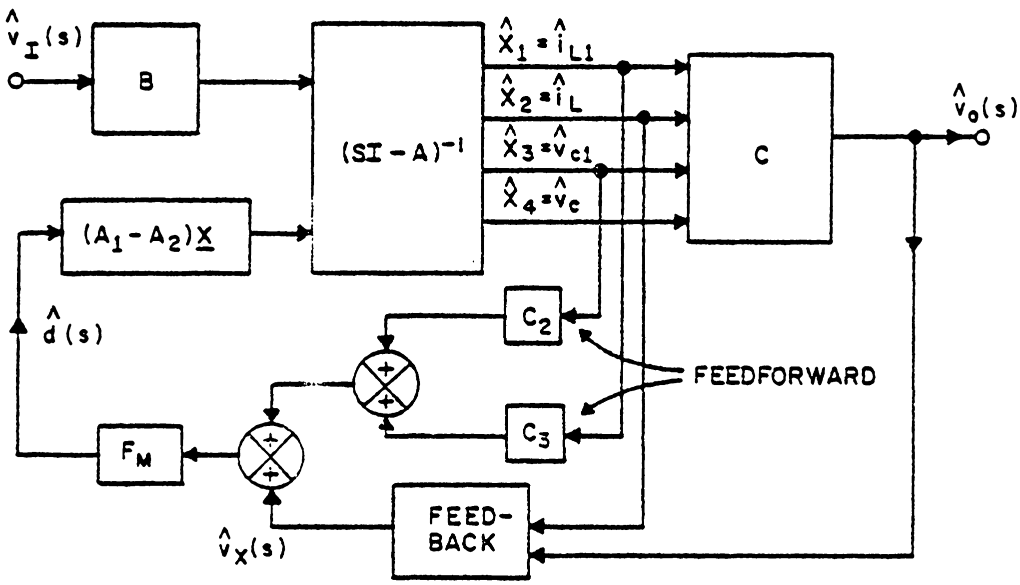


Figure 27: State space model of the buck regulator

## 5.2 GENERALIZED SMALL SIGNAL MODEL OF BUCK REGULATOR

The generalized small signal model of the buck regulator is shown in Figure 28 . The regulator is modelled according to the three basic functional blocks: power stage, error processor and duty cycle pulse modulator. The power stage model consists of two inputs: disturbances from the line $\hat{v}_I$ and the duty cycle control $\hat{d}$, and four outputs: the output voltage $\hat{v}_O$, the output filter inductor current $\hat{i}_L$, the input filter capacitor voltage $\hat{v}_{C1}$ and the input filter inductor current $\hat{i}_{L1}$. The error processor has as its input information regarding the output filter and the input filter state variables. The transfer functions $F_3$, $F_{AC}$ and $F_{DC}$ constitute the two loop standardized control module (SCM) developed earlier [2,7,8], whereas the feedforward loop gains $c_2$ and $c_3$ are as yet unknown. The error processor processes information regarding the state variables of the input and output filters and feeds a total error signal to the pulse modulator, whose transfer function $F_M$ was developed earlier [2,7,8].

The power stage transfer functions $F_{11}$ etc. are written using the following equations:

$$\begin{aligned} T_{11}\hat{v}_I + T_{12}\hat{d} &= \hat{v}_O \\ T_{21}\hat{v}_I + T_{22}\hat{d} &= \hat{i}_L \\ T_{31}\hat{v}_I + T_{32}\hat{d} &= \hat{v}_{C1} \\ T_{41}\hat{v}_I + T_{42}\hat{d} &= \hat{i}_{L1} \end{aligned} \tag{5-1}$$

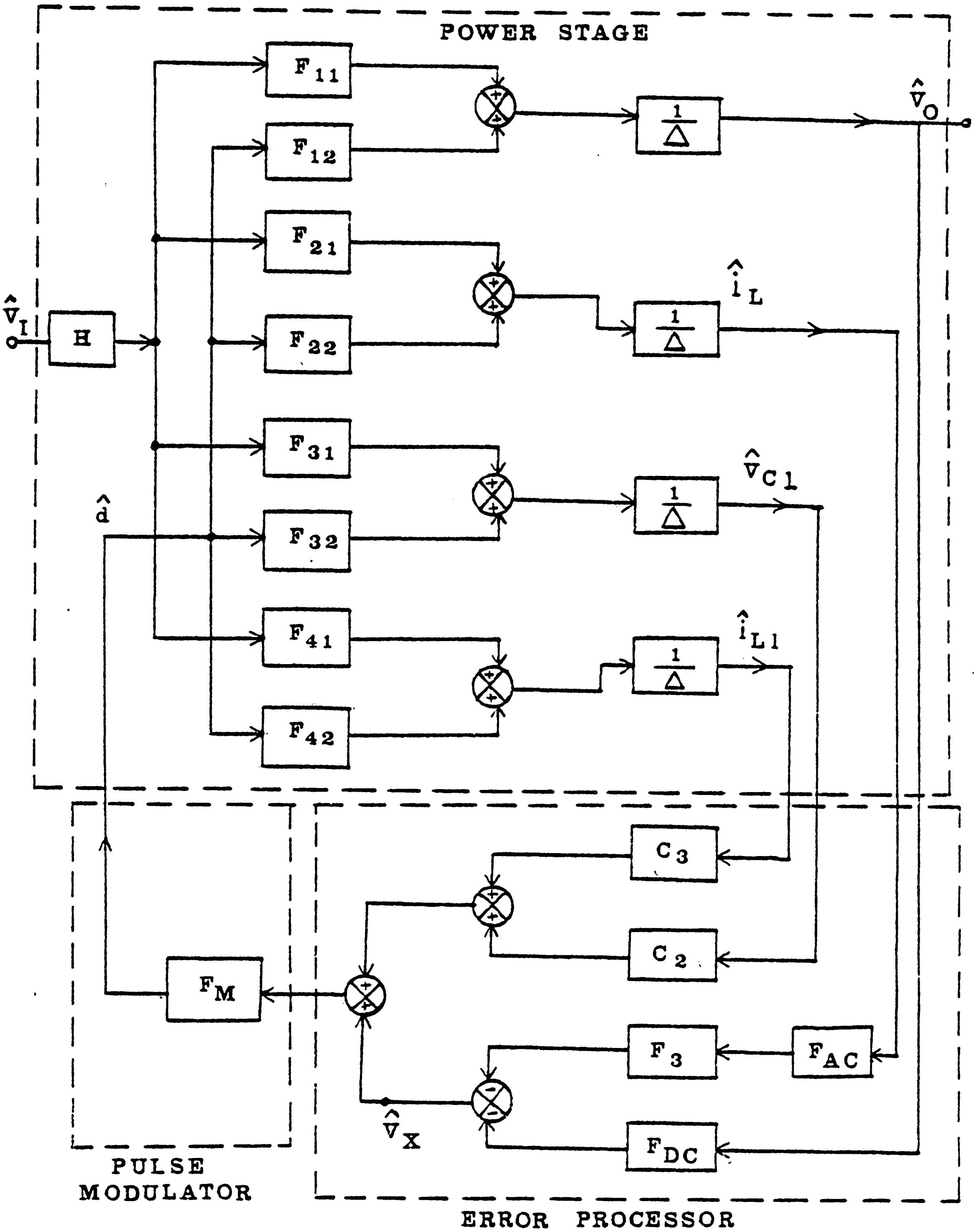


Figure 28: Generalized Small Signal Model

Thus it can be seen that

$$T_{11} = \left.\frac{\hat{v}_O}{\hat{v}_I}\right|_{\hat{d} = 0} \tag{5-2}$$

and

$$T_{11} = \frac{H\ F_{11}}{\Delta}$$
$$T_{12} = \frac{F_{12}}{\Delta} \tag{5-3}$$

5.2.1 <u>Development of Power Stage Transfer Functions</u>

As can be seen from equations (5-1) $T_{11}$, $T_{21}$, $T_{31}$ and $T_{41}$ can be evaluated with $\hat{d} = 0$ and the other four with $\hat{v}_I = 0$. The starting point for the evaluation of the transfer functions is the small signal equivalent circuit model for the buck regulator power stage developed in Chapter 4, Figure 22

5.2.1.1 Evaluation of $T_{11}$, $T_{21}$, $T_{31}$ and $T_{41}$

These transfer functions are evaluated with $\hat{d} = 0$ in Figure 22 . The resulting circuit is shown in Figure 29 . In Figure 29 the input filter has been replaced by its forward transfer function H(s) and its output impedance Z(s).

$$H(s) = \frac{1 + sC1R_{C1}}{s^2L1\ C1 + sC1(R_{L1} + R_{C1}) + 1} \tag{5-4}$$

$$Z(s) = \frac{s^2 L1C1R_{C1} + sC1R_{C1}R_{L1} + sL1 + R_{L1}}{s^2 L1C1 + sC1(R_{L1} + R_{C1}) + 1} \tag{5-5}$$

From the equivalent circuit of Figure 29 the following can be derived:

$$\begin{aligned} T_{11} &= \frac{\hat{v}_O}{\hat{v}_I} = \frac{DR_L(1 + sCR_C)H}{\Delta} \\ T_{21} &= \frac{\hat{i}_L}{\hat{v}_I} = \frac{D(1 + sCR_L)H}{\Delta} \\ T_{31} &= \frac{\hat{v}_{C1}}{\hat{v}_I} = \frac{a_1 H}{\Delta} \\ T_{41} &= \frac{\hat{i}_{L1}}{\hat{v}_I} = \frac{\Delta - a_1 H}{(R_{L1} + sL1)\Delta} \end{aligned} \tag{5-6}$$

where

$$\begin{aligned} a_1 &= s^2 LCR_L + sCR_L(R_\ell + R_C + \frac{L}{CR_L}) + R_L \\ \Delta &= a_1 + D^2 Z(1 + sCR_L) \\ D &= \text{duty cycle} = \frac{V_O}{V_I},\ V_I = \text{supply voltage} \end{aligned} \tag{5-7}$$

$$R_L + R_\ell \approx R_L$$

Using equations (5-3) and (5-6) the following are derived:

$$
\begin{aligned}
F_{11} &= DR_L(1 + sCR_C) \\
F_{21} &= D(1 + sCR_L) \\
F_{31} &= a_1 \\
F_{41} &= \frac{\Delta/H - a_1}{R_{L1} + sL1}
\end{aligned}
\tag{5-8}
$$

In the derivation of equations (5-6) the resistance $R_{C1}$ has been assumed negligibly small. This is not an unrealistic assumption since the ESR of the input filter capacitor ($R_{C1}$) can be assumed negligibly small compared with the other resistances; also in the derivation of $T_{41}$ the following is used:

$$\frac{\hat{v}_I - \hat{v}_{C1}}{R_{L1} + sL1} = \hat{i}_{L1} \tag{5-9}$$

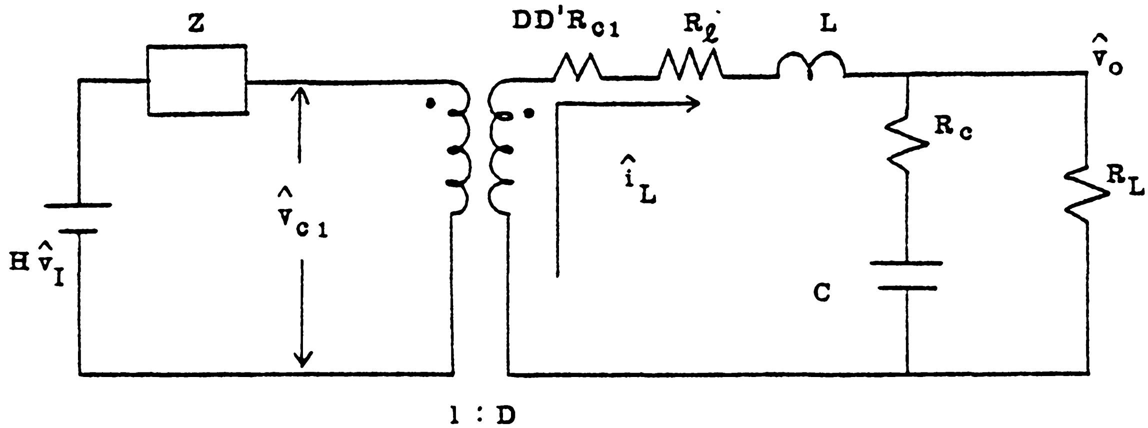


Figure 29: Small signal equivalent circuit with $\hat{d} = 0$

5.2.1.2 Evaluation of $T_{12}$, $T_{22}$, $T_{32}$ and $T_{42}$.

These transfer functions are evaluated with $\hat{v}_I = 0$ in Figure 22 . The resulting circuit is shown in Figure 30

From the equivalent circuit of Figure 30 the following are derived:

$$T_{12} = \frac{\hat{v}_o}{\hat{d}} = \frac{V_o(R_L - D^2 Z)(1 + sCR_C)}{D\Delta}$$

$$T_{22} = \frac{\hat{i}_L}{\hat{d}} = \frac{V_o(R_L - D^2 Z)(1 + sCR_L)}{DR_L\Delta} \qquad (5\text{-}10)$$

$$T_{32} = \frac{\hat{v}_{C1}}{\hat{d}} = \frac{-ZV_o[a_1 + R_L(1 + sCR_L)]}{R_L\Delta}$$

$$T_{42} = \frac{\hat{i}_{L1}}{\hat{d}} = \frac{ZV_o[a_1 + R_L(1 + sCR_L)]}{(R_{L1} + sL1)R_L\Delta}$$

Using equations (5-1) and (5-10) the following are derived:

$$F_{12} = \frac{V_o(R_L - D^2 Z)(1 + sCR_C)}{D}$$

$$F_{22} = \frac{V_o(R_L - D^2 Z)(1 + sCR_L)}{DR_L} \qquad (5\text{-}11)$$

$$F_{32} = \frac{-ZV_o[a_1 + R_L(1 + sCR_L)]}{R_L}$$

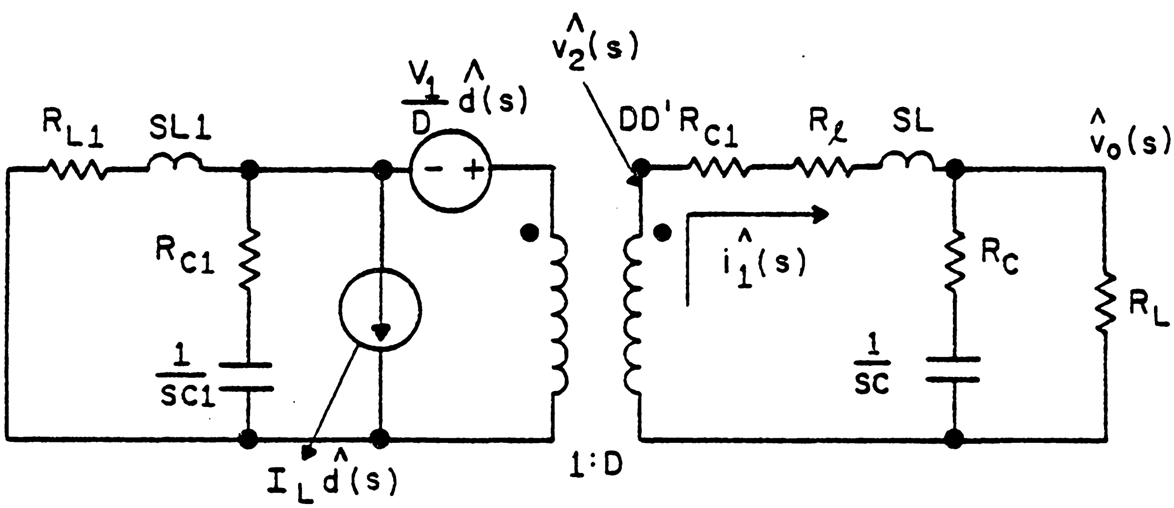


Figure 30: Small signal equivalent circuit with $\hat{v}_I = 0$

$$F_{42} = \frac{ZV_o[a_1 + R_L(1 + sCR_L)]}{(R_{L1} + sL1)R_L}$$

where $\Delta$ and $a_1$ are as defined in equation (5-7) and

$$V_1 \simeq \frac{V_o}{D}$$

$$R_{C1} \simeq 0 \qquad (5-12)$$

5.2.2 Feedback Transfer Functions

Transfer functions $F_3$, $F_{AC}$, $F_M$ and $F_{DC}$ constitute the feedback. A two loop standardized control module (SCM) controlled [2,7,8] buck regulator was used to obtain experimental results that are discussed later in this dissertation. The buck regulator used is shown in Figure 31 , and with reference to that figure the following are defined [2,7,8] :

$$F_3 = snL$$

$$F_{AC} = \frac{1}{sC_1' R_4}$$

$$F_{DC} = \frac{1}{sC_1'}\left(\frac{g}{R_{14} + R_x} + \frac{1}{Z_C}\right) \qquad (5-13)$$

$$R_x = R_{11}//R_{12} \ , \ g = \frac{R_x}{R_{11}}$$

$$Z_C = R_{13} + \frac{1}{sC_2}$$

$$F_M = \frac{2R_4C_1'}{nM} \quad \text{(Pulse Modulator Transfer Function)}$$

M = Constant depending on the type of control used.

## 5.3 DESIGN OF THE FEEDFORWARD LOOP.

The transfer function $\hat{v}_0/\hat{v}_x$ is used to design the feedforward. With $\hat{v}_1 = 0$ the following equations are derived from Figure 28 :

$$[\hat{v}_x + c_2\hat{v}_{C1} + c_3\hat{i}_{L1}]F_M = \hat{d} \tag{5-14}$$

and

$$\begin{aligned} \frac{\hat{d}F_{12}}{\Delta} &= \hat{v}_o \\ \hat{v}_{C1} &= \frac{\hat{d}F_{32}}{\Delta} \\ \hat{i}_{L1} &= \frac{\hat{d}F_{42}}{\Delta} \end{aligned} \tag{5-15}$$

Substituting for $\hat{v}_{C1}$, $\hat{i}_{L1}$ and $\hat{d}$ from (5-15) in (5-14) results in

$$\frac{\hat{v}_o}{\hat{v}_x} = \frac{(\frac{F_{12}}{\Delta})F_M}{1 - c_2(\frac{F_{32}}{\Delta})F_M - c_3(\frac{F_{42}}{\Delta})F_M} \tag{5-16}$$

In the absence of feedforward i.e. with $c_2 = c_3 = 0$ it can be seen that:

$$\frac{\hat{v}_o}{\hat{v}_x} = \frac{V_o(R_L - D^2Z)(1 + sCR_c)F_M}{a_1 + D^2Z(1 + sCR_L)} \tag{5-17}$$

The effect of peaking of the output impedance of the input filter Z is to cause a reduction in the term $(R_L - D^2Z)$ and also an increase in the denominator, thus resulting in a substantial loss of loop gain.

With feedforward the detrimental effect of peaking of Z could be avoided by a proper choice of the feedforward loop gains $c_2$ and $c_3$. Choosing

$$c_2 = \frac{-D^2}{V_oF_M} \tag{5-18}$$

$$c_3 = 0$$

leads to

$$\frac{\hat{v}_o}{\hat{v}_x} = \frac{\dfrac{V_oF_M(R_L - D^2Z)(1 + sCR_c)}{D\Delta}}{1 + \dfrac{D^2}{V_oF_M}F_M\left\{\dfrac{-ZV_o[a_1 + R_L(1 + sCR_L)]}{R_L\Delta}\right\}} \tag{5-19}$$

which can be simplified to

$$\frac{\hat{v}_o}{\hat{v}_x} = \frac{V_o F_M (R_L - D^2 Z)(1 + sCR_c) R_L \Delta}{D \Delta a_1 (R_L - D^2 Z)} \qquad (5\text{-}20)$$

Cancellation of the two terms leads to

$$\frac{\hat{v}_o}{\hat{v}_x} = \frac{V_o F_M (1 + sCR_c) R_L}{D a_1} \qquad (5\text{-}21)$$

Thus a proper choice of the feedforward loop gains has resulted in the transfer function $\hat{v}_0/\hat{v}_x$ being completely independent of the input filter output impedance Z. It is also noted from equations (5-11) and (5-16) that at frequencies other than the resonant frequencies at which Z peaks, the gain of $F_{32}$ is fairly small since Z would be small at those frequencies. Thus the addition of feedforward would not affect, in any noticable manner, the open loop gain and phase margin at any frequency other than those at which Z peaks.

The following points regarding the feedforward loop design can be made:

1. It has been shown analytically that a proper choice of feedforward loop gains results in eliminating completely the effect of peaking of Z on the loop gain.

2. The gain $c_3 = 0$, thus the inductor current information is not needed, only the input filter capacitor voltage information is used.
3. The feedforward loop gains are independent of the input filter parameter values, and are free of any frequency dependent term.
4. The feedforward loop gains are independent of the type of feedback control used. The pulse modulator transfer function $F_M$ is, however, an integral part of the design and thus the compensation depends on the type of duty cycle control used. The feedforward loop design process is independent of the particular type of control used and thus the same design can be used for other types of control, for example for single loop control, current injected control and others.

## 5.4 IMPLEMENTATION OF FEEDFORWARD

The buck regulator used to obtain experimental results that are discussed later is shown in Figure 31 . The feedforward circuit processes the small signal variation across the input filter capacitor and adds this processed information to the feedback signal.

Two circuit implementations of the feedforward design were used in making measurements and they are discussed next.

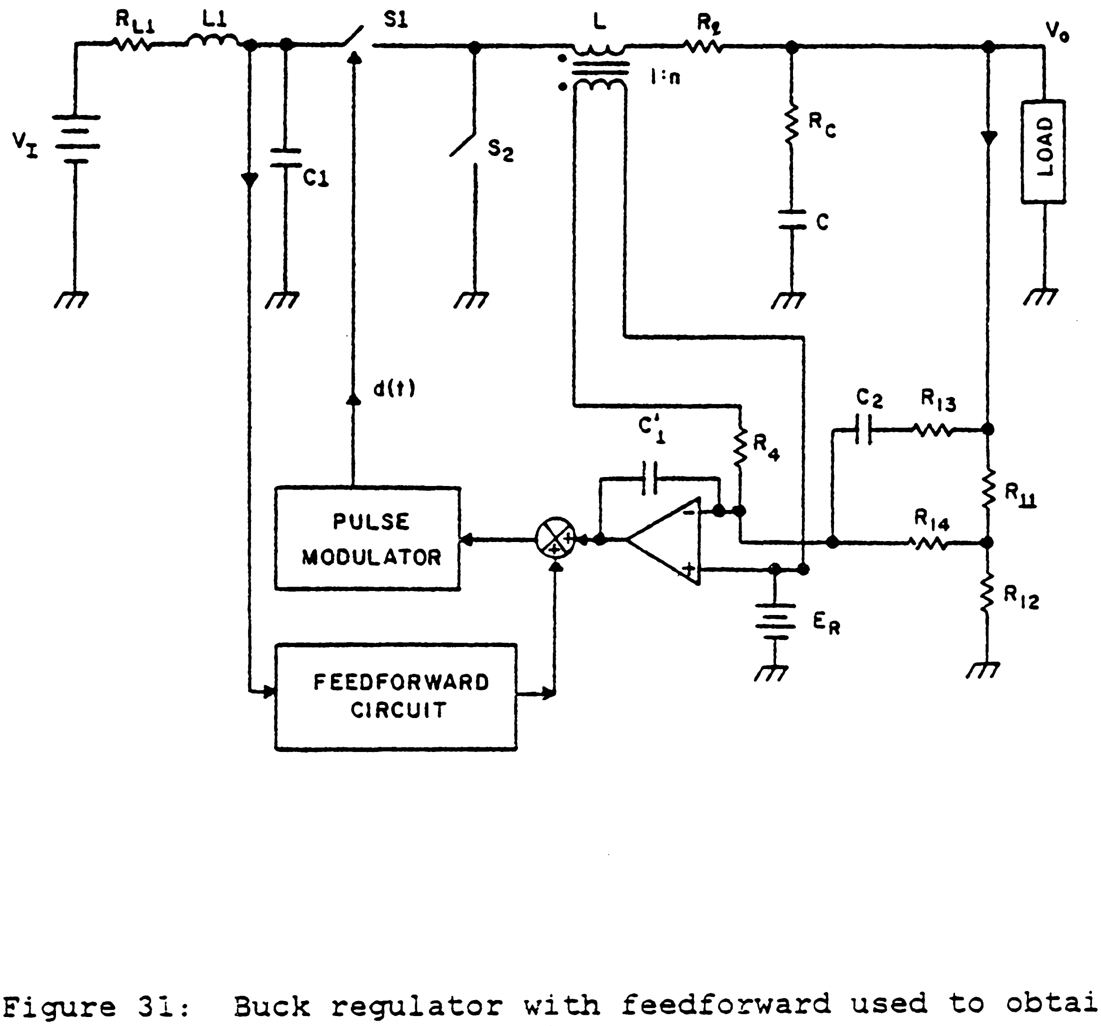


Figure 31: Buck regulator with feedforward used to obtain exprimental results

### 5.4.1 Nonadaptive Feedforward Circuit

It was shown earlier that the feedforward loop gain is

$$c_2(s) = -D^2/V_0 F_M \quad \text{, equation (5-18)}$$

The nonadaptive feedforward circuit was developed for the buck regulator of Figure 31 . The key parameters of the regulator are as follows -

Input-Output Parameters

$V_I$ = 25-40 volts   $V_O$ = 20 volts   $P_O$ = 40 watts

Power Stage Parameters

L = 230 micro H   C = 300 micro F   $R_\ell$ = 0.2 ohm

$R_C$ = 0.067 ohm (nominal)   $R_L$ = 20 ohm (load)

Pulse Modulator Parameters

$M = V_I T_{ON} = 0.88 * 10^{-3}$ V-sec

Control Circuit Parameters

$E_R$ = 6.7 volts   $R_{11}$ = 33.3 Kohm   $R_{12}$ = 16.7 Kohm

$R_{13}$ = 2 Kohm   $R_{14}$ = 47 Kohm   $R_4$ = 40.7 Kohm

n = 0.65   $C_1'$ = 5600 picoF   $C_2$ = 0.01 microF

The buck regulator was operated in a predetermined duty cycle control mode (constant $V_I T_{ON}$ control), [2,7,8]. Substituting for $F_M$, [2,8] and for D leads to

$$c_2(s) = \frac{-V_O nM}{2V_I^2 R_4 C_1'} \qquad (5\text{-}22)$$

where $M = V_I T_{ON}$ is constant.

For the nonadaptive design the input voltage was kept constant at $V_I = 30$ volts. Substituting in equation (5-22) it is calculated that $c_2(s) = -0.03$. The nonadaptive feedforward circuit implementation is shown in Figure 32 . The input to the circuit is the input filter capacitor voltage and a series capacitor (27 microF) blocks out the dc component. The input is then multiplied by the gain of 0.03 implemented by the 5.1 Kohm and 164 ohm resistances. The feedforward signal available at the potential devider network is then subtracted from the feedback signal available at the output of the integrator in the feedback loop. The result is then fed to the pulse modulator. The capacitor voltage fed into the operational amplifier subtracting circuit consists of two components - a small signal variation and a component corresponding to the switching frequency. The feedback signal is also at the switching frequency, but the amplitude of the feedback signal is large compared to the switching frequency information in the capacitor voltage, and thus the second component has negligible effect. It is to be noted that the circuit of Figure 32 constitutes the feedforward circuit and also the summing junction shown in Figure 31 .

The nonadaptive circuit has the advantage of being extremely simple and easy to implement. The gain of the potential devider in the feedforward circuit is, however, a function of supply voltage and thus the circuit of Figure 32 cannot be used at any other value of supply voltage. Measurements made using this circuit are discussed in the next chapter.

### 5.4.2 Adaptive Feedforward Circuit

The adaptive feedforward circuit is shown in Figure 33 . From equation (5-22) it is clear that changes in supply voltage $V_I$ will change the gain $c_2$ of the feedforward loop, the circuit of Figure 33 implements the feedforward of equation (5-22) and adjusts the gain automatically as $V_I$ changes.

The input voltage in Figure 33 is allowed to vary between 25v and 40v. It is fed to a voltage devider and then squared. The input filter capacitor voltage consists of a large dc component and this is blocked out by the 27 microF capacitor in series with the feedforward path. The small signal variation and the small magnitude component at switching frequency are then devided by the squared input voltage. A pair of resistances provides the final gain; the

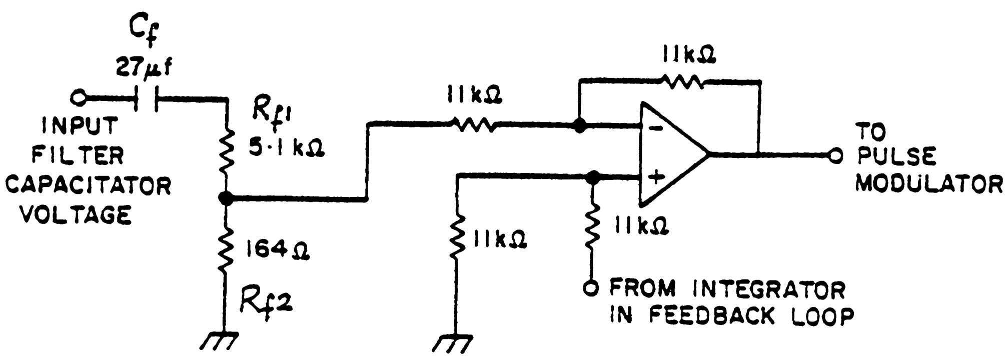


Figure 32: Nonadaptive Feedforward Circuit

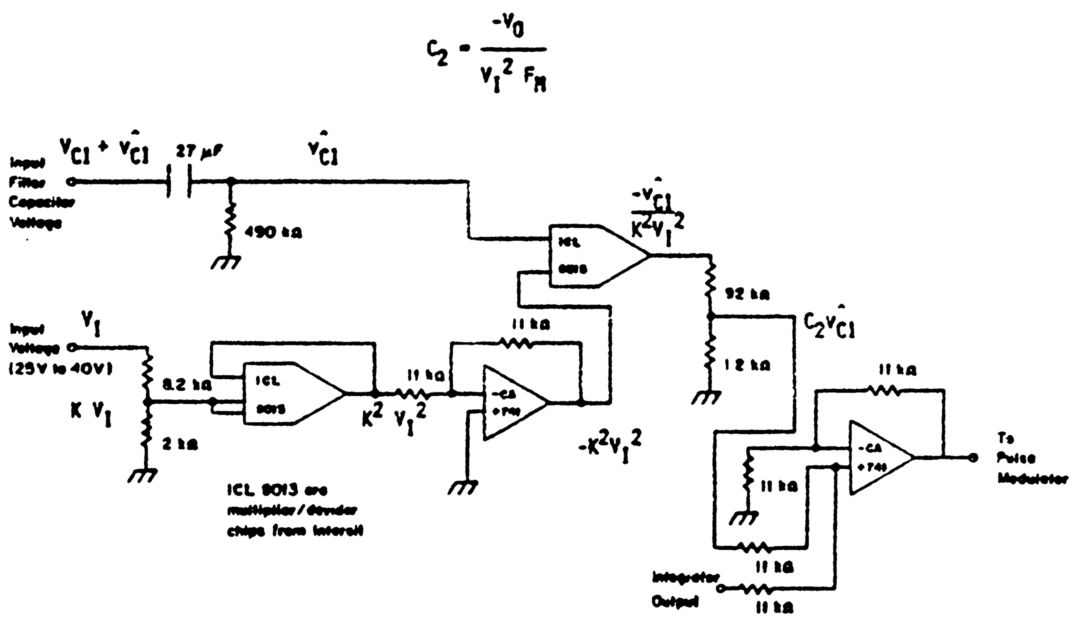


Figure 33: Adaptive feedforward implementation for a variable voltage supply.

feedforward signal now available is then added to the feedback signal at the output of the integrater. As for the nonadaptive circuit the switching frequency component in the input filter capacitor voltage is small compared to the corresponding component in the feedback signal and thus its effect on the duty cycle implementation is negligible.

The gain of the feedforward circuit is thus a function of input voltage $V_I$ and is made adaptive to changes in $V_I$. The feedforward is thus capable of tracking any variations in supply voltage.

# Chapter VI

## ANALYTICAL AND EXPERIMENTAL VERIFICATION OF THE FEEDFORWARD DESIGN

This chapter presents extensive measurement data that was made to verify experimentally the feedforward design outlined earlier. The feedforward control was designed for a buck regulator and the same regulator is used in obtaining measurements.

Measurement data pertaining to the open loop gain and phase margin are presented first; data made using the adaptive feedforward circuit designed earlier confirm the adaptive nature of the circuit. The audiosusceptibility and output impedance measurements presented next show that the feedforward significantly improves performance in both categories. Lastly, measurements of transient response are included that show that the feedforward improves the transient response.

## 6.1 MEASUREMENTS OF THE NONADAPTIVE FEEDFORWARD CONTROL

The buck regulator with feedforward used to obtain experimental results is shown in Figure 34 , and is the same as that presented earlier in Chapter V. The parameters of the regulator are the same as given earlier in Chapter V with the single-stage input filter parameters specified as:

$R_{L1}$ = 0.2 ohm     L1 = 116 micro-H     C1 = 20 micro-F

The feedforward circuit used was the nonadaptive feedforward circuit for a fixed input voltage discussed in Chapter V, with $V_I$ = 30 V. The small signal open loop transfer function of the multiloop controlled buck regulator of Figure 34 without feedforward can be expressed as [2,7,8]

$$G_T(s) = F_{DC}F_M F_{12} + F_3 F_{AC} F_{22} F_M \qquad (6\text{-}1)$$

In equation (6-1) $F_{12}$ and $F_{22}$ are the power stage transfer functions, $F_{DC}$, $F_M$, $F_3$ and $F_{AC}$ are the feedback control loop transfer functions, as discussed in Chapter 5 (section 5.2). The peaking of the output impedance of the input filter, Z(s), affects the transfer functions $F_{12}$ and $F_{22}$ as is seen below:

$$F_{12} = \frac{V_O(R_L - D^2 Z)\ (1 + sCR_C)}{D[\ D^2 Z(\ 1 + sCR_L) + a_1]} \qquad (6\text{-}2)$$

$$F_{22} = \frac{V_O(R_L - D^2 Z)(\ 1 + sCR_L)}{DR_L[\ D^2 Z(\ 1 + sCR_L) + a_1]} \qquad (6\text{-}3)$$

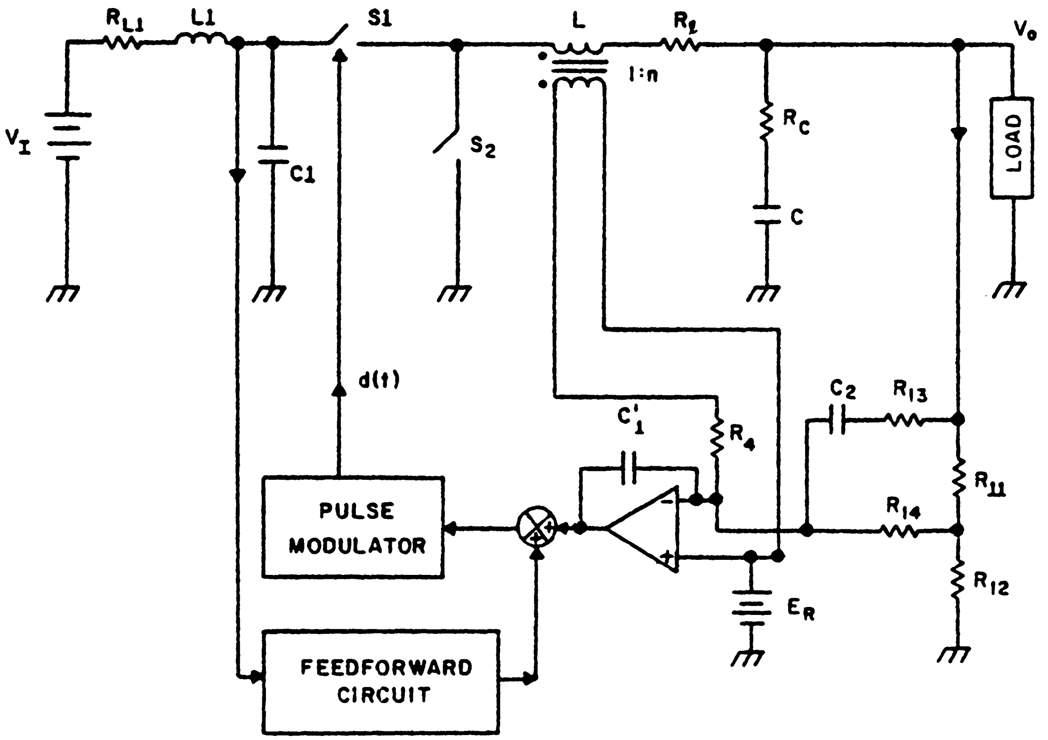


Figure 34: Buck regulator with feedforward used to obtain experimental results

The peaking of Z(s) reduces the gain of both $F_{12}$ and $F_{22}$ and thus reduces the open loop gain at the resonant frequency of the input filter.

The addition of the feedforward loop modifies the open loop transfer function as shown below --

$$G'_T(s) = \frac{F_{DC}F_M V_O R_L(1 + sCR_C)}{D\ a_1} + \frac{F_3 F_{AC} F_M V_O(1 + sCR_L)}{D\ a_1} \qquad (6\text{-}4)$$

The addition of feedforward modifies the transfer functions $F_{12}$ and $F_{22}$ and thus it can be seen from equation (6-4) that the open loop gain with feedforward is not affected by the peaking of the input filter output impedance Z(s). $G'_T(s)$ is now independent of Z(s) and is a function only of the feedback loop parameters and the power stage parameters, unlike $G_T(s)$ of equation (6-1) which is affected by the peaking of Z(s). Equation (6-4) is also the open loop gain of the buck regulator without input filter, as can be seen from equations (6-1), (6-2) and (6-3) by setting Z(s) = 0, and it can thus be concluded that the addition of the feedforward loop should eliminate completely the peaking effect of the input filter output impedance and that the open loop gain with feedforward should be identical with the open loop gain without the input filter [10,11].

SINGLE STAGE INPUT FILTER

Measurements of the open loop gain and phase margin of the buck regulator of Figure 34 were made with and without feedforward, and are presented in Figure 35 (a) and (b). The input filter resonates at around 3 KHz and results in disturbances in the open loop gain and phase margin at that frequency. The feedforward eliminates all these undesirable disturbances as is evident in the figures, thus providing close agreement with theory. It can also be seen from Figure 35 that the characteristics with feedforward are almost identical to the gain and phase margin plots of the buck regulator without input filter, thus providing close agreement with the analytical prediction made earlier.

TWO-STAGE INPUT FILTER

The experiment was further extended to the buck regulator with a two-stage input filter. The two-stage filter of Figure 36 was used with the following parameter values:

$R_1$= 0.2 ohm    $L_1$= 325 micro H    $C_1$= 200 micro F

$R_2$= 0.02 ohm    $L_2$= 116 micro H    $C_2$= 20 micro F

$R_3$= 0.075 ohm (ESR of $C_1$).

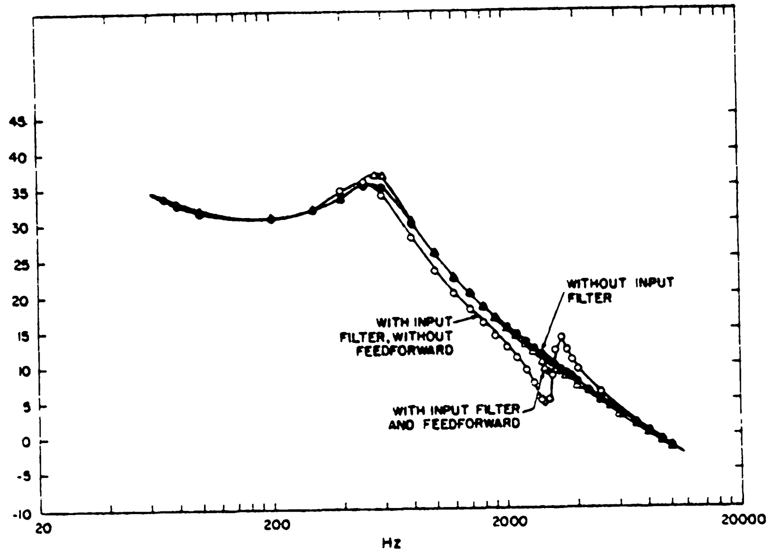


(a)

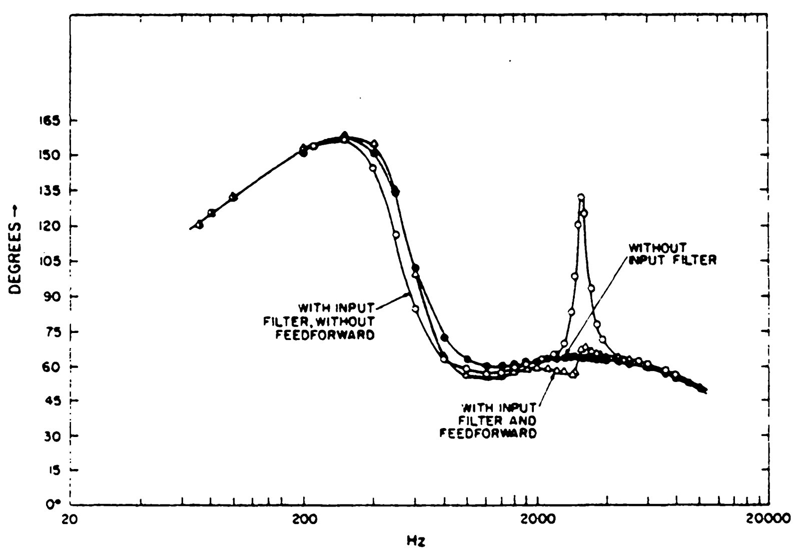


(b)

Figure 35: Open loop transfer function measurements with single-stage input filter. (a) gain (b) phase margin.

The feedforward circuit used was the same nonadaptive feed-forward circuit used to obtain the measurements of Figure 35 with the feedforward input being the voltage at capacitor $C_Z$. The other parameters of the circuit are the same as used to obtain Figure 35 . Measurements of the open loop gain and phase margin were made with and without feedforward and the results are shown in Figure 37 (a) and (b). The open loop gain and phase are affected at the resonant frequencies of the two stages of the input filter because the output impedance of the input filter Z(s) peaks at both resonant frequencies. The use of the feedforward circuit eliminates the detrimental effects of the input filter, as is evident from Figure 37 .

REMARKS

The following points regarding the above measurements are noteworthy:

(1) Measurements of the open loop gain and phase margin show that the input filter output impedance causes disturbances in the gain and phase margin at the filter resonant frequencies and the addition of feedforward eliminates these disturbances, providing close agreement with theory.

(2) The feedforward compensation circuit is independent of the input filter parameter values.

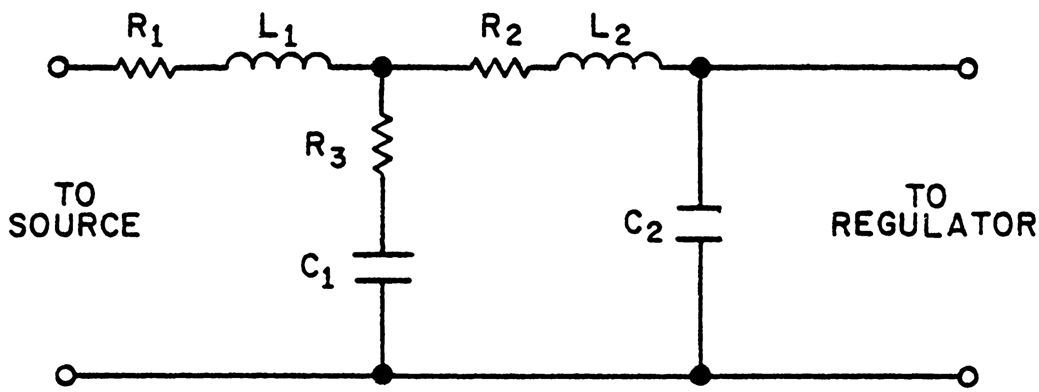


Figure 36: Two- stage input filter.

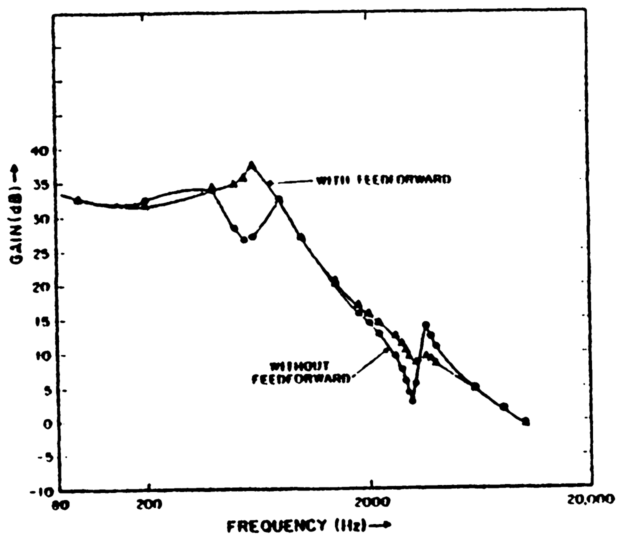


(a)

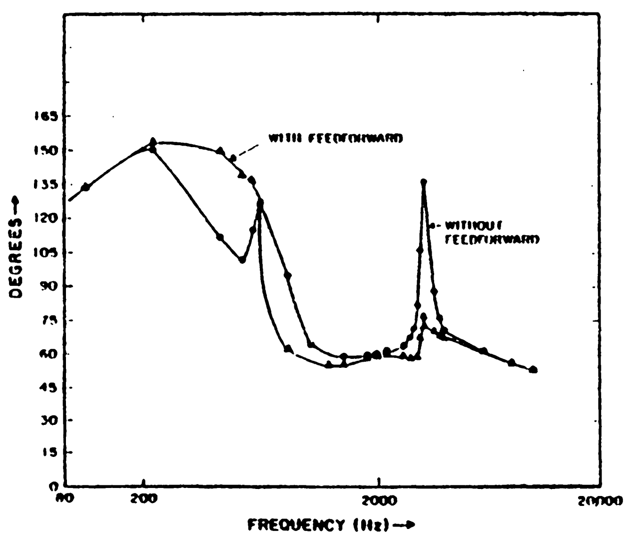


(b)

Figure 37: Open loop transfer function measurements with two-stage input filter. (a) gain (b) phase margin.

(3) The feedforward compensation scheme is independent of the input filter configuration. It was demonstrated above that the same feedforward compensation network is equally applicable to a single stage input filter and a two-stage input filter. These observations lead to a stronger conclusion that the feedforward can provide effective compensation for an unknown source impedance. For example, a preregulator which often has an unknown, dynamic output impedance can interact with a DC-DC converter downstream and result in system instability. The feedforward compensation scheme outlined can be used to isolate the switching converter from the source thus preventing interaction between the switching converter and equipment upstream.

## 6.2 ADAPTIVE FEEDFORWARD MEASUREMENTS.

The buck regulator with feedforward used to obtain experimental results is shown in Figure 34 and the parameters of the circuit are as specified in section 6.1. The adaptive feedforward circuit for variable input voltage presented in Chapter 5 was used in obtaining measurements .The two-stage input filter of Figure 36 was used with the same parameter values as in section 6.1 with the feedforward input being the voltage at capacitor $C_2$ . The value of $R_3$ was changed to-

$R_3$= 0.2 ohm (ESR of $C_2$ plus external damping resistance)

Measurements were obtained at four values of supply voltage using the same adaptive feedforward circuit in all cases - this was done to confirm the adaptive nature of the feedforward circuit.

A computer program was written to calculate the gain and phase margin of the open loop transfer function with and without two-stage input filter, at various input voltages. Equation (6-1) was used to calculate the gain and phase margin; setting Z(s) = 0 in the equation gives the gain and phase margin without input filter. The following expression for the two-stage input filter was used:

$$Z(s) = \frac{Z_1 + R_2 + sL_2}{1 + sC_2( Z_1 + R_2) + s^2 L_2 C_2} \qquad (6\text{-}5)$$

where

$$Z_1(s) = (R_1 + sL_1) \;//\; (R_3 + 1/sC_1) \qquad (6\text{-}6)$$

Figures 38 - 41 show the computed values of open loop gain and phase margin with and without the two-stage input filter for input voltages $V_I$ = 25v, 30v, 35v and 40v. It can be seen that the two-stage input filter resonates at two frequencies and at each frequency the output impedance Z(s) peaks, thus causing sharp fluctuations in the open loop gain and phase margin. Measurements of the open loop gain and phase margin at each of the above values of supply voltage were obtained with and without feedforward and are also plotted on the figures. It can be seen clearly that the addition of feedforward removes the sharp fluctuations in open loop gain and phase margin caused by the input filter, providing close agreement with theoretical prediction made earlier. The analytical prediction that the open loop gain and phase margin with feedforward are identical to the characteristics without input filter is also confirmed, as examination Figures 38 - 41 show.

The two stage input filter was modified so that $R_3$ = 0.075 ohm (ESR of $C_2$) and measurements of the open loop gain and phase margin with and without feedforward were made. Figure 42 shows the calculated values of open loop gain and phase margin together with the measured values at $V_I$ = 25v. With the external damping resistance set to zero the effect of the input filter is seen to be more pronounced. Measurements without feedforward shown plotted on the figure also show the pronounced effect of the input filter. The addition of feedforward effectively eliminates the sharp fluctuations in gain and phase margin caused by the undamped input filter.

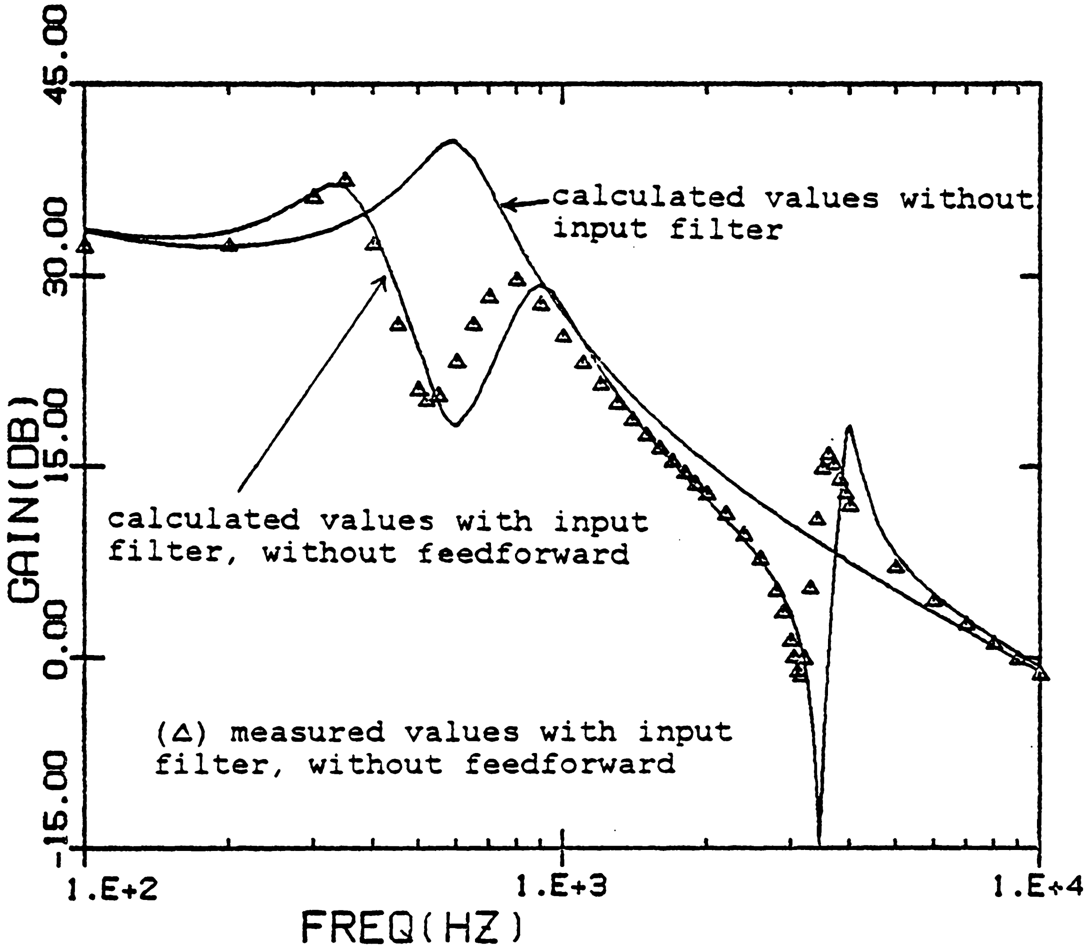


Figure 38: (a) Open loop gain at $V_I$=25v: Calculated values and measured values (Δ) without feedforward

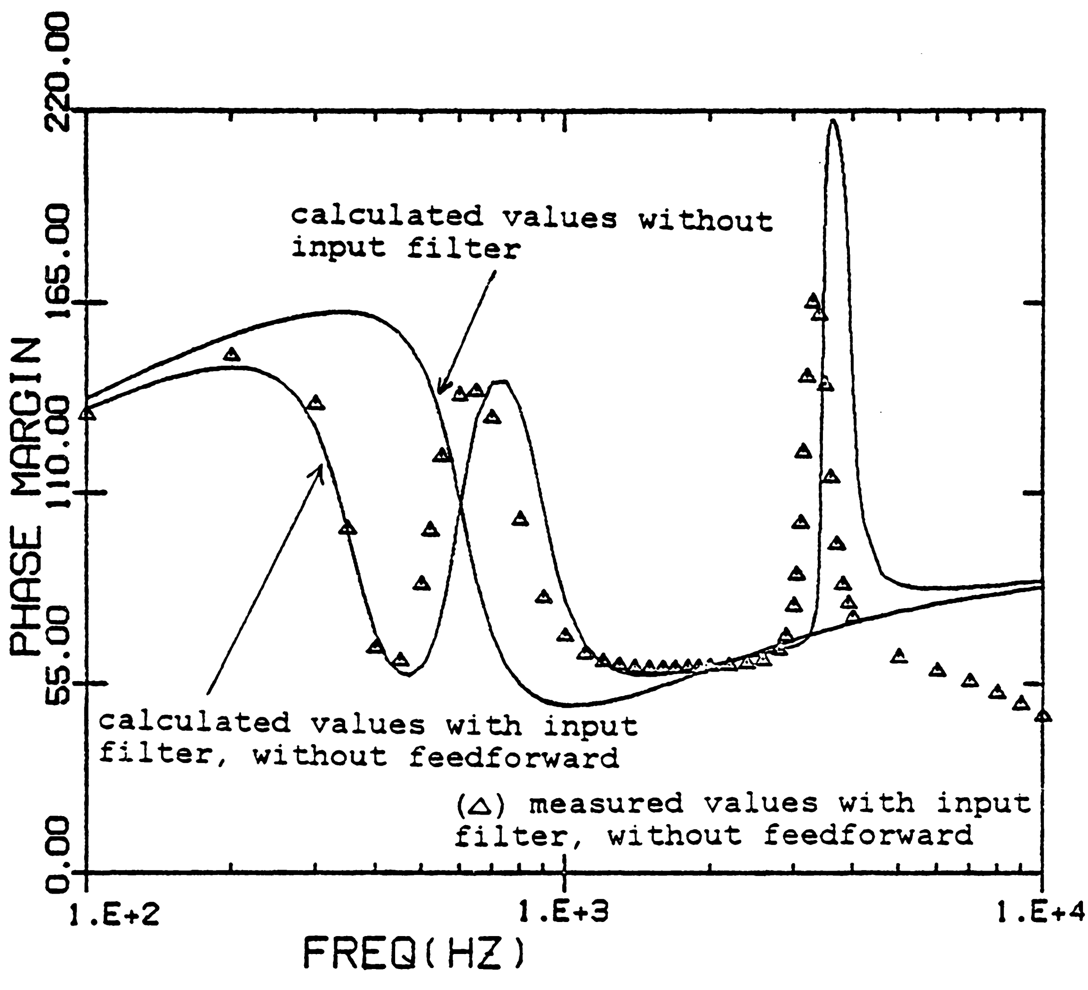


Figure 38: (b) Open loop phase margin at $V_I$ =25v: Calculated values and measured values (△) without feedforward

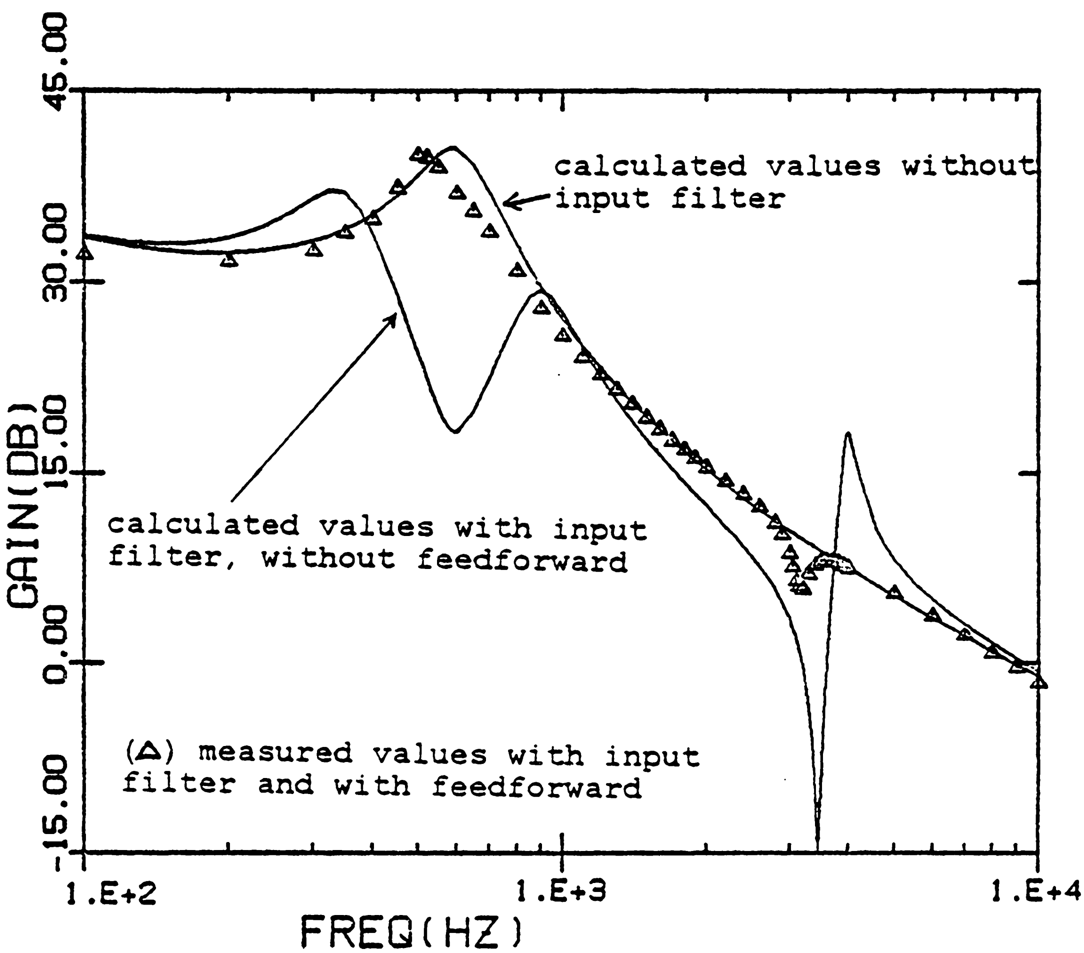


Figure 38: (c) Open loop gain at $V_I$=25v: Calculated values and measured values (△) with feedforward

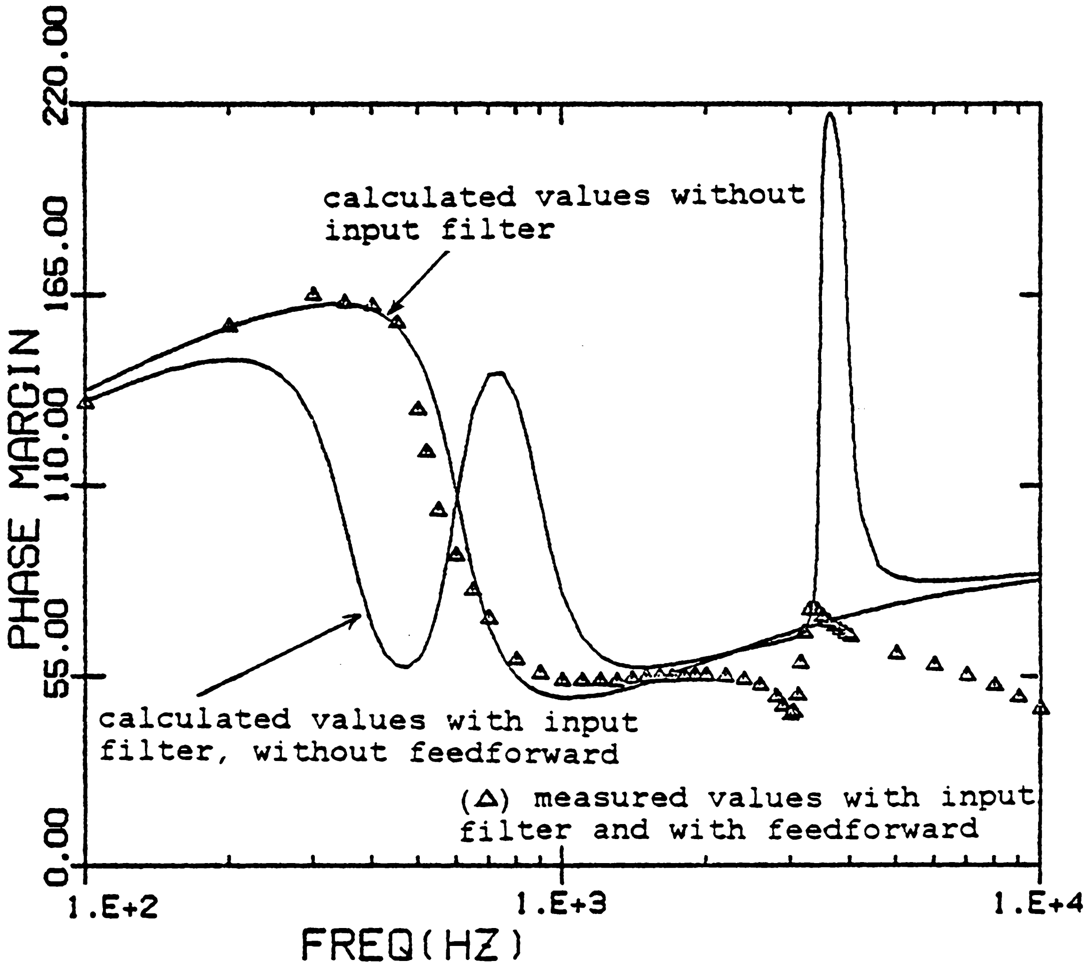


Figure 38: (d) Open loop phase margin at $V_I$=25v: Calculated values and measured values(Δ) with feedforward

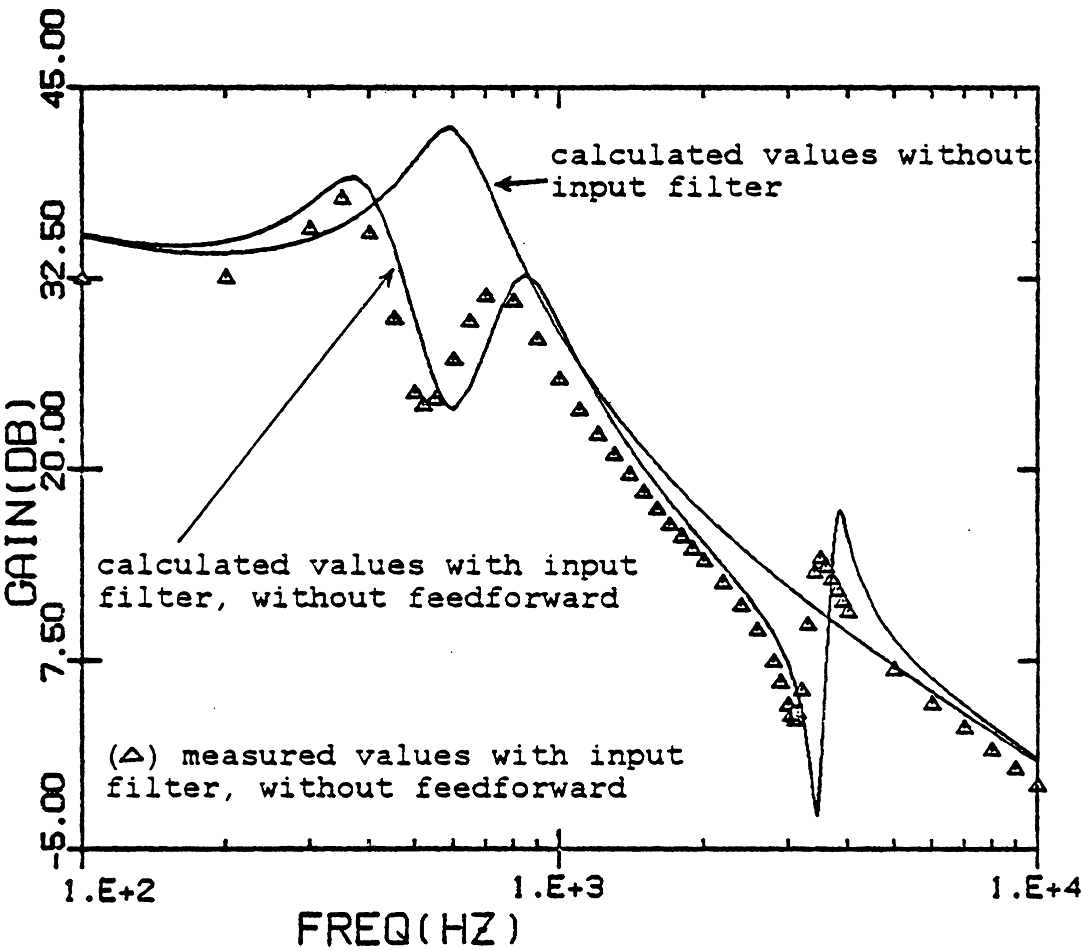


Figure 39: (a) Open loop gain at $V_I$=30v: Calculated values and measured values (△) without feedforward

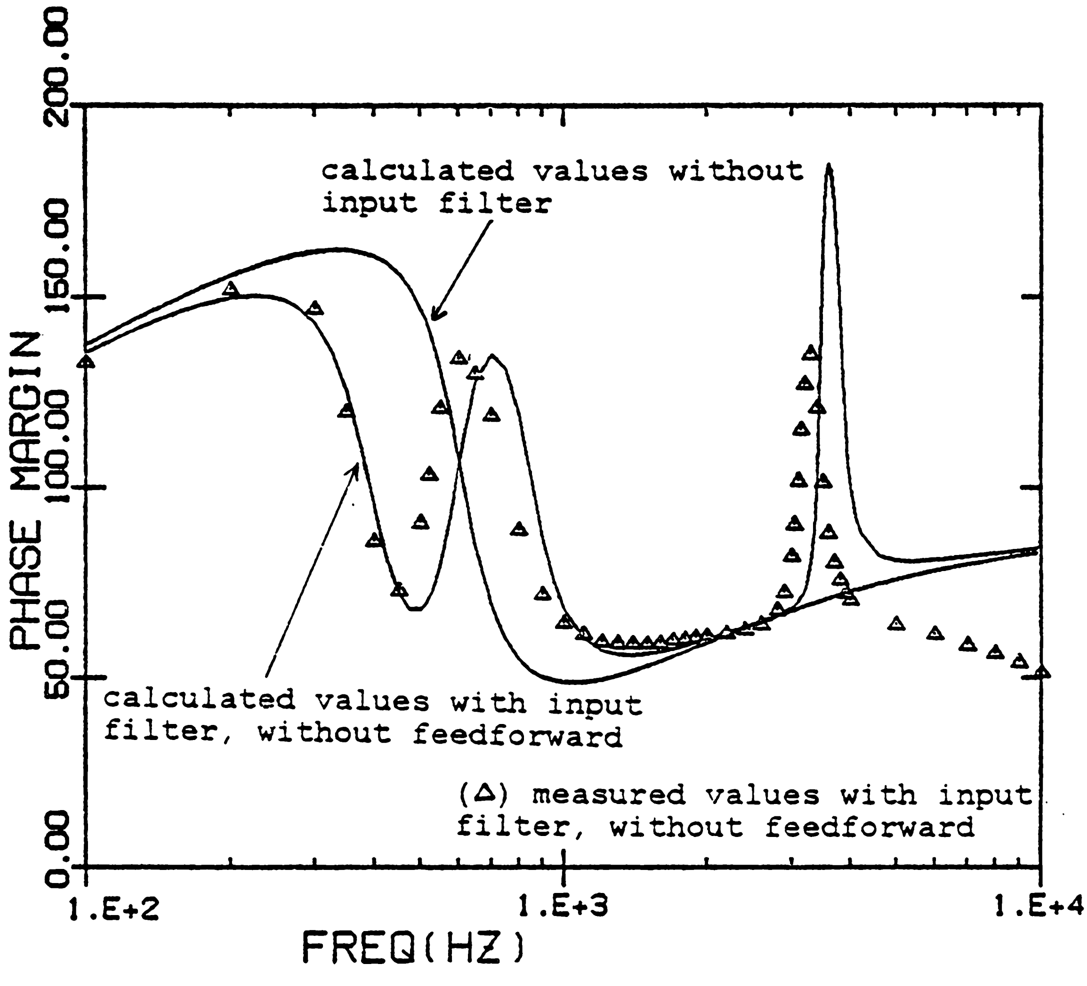


Figure 39: (b) Open loop phase margin at $V_I$=30v: Calculated values and measured values (Δ) without feedforward

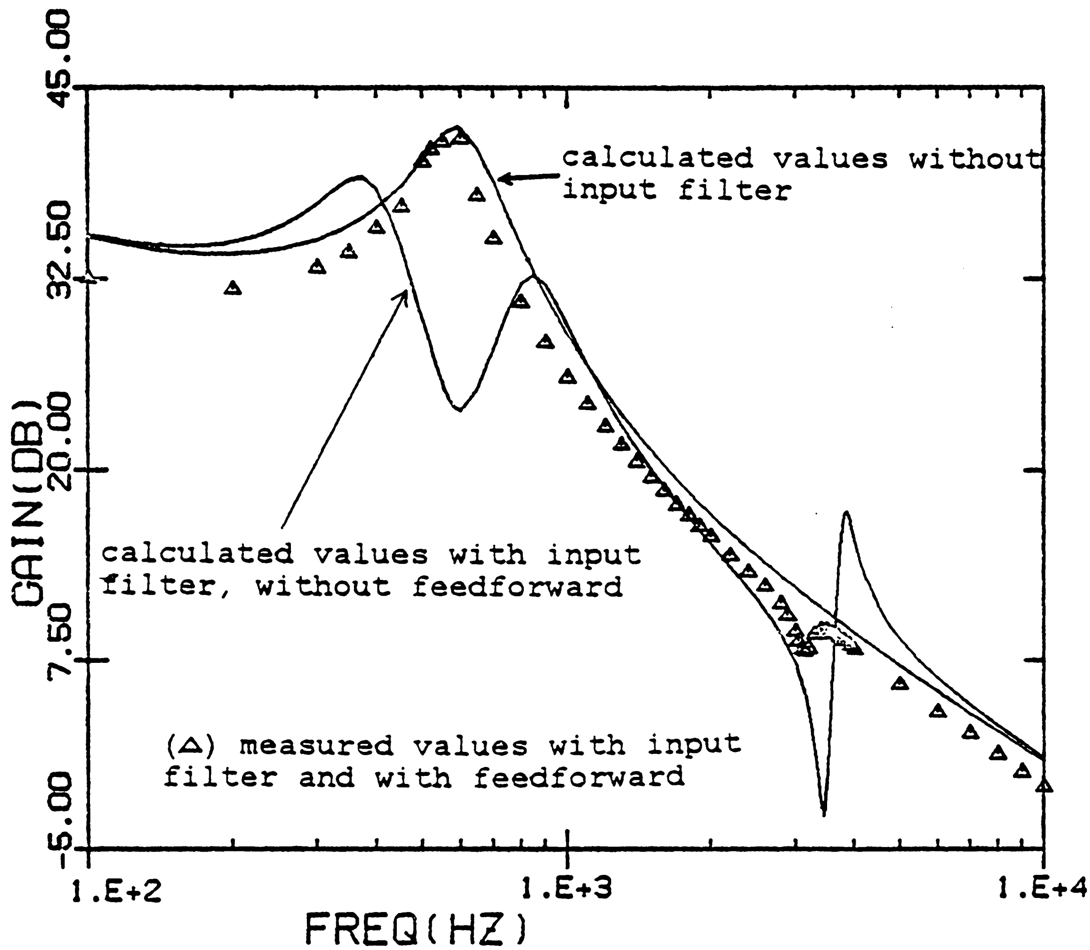


Figure 39: (c) Open loop gain at $V_I$ =30v: Calculated values and measured values (△) with feedforward

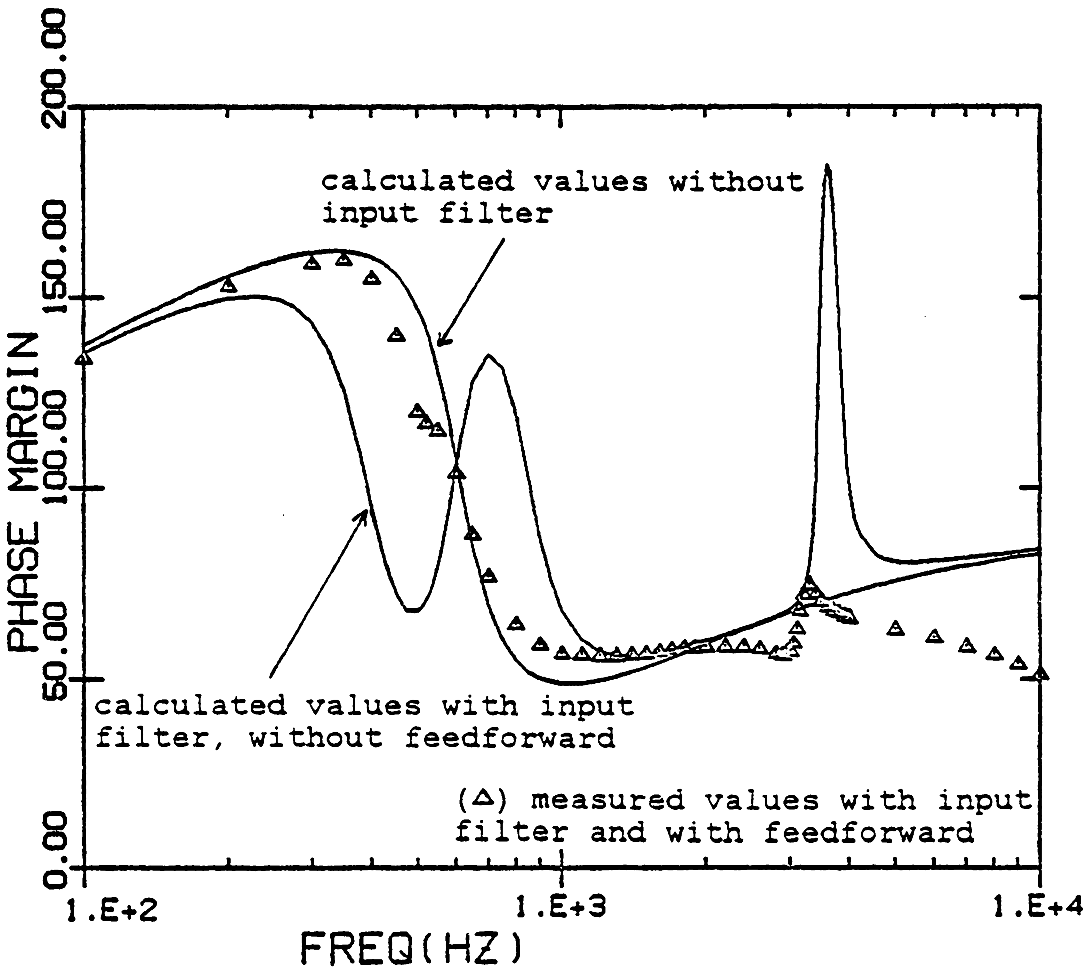


Figure 39: (d) Open loop phase margin at $V_I$=30v: Calculated values and measured values (△) with feedforward

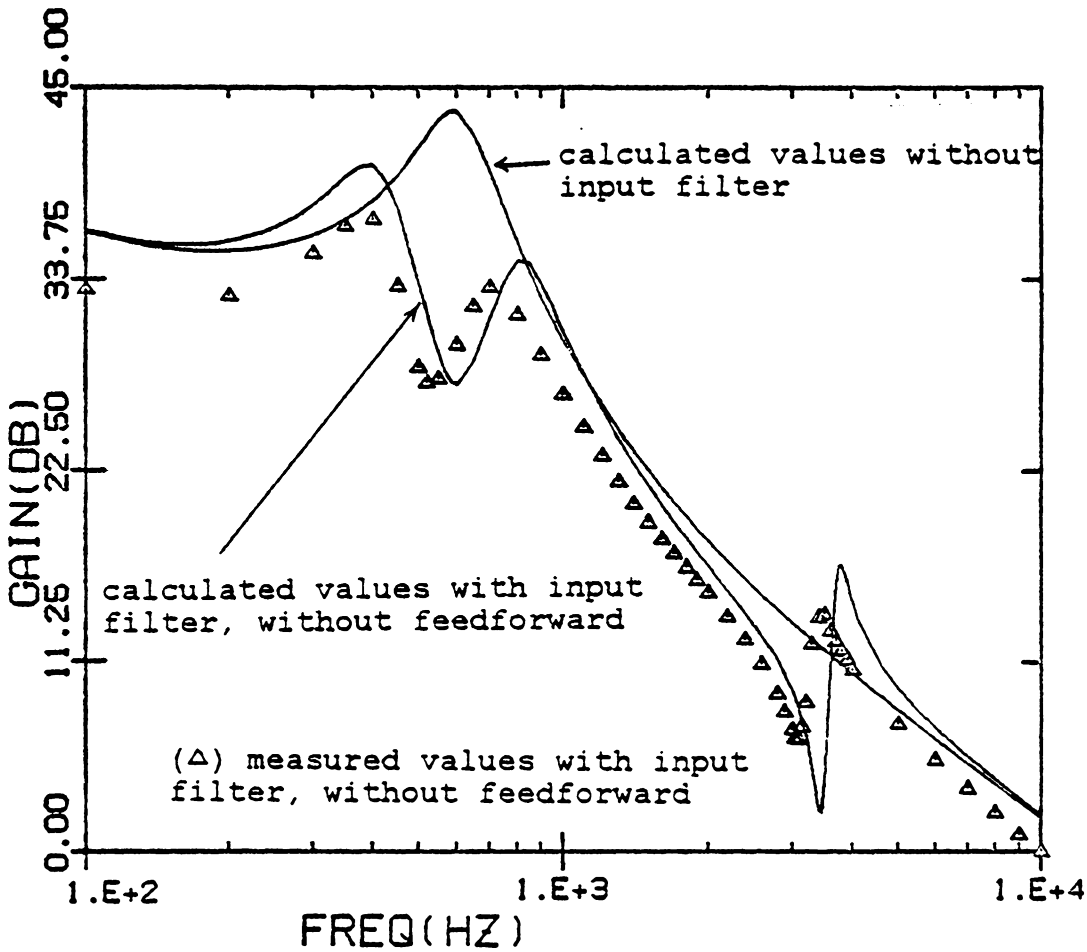


Figure 40: (a) Open loop gain at $V_I$=35v: Calculated values and measured values (△) without feedforward

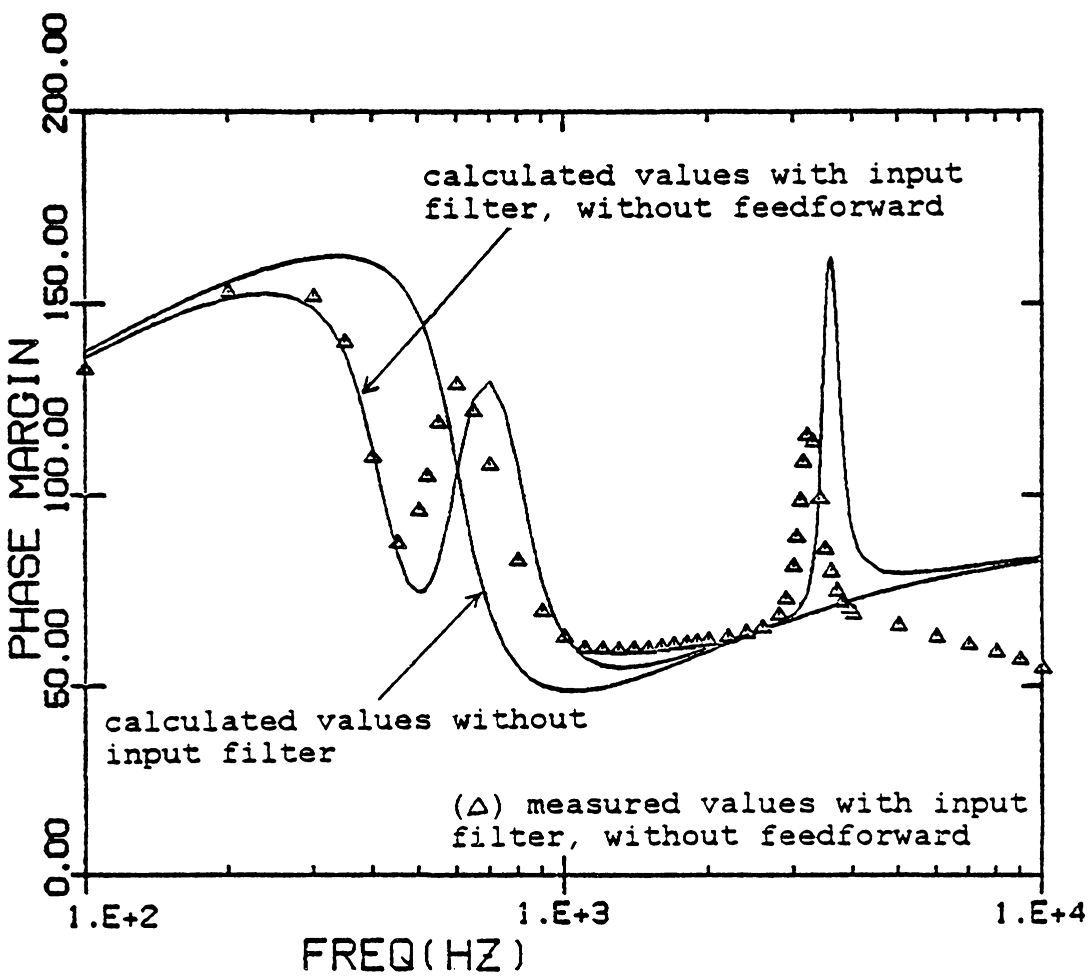


Figure 40: (b) Open loop phase margin at $V_I$=35v: Calculated values and measured values (Δ) without feedforward

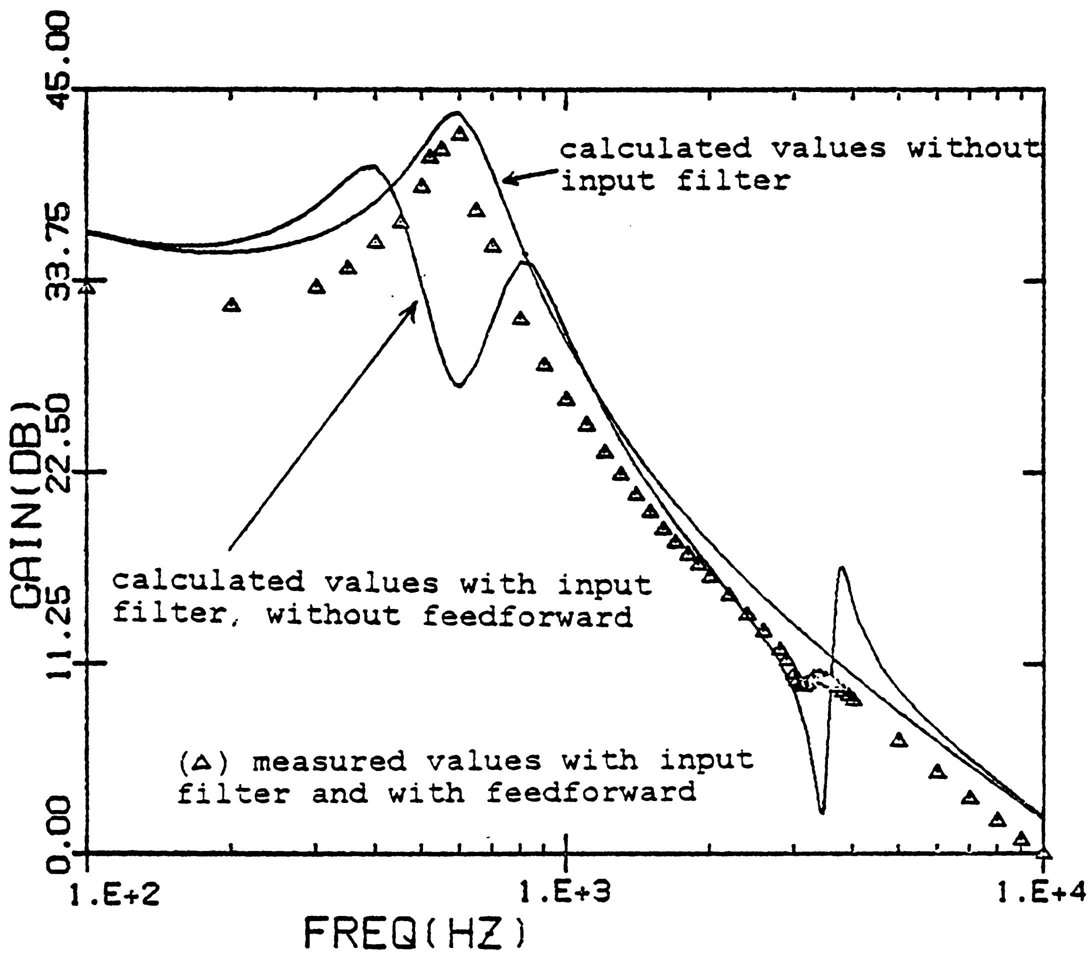


Figure 40: (c) Open loop gain at $V_I$ =35v: Calculated values and measured values (Δ) with feedforward

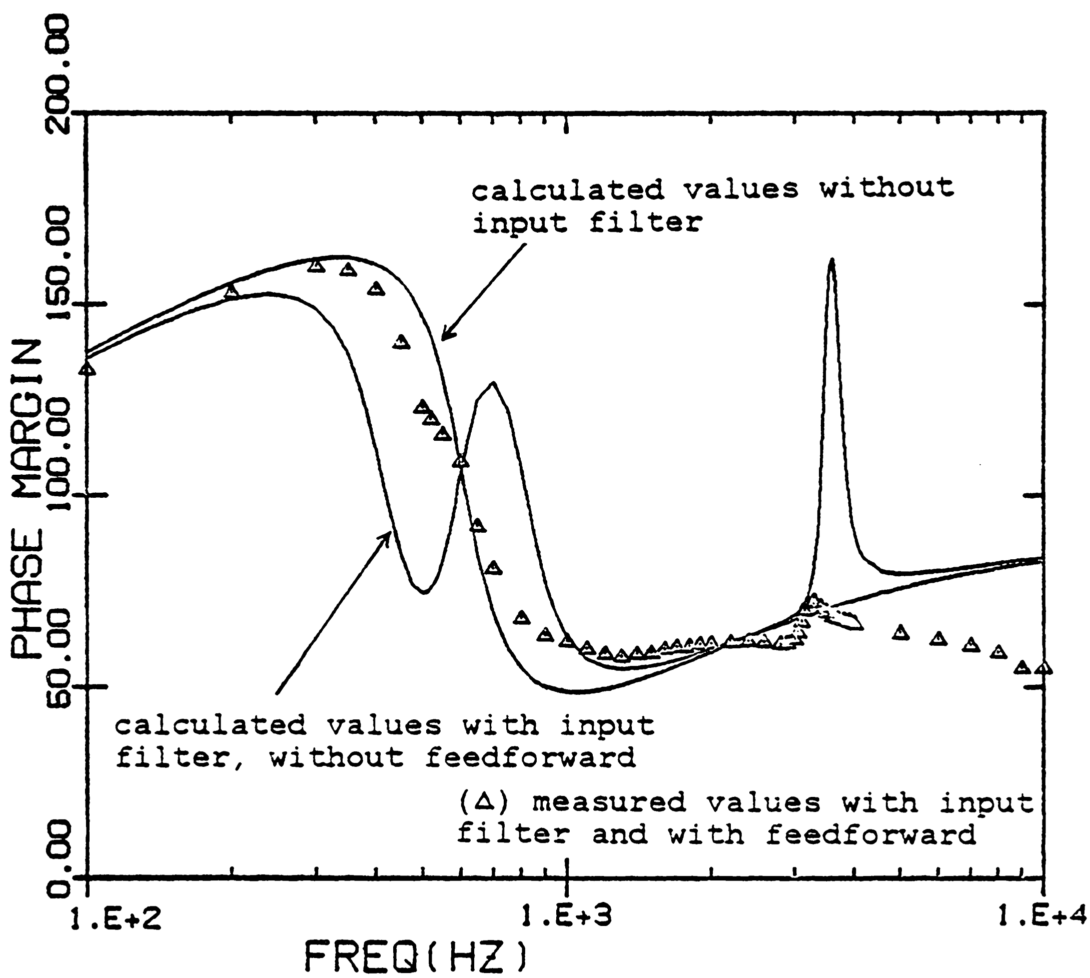


Figure 40: (d) Open loop phase margin at $V_I$ =35v: Calculated values and measured values (Δ) with feedforward

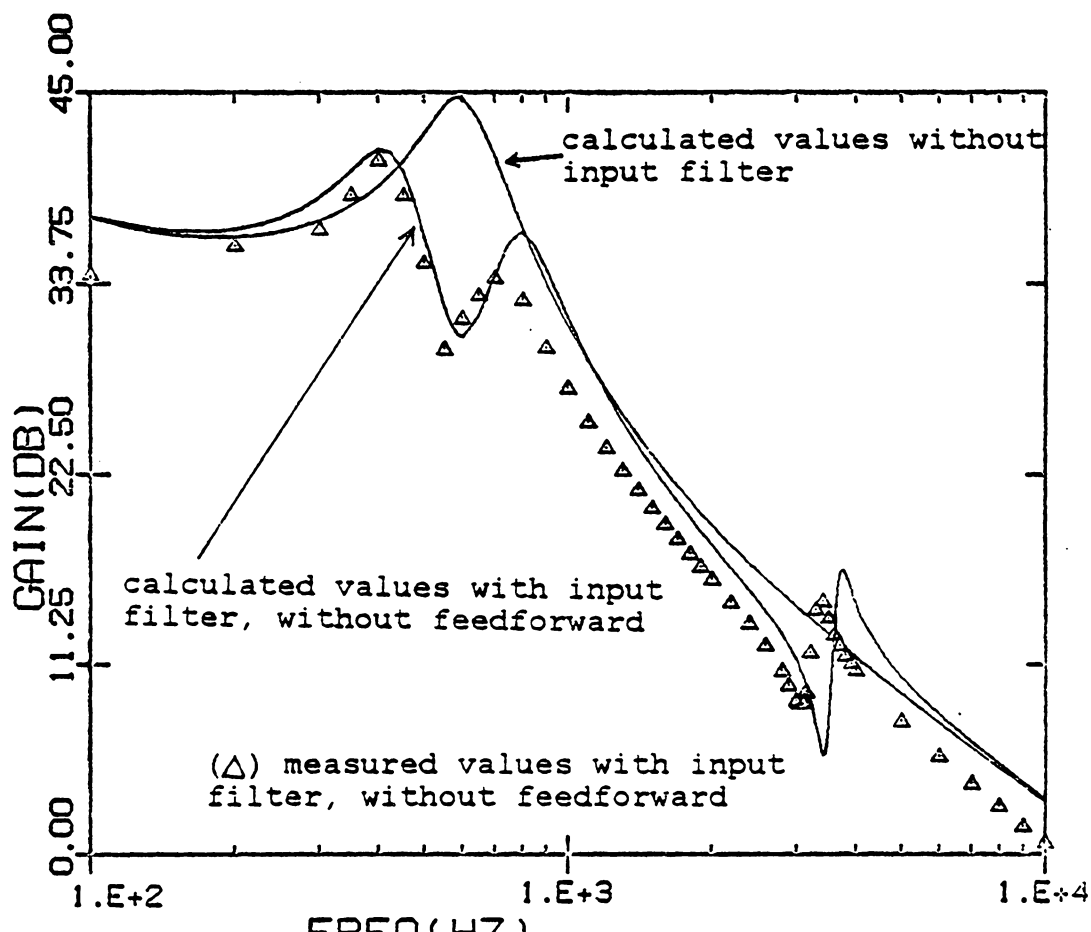


Figure 41: (a) Open loop gain at $V_I$=40v: Calculated values and measured values (△) without feedforward

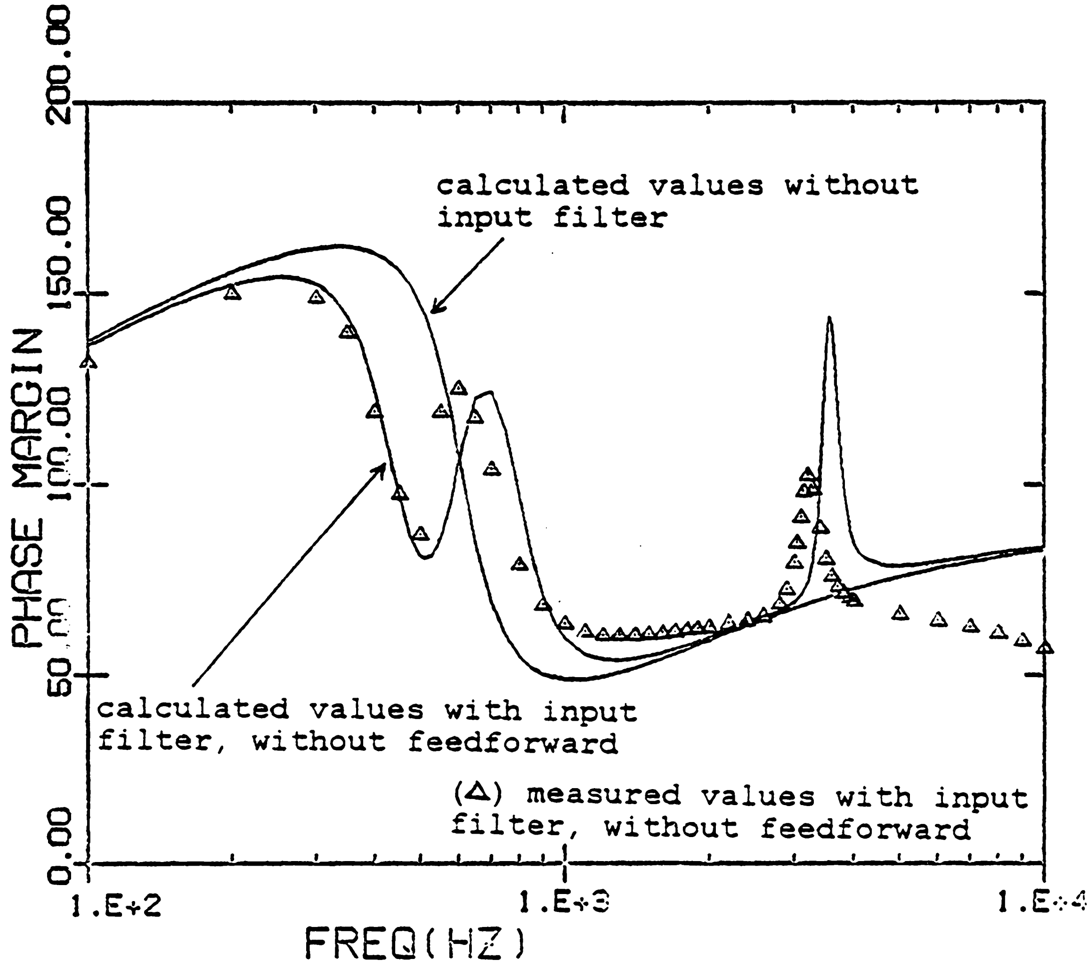


Figure 41: (b) Open loop phase margin at $V_I$=40v: Calculated values and measured values (Δ) without feedforward

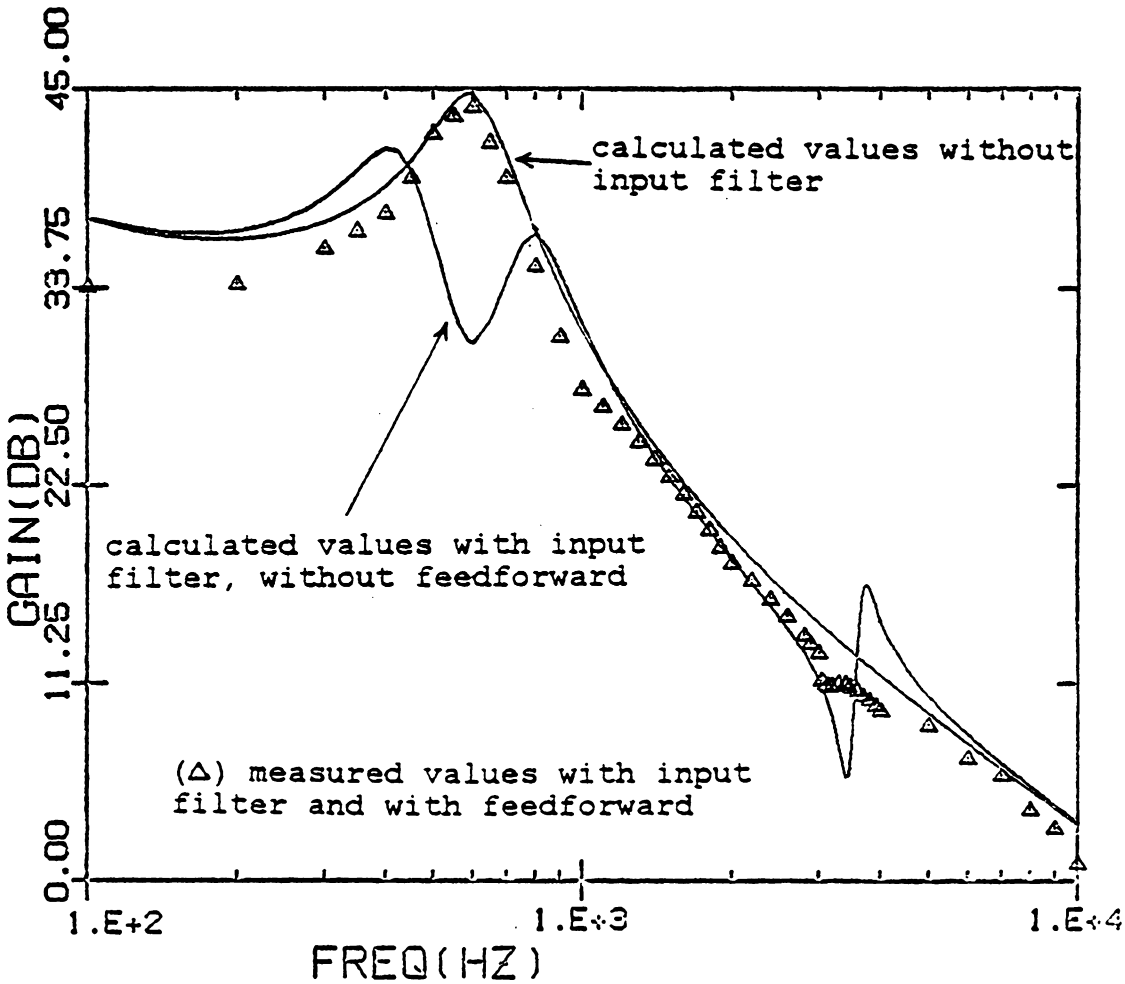


Figure 41: (c) Open loop gain at $V_I$=40v: Calculated values and measured values (Δ) with feedforward

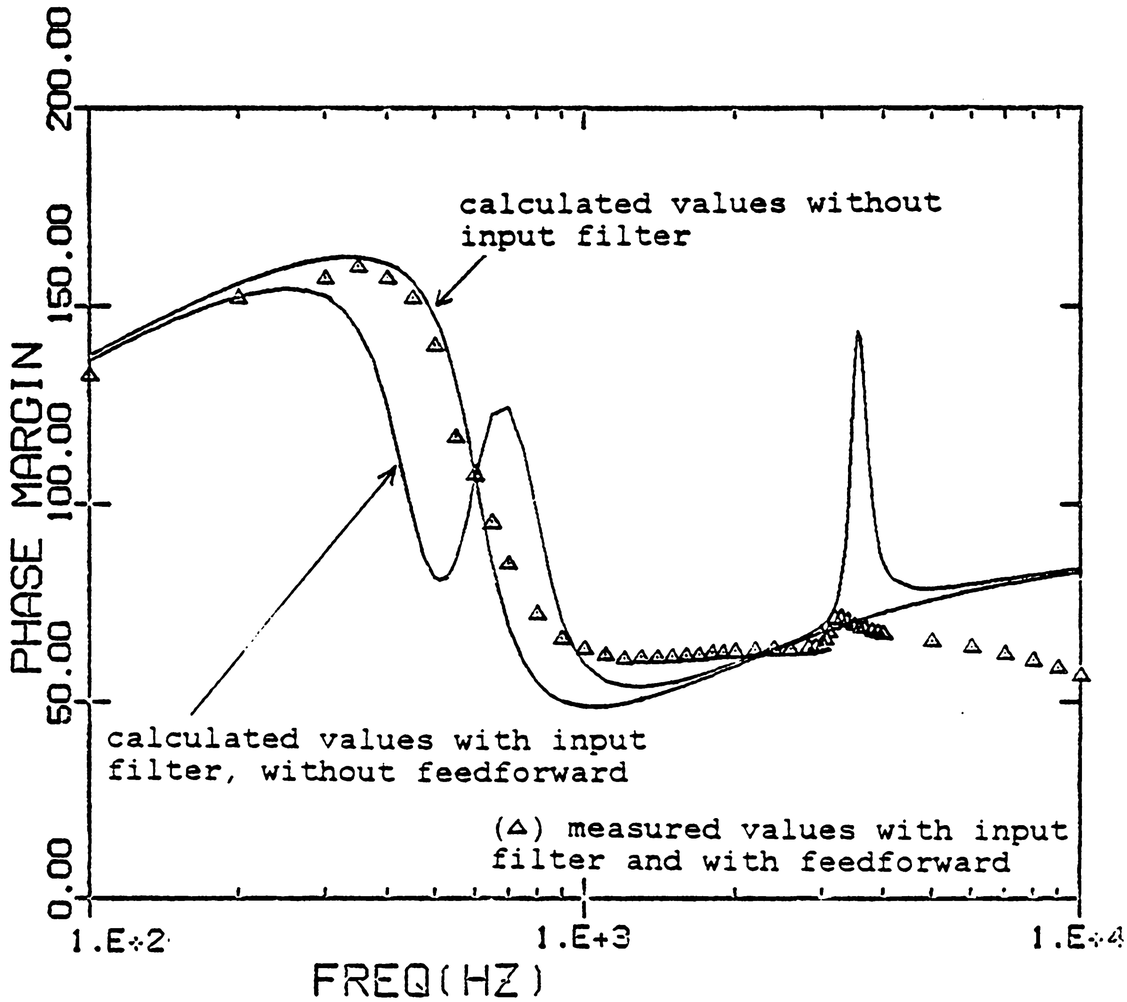


Figure 41: (d) Open loop phase margin at $V_I$ =40v: Calculated values and measured values (△) with feedforward

The following observations regarding the measurements are made:

(1) The peaking of the output impedance of the first stage is more pronounced and has a greater effect on the regulator than the peaking of the second stage.

(2) Both analysis and measurement results indicate that the open loop gain is higher at lower values of duty cycle D. This is further manifested by examining eqation (6-4). It shows that a lower value of D results in a higher gain.

(3) The effect of input filter peaking varies with the input voltage. This is explained by noting that both $F_{12}$ and $F_{22}$, equations (6-2) and (6-3) depend on the duty cycle D. The effect of peaking of Z(s) is to cause a reduction in the term $(R_L - D^2 Z)$ and the amount of reduction would be greater if D is larger. Consequently it is expected that at small values of $V_I$, when D is larger, the effect of peaking would be more pronounced. This is confirmed by examination of Figures 38 - 41 .

(4) The addition of the feedforward loop effectively eliminates the perturbation in open loop gain and phase caused by the input filter. The feedforward works effectively at all four values of supply voltage $V_I$ . Since the same feedforward circuit was used in making all the measurements of Figures 38 - 42 the adaptive nature of the feedforward circuit is confirmed.

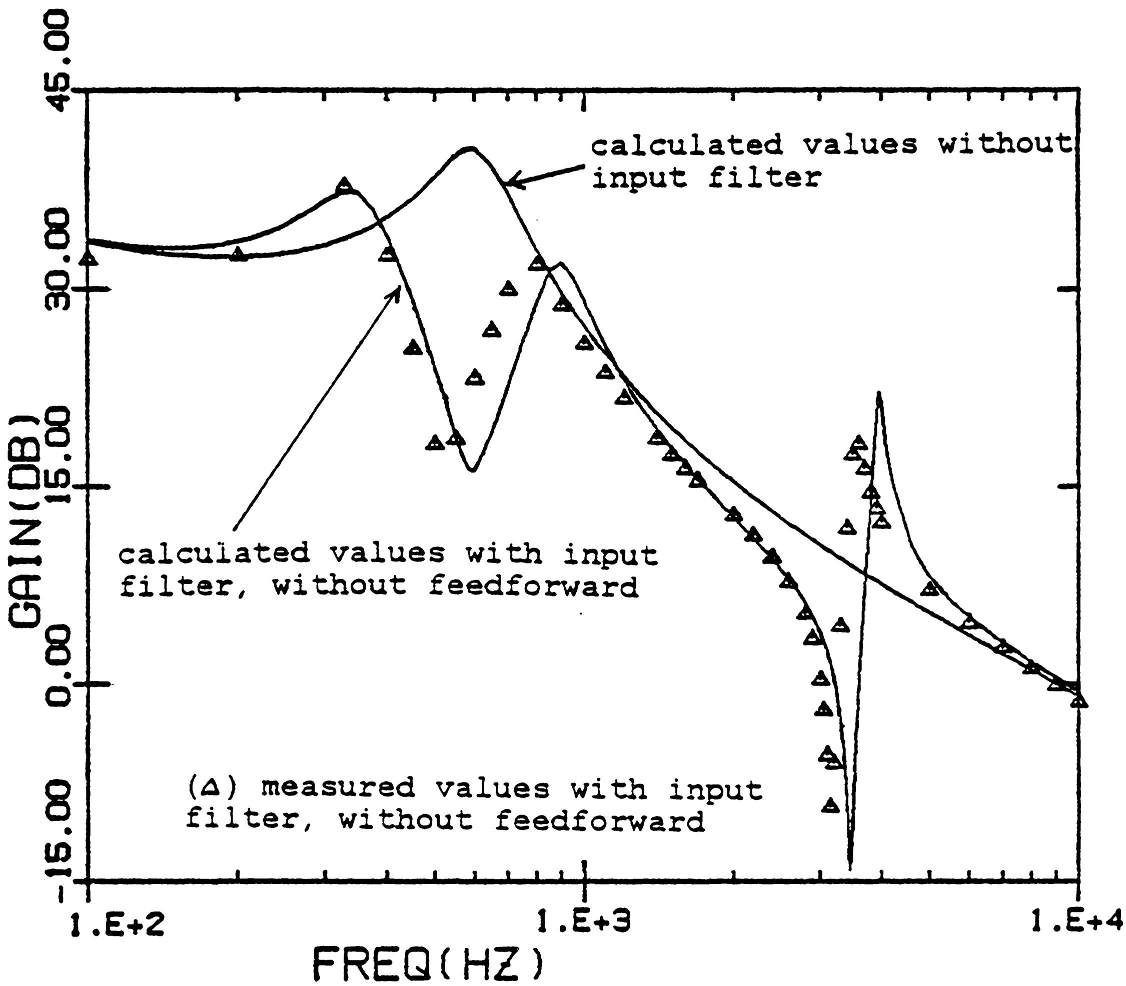


Figure 42: (a) Open loop gain at $V_I$=25v: Calculated values and measured values (Δ) without feedforward

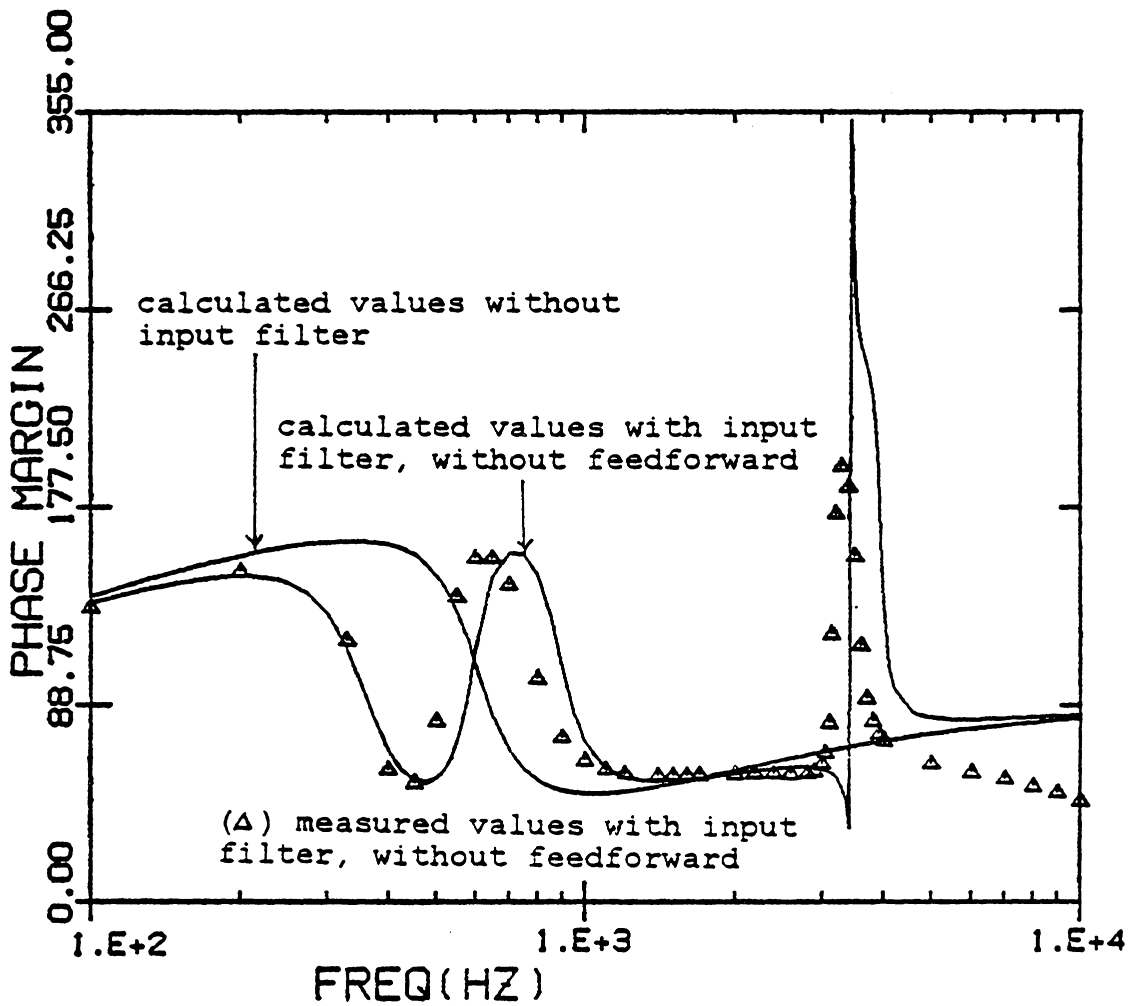


Figure 42: (b) Open loop phase margin at $V_I$=25v: Calculated values and measured values (Δ) without feedforward

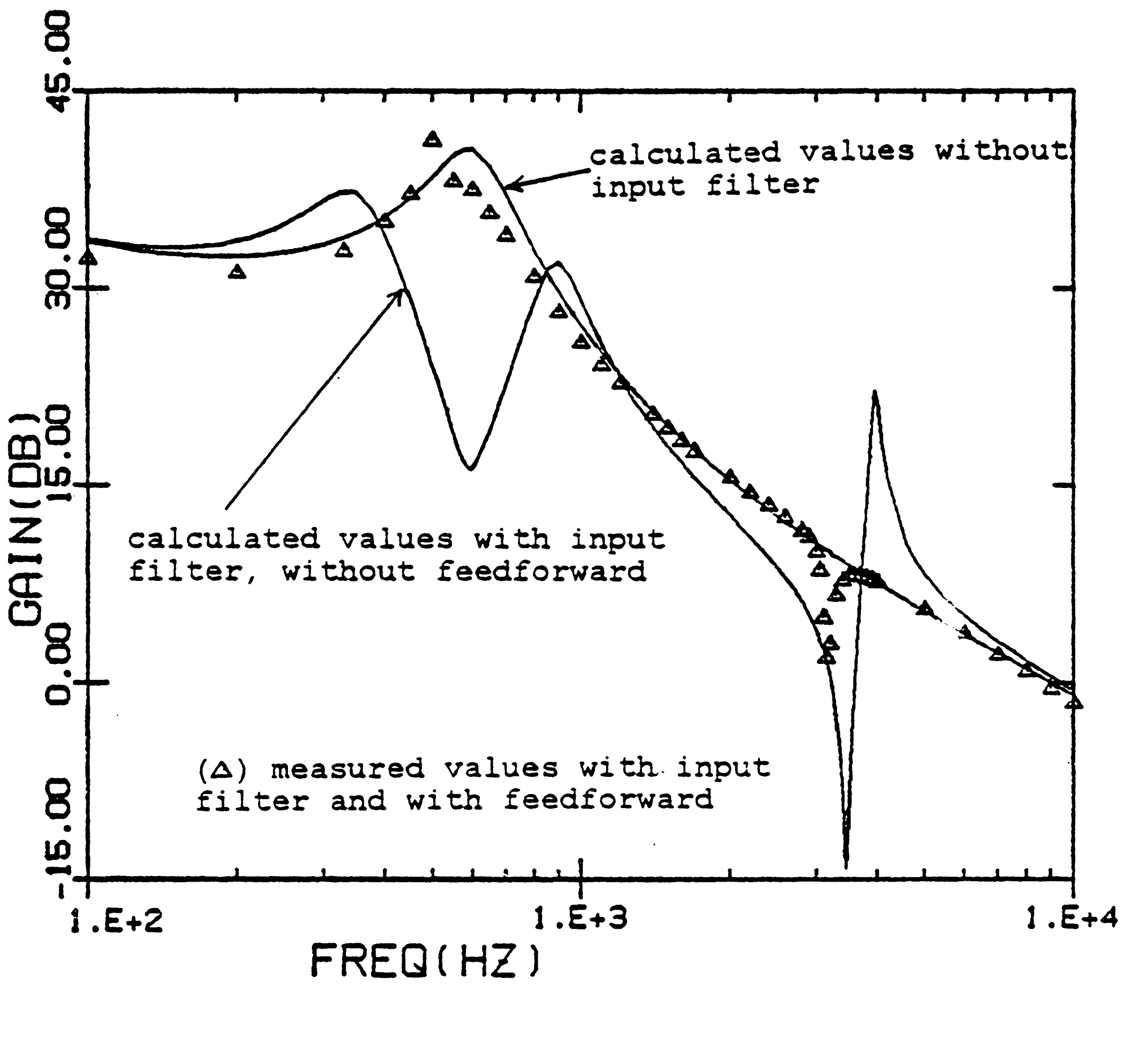


Figure 42: (c) Open loop gain at $V_I$ =25v: Calculated values and measured values (Δ) with feedforward

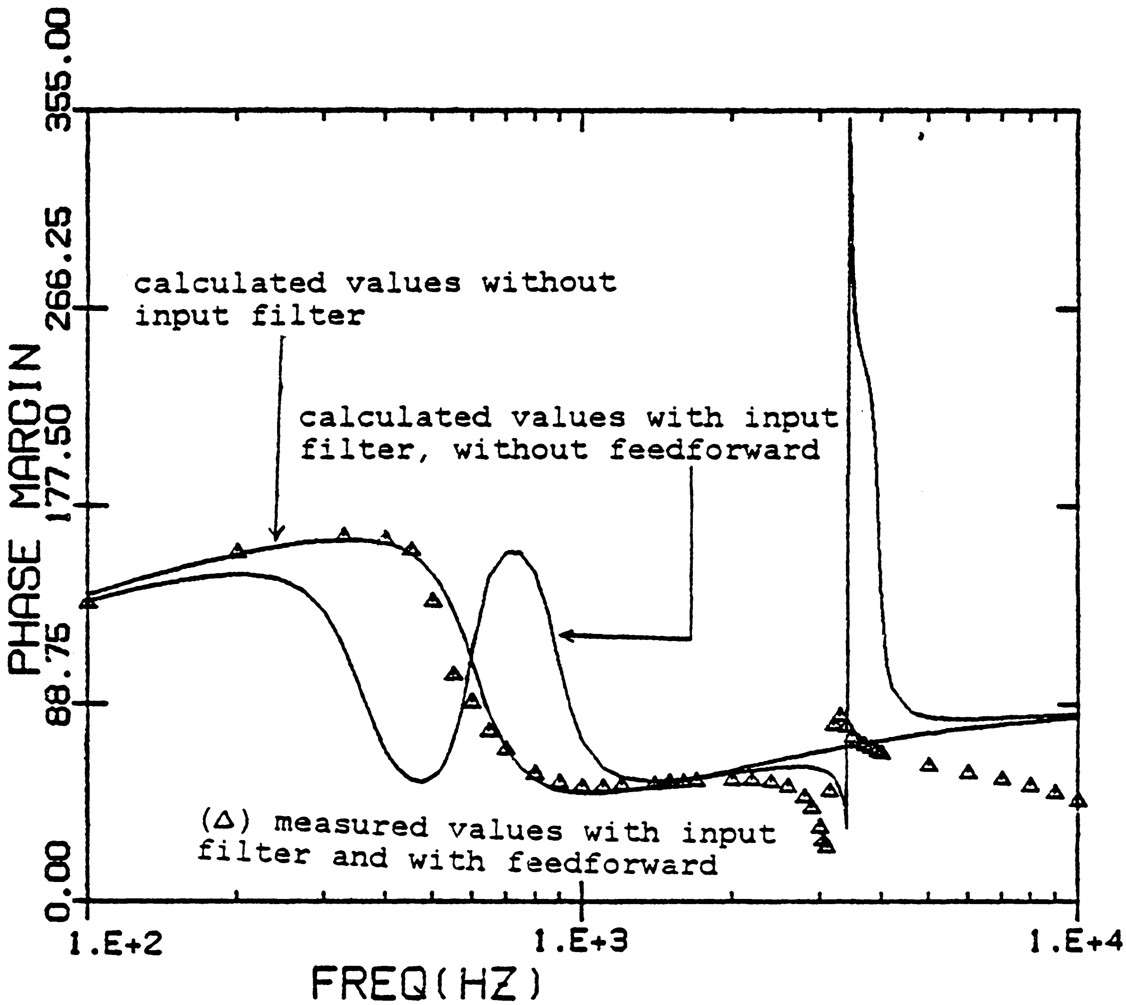


Figure 42: (d) Open loop phase margin at $V_I$=25v: Calculated values and measured values (Δ) with feedforward

(5) From the results presented in section 6.1 and from measurements presented in this section it is logical to conclude that the adaptive feedforward circuit can provide effective compensation for an arbitrary, unknown source impedance for a variable supply voltage. The adaptive feedforward circuit has been shown to be able to track the supply voltage and adjust the gain in accordance with supply voltage changes. The adaptive feedforward circuit can effectively isolate the switching regulator from its source impedance, thus preventing any interaction between the switching converter and equipment upstream.

## 6.3 MEASUREMENTS OF CLOSED LOOP INPUT-TO-OUTPUT TRANSFER FUNCTION (AUDIOSUSCEPTIBILITY).

The closed loop input-to-output transfer function (audiosusceptibility) of a switching regulator is an important characteristic. It refers to the regulator's ability in attenuating small signal sinusoidal disturbances propagating from the regulator input to its output. The gain of the closed loop input-to-output transfer function should be as small as possible; thus the regulator will effectively attenuate noise at the input so as not to affect operation of the regulator payloads. Unfortunately, as pointed out in Chapter 2, the peaking of the output impedance of the input filter and the peaking of the forward transfer function of the input filter increase the audiosusceptibility. Measurements of audiosusceptibility with and without feedforward were made using the two-stage input filter of Figure 36 with a damping resistor so that $R_3$ = 0.2 ohm. Measurements were made by injecting a small sinusoidal signal at the input to the converter and then using a HP network analyser to measure the audiosusceptibility [8]. The feedforward circuit used was the adaptive feedforward circuit of Figure 33 and the buck regulator used is shown in Figure 34 , with its parameters as specified in section 6.1.

Figures 43 - 46 show the measured values of audiosusceptibility with and without feedforward at four values of supply voltage $V_I$ = 25v, 30v, 35v and 40v using the same feedforward circuit in all cases. The top trace in each figure is the plot without feedforward and it can be seen clearly that the audiosusceptibility is degraded at the two resonant frequencies where the output impedance Z(s) and the transfer function H(s) of the input filter peak , with the first stage resonating around 600 Hz and the second stage around 3 KHz. It is also evident from the figures that the audiosusceptibility is dependent on duty cycle D or the supply voltage. At higher values of supply voltage when the duty cycle is low the audiosusceptibility is lower, specially at the lower frequencies.

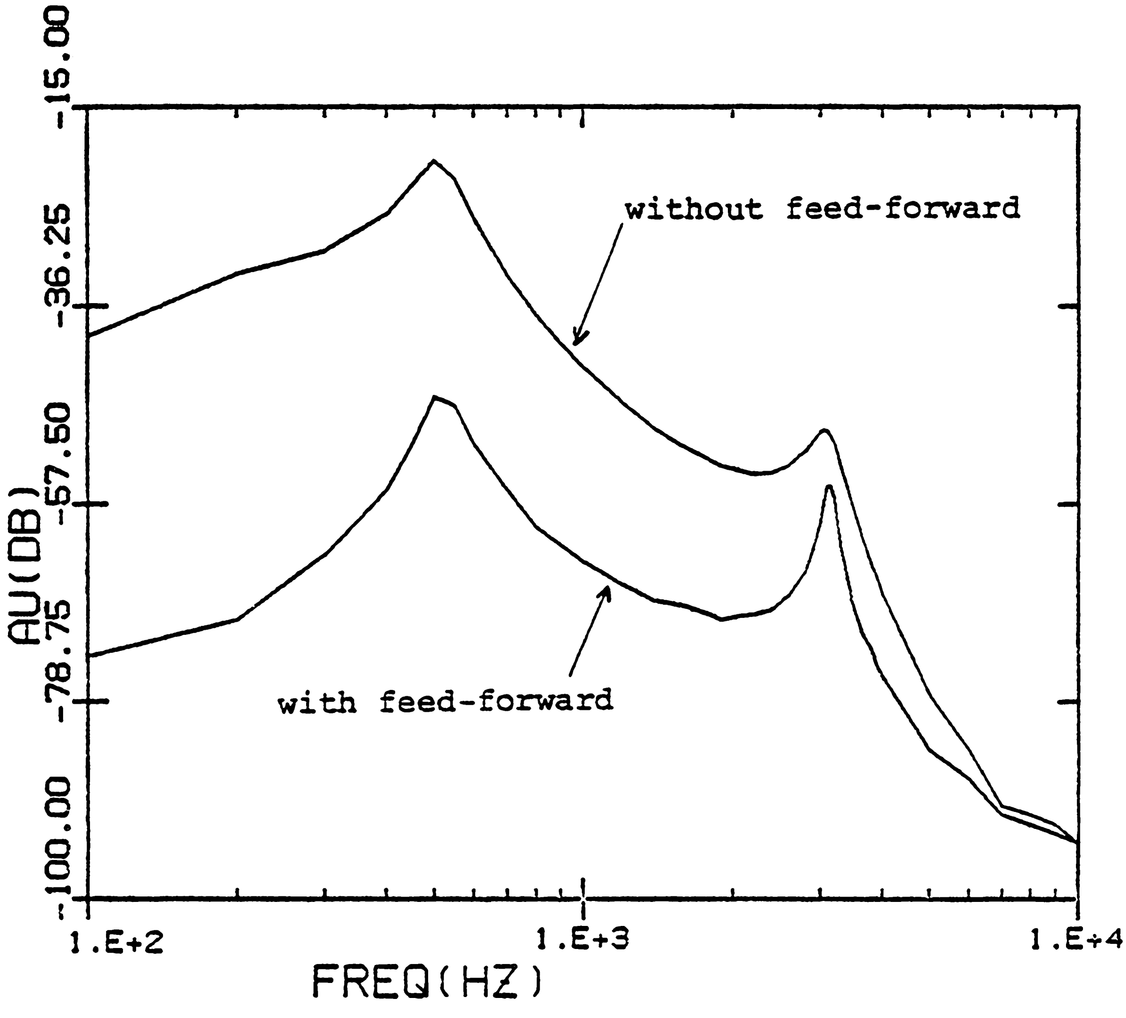


Figure 43: Measurement of audiosusceptibility $[\hat{v}_o(s)/\hat{v}_x(s)]$ with and without feedforward at $V_I$ =25v

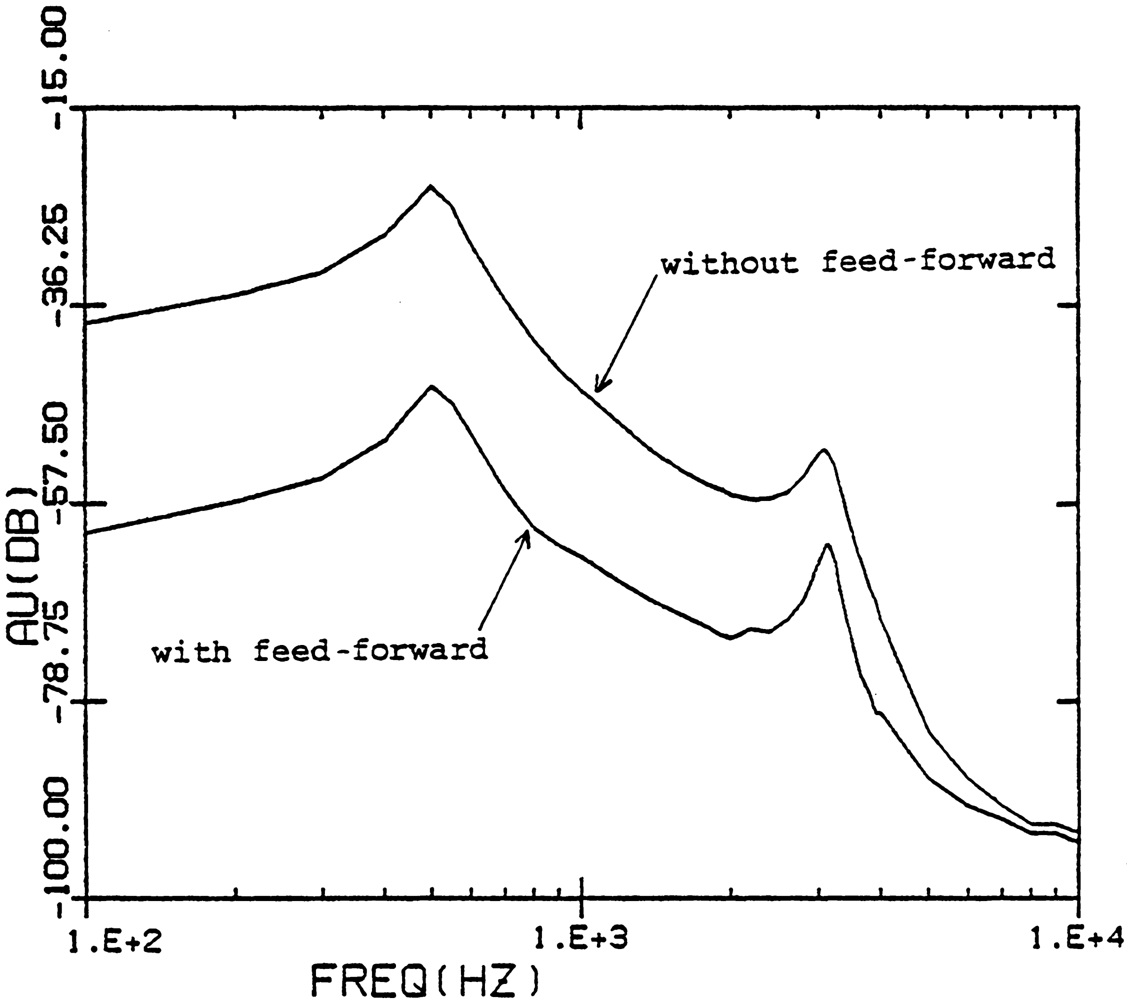


Figure 44: Audiosusceptibility with and without feedforward at $V_I$=30v (measurements)

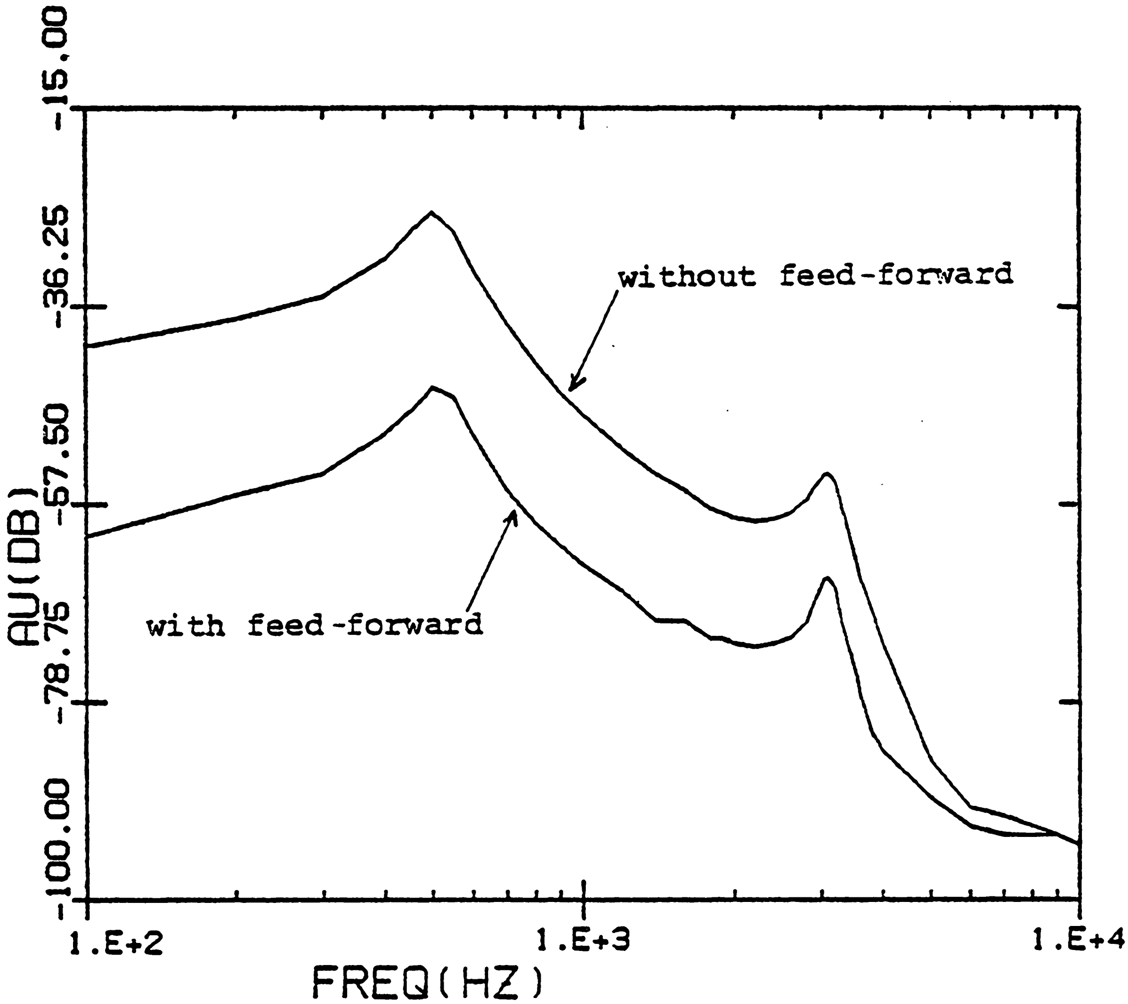


Figure 45: Audiosusceptibility with and without feedforward at $V_I$=35v (measurements)

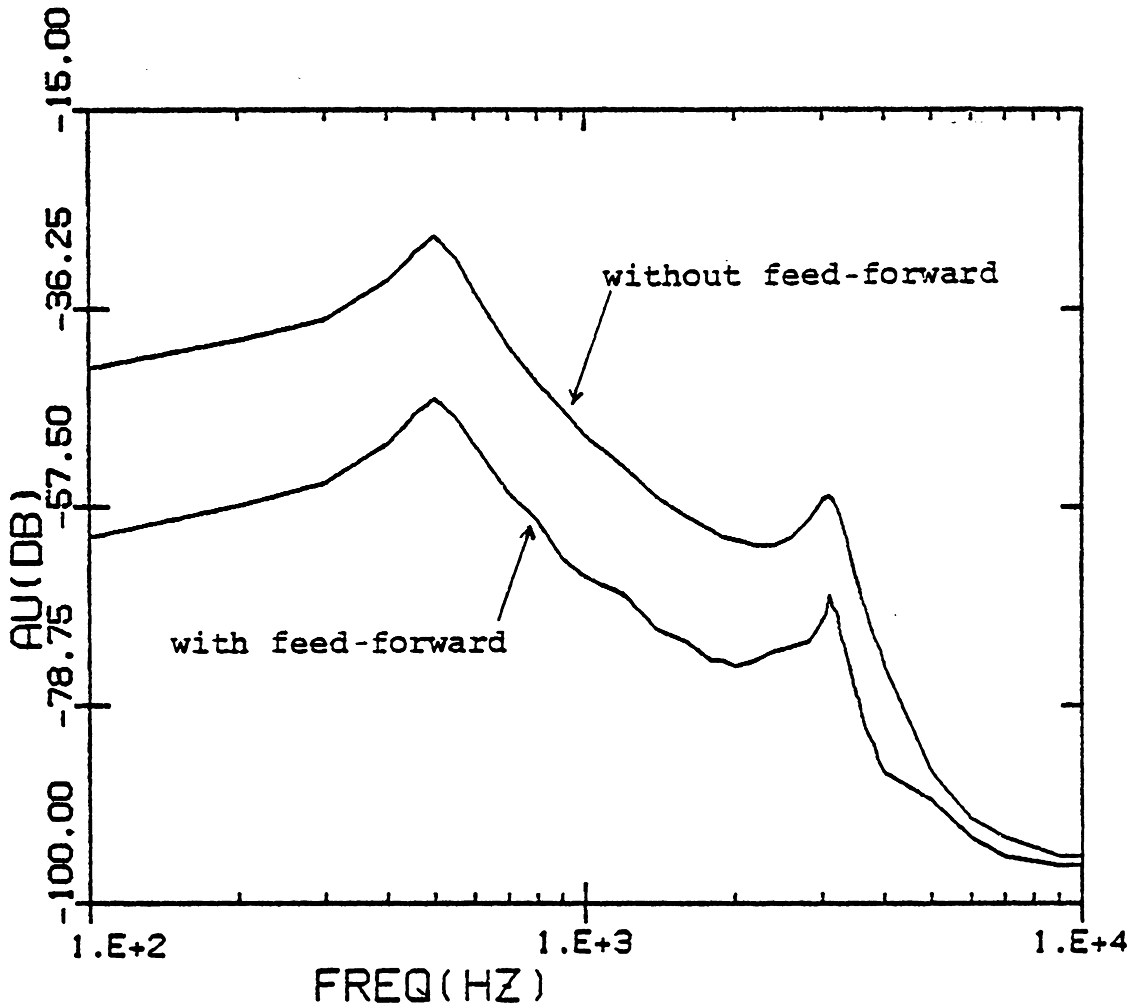


Figure 46: Audiosusceptibility with and without feedforward at $V_I$=40v (measurements)

The addition of feedforward substantially improves the audiosusceptibility, specially at the lower frequencies, as is evident upon examination of Figures 43 - 46 . The peaking effect of audiosusceptibility with feedforward loop is however, more pronounced at the two resonant frequencies of the two-stage input filter; this is explained by noting that in equation (2-6), Chapter 2, the audiosusceptibility is shown to be affected both by the peaking of Z(s) and by the peaking of the forward transfer function H(s) of the input filter. The peaking of H(s) cannot be controlled in any fashion by the addition of a feedforward loop since the control loop is not affected by H(s); thus the feedforward loop is effective in cancelling Z(s) while the peaking effect of H(s) is manifested in audiosusceptibility. Figures 47 and 48 show the transfer functions H(s) and Z(s) of the two-stage input filter used. The peaking of H(s) at the two resonant frequencies is clearly seen.

The two-stage input filter was modified by removing the damping resistor so that $R_3$ = 0.075 ohm. Measurement data of the audiosusceptibility with and without feedforward are shown in Figures 49 - 52 . The top trace in all these figures is the closed loop input-to-output transfer function without feedforward and it can be seen that the gain is higher than in the earlier case (with damping resistance).

Figures 53 and 54 show the forward transfer function H(s) and the output impedance Z(s) of the input filter used. Comparing Figures 47 and 48 with Figures 53 and 54 it can be seen clearly that both Z(s) and H(s) peak at significantly higher values when the external damping resistance is removed.

The addition of feedforward substantially improves the audiosusceptibility as is evident from Figures 49 - 52 . The audiosusceptibility with feedforward peaks at the two resonant frequencies of the two-stage input filter as before, but in this case the peaks are higher. This is explained by noting that H(s) of the two-stage input filter without damping resistance peaks at a significantly higher value, as shown in Figures 53 and 54 , than that with a damping resistance as shown in Figures 47 and 48 ; thus the effect of H(s) on the closed loop gain would be expected to be greater in the former case.

It can therefore be concluded that the addition of feedforward significantly improves the audiosusceptibility, specially at the lower frequencies. The audiosusceptibility with feedforward is affected by the peaking of H(s) since the effect of peaking cannot be eliminated via any control means. The same adaptive feedforward circuit was used in making all the closed loop gain measurements mentioned

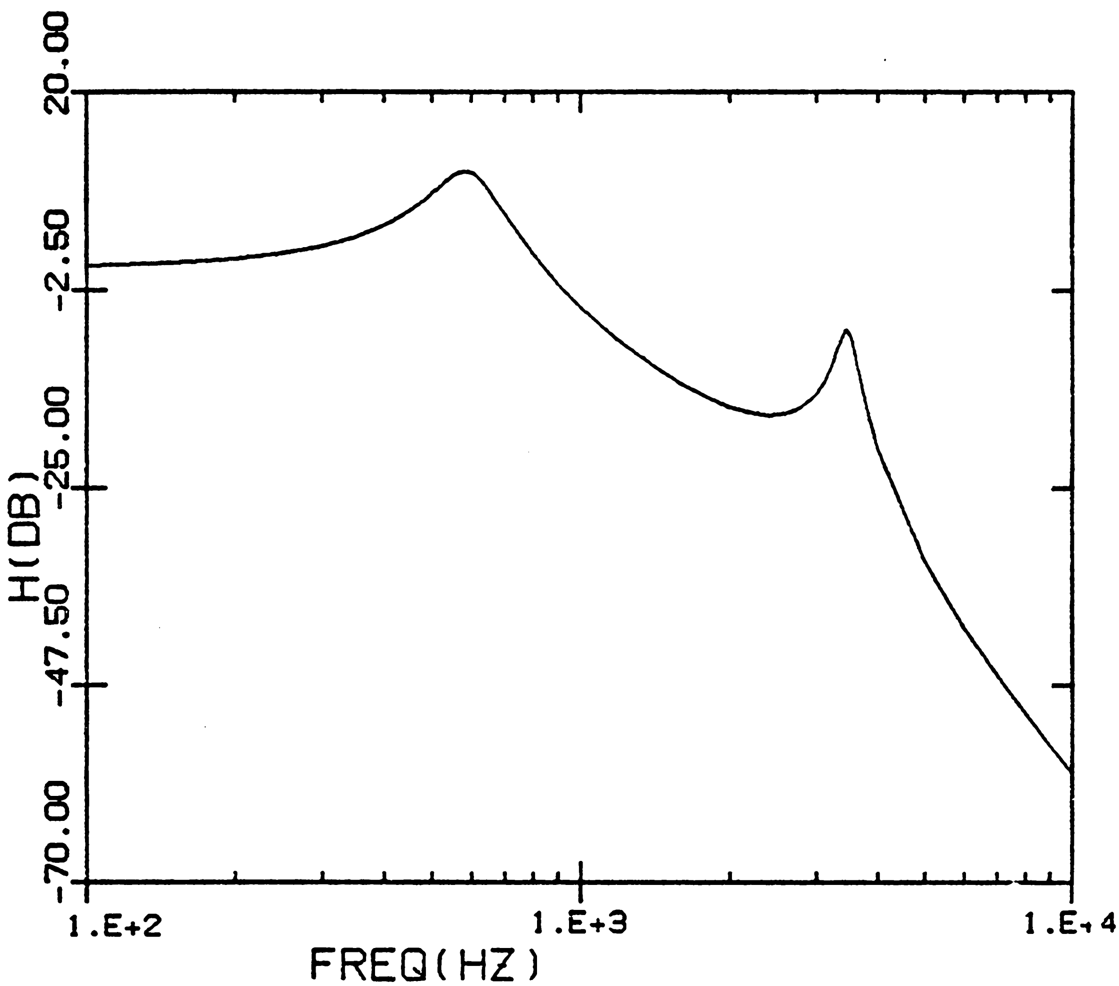


Figure 47: H(s) of two stage input filter, with $R_3$=0.2 ohm

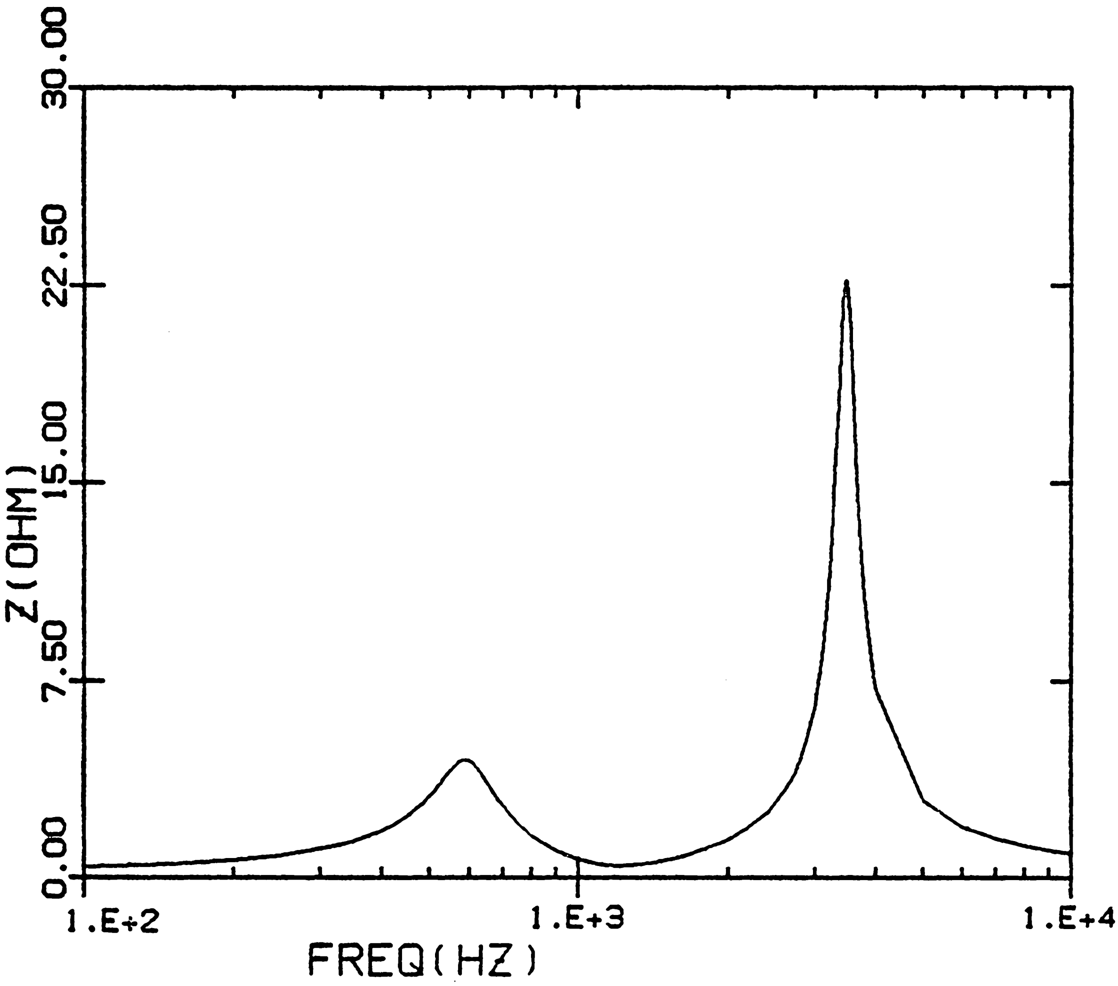


Figure 48: Z of two stage input filter, with $R_3$=0.2 ohm

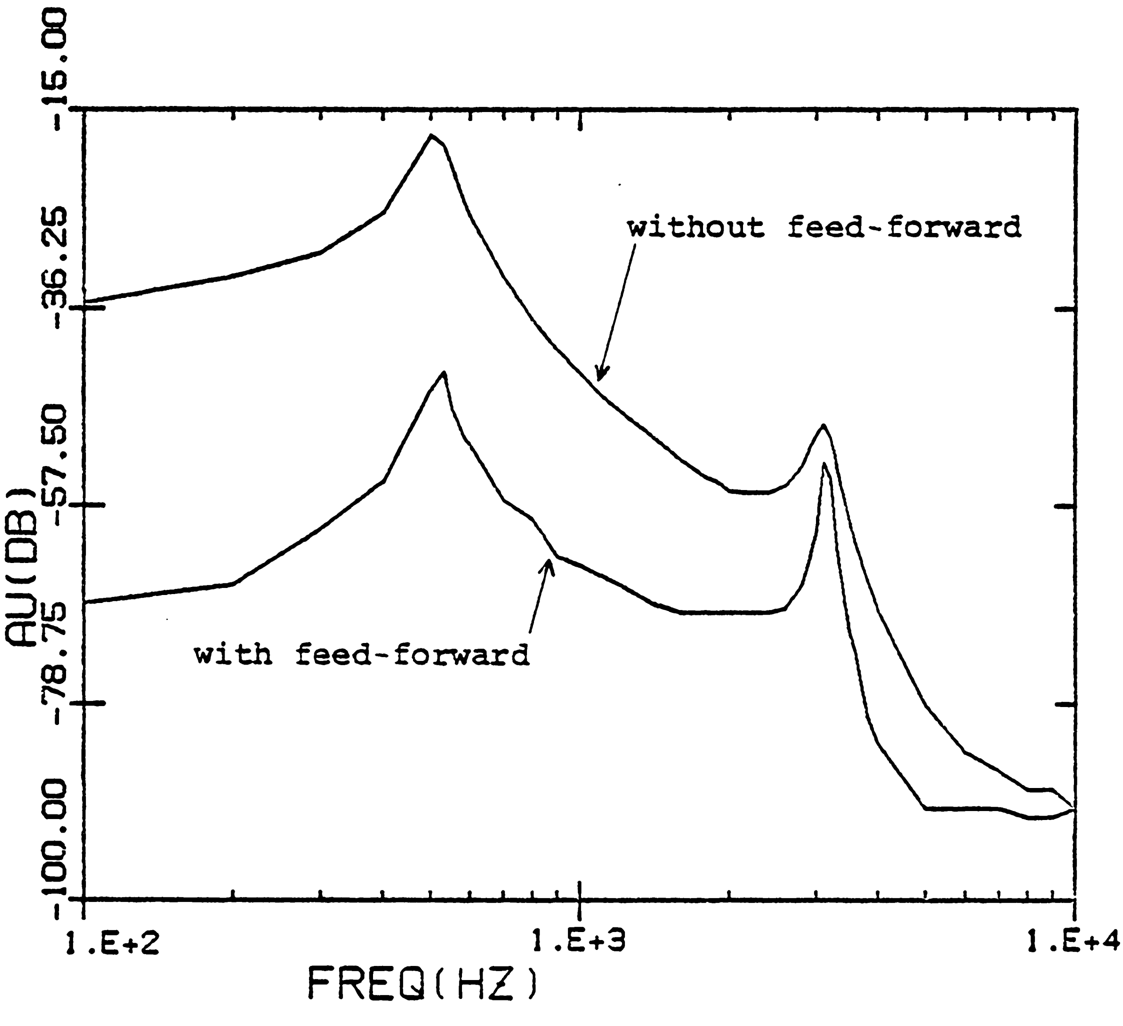


Figure 49: Audiosusceptibility with and without feedforward at $V_I$=25v (measurements)

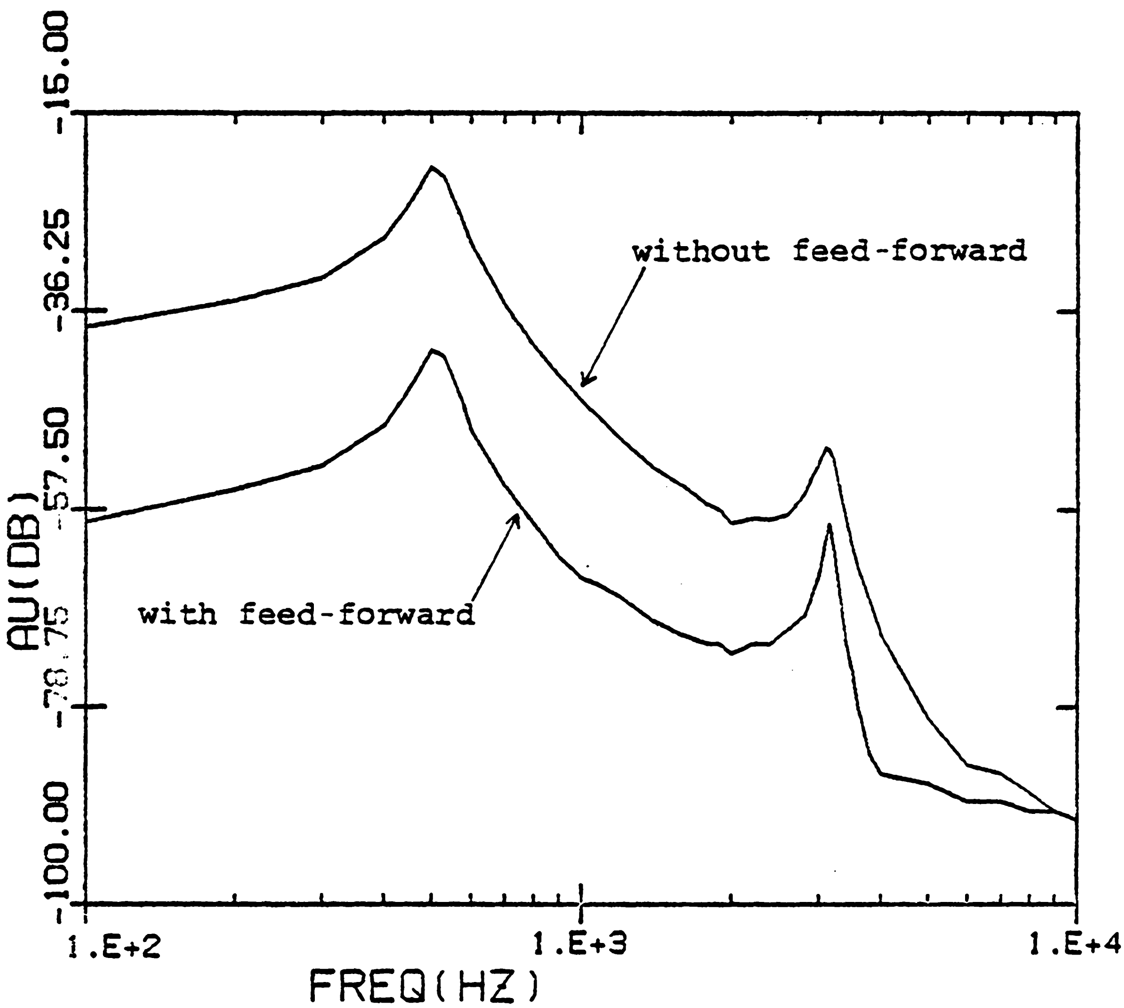


Figure 50: Audiosusceptibility with and without feedforward at $V_I$=30v (measurements)

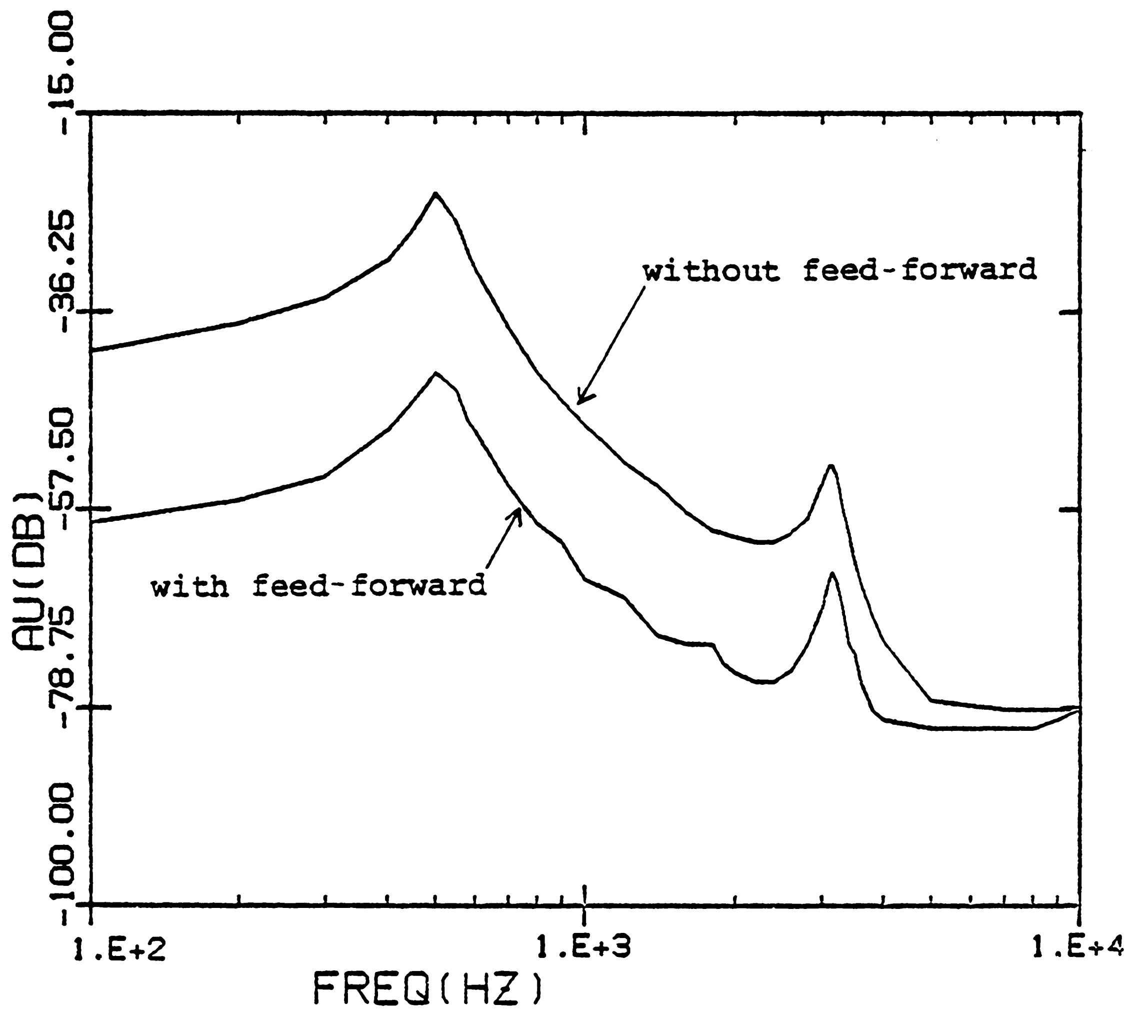


Figure 51: Audiosusceptibility with and without feedforward at $V_I$=35v (measurements)

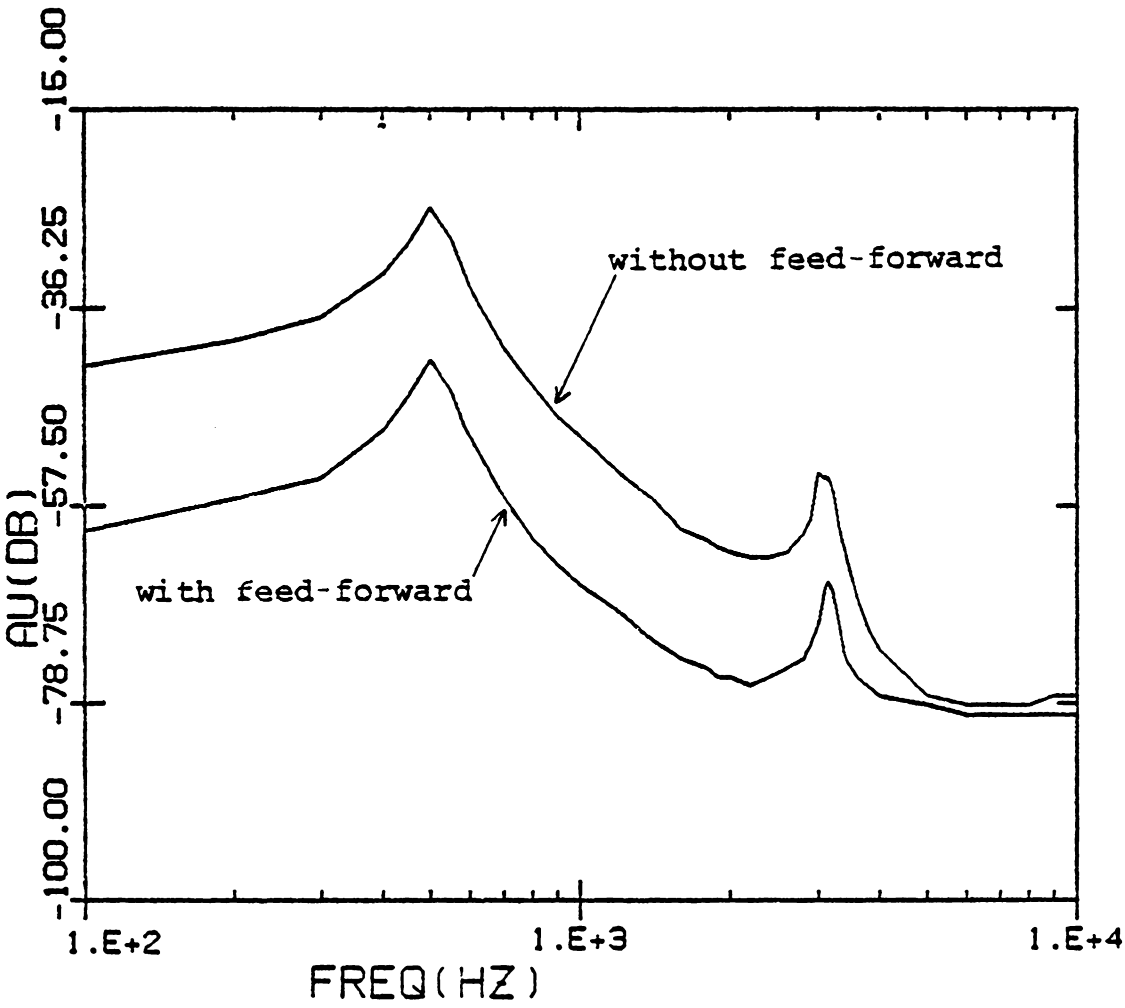


Figure 52: Audiosusceptibility with and without feedforward at $V_I$ =40v (measurements)

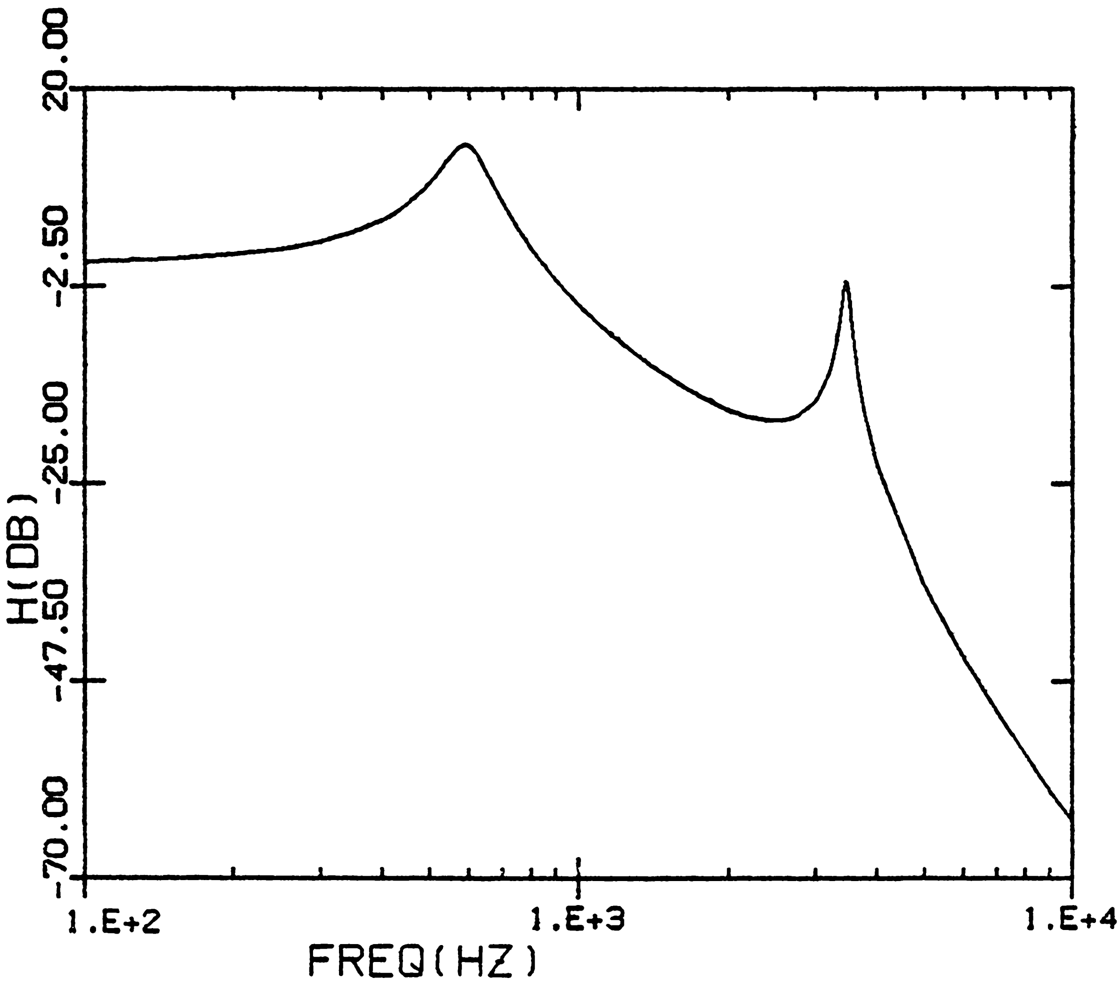


Figure 53: H(s) of two stage input filter, $R_3$=0.075 ohm

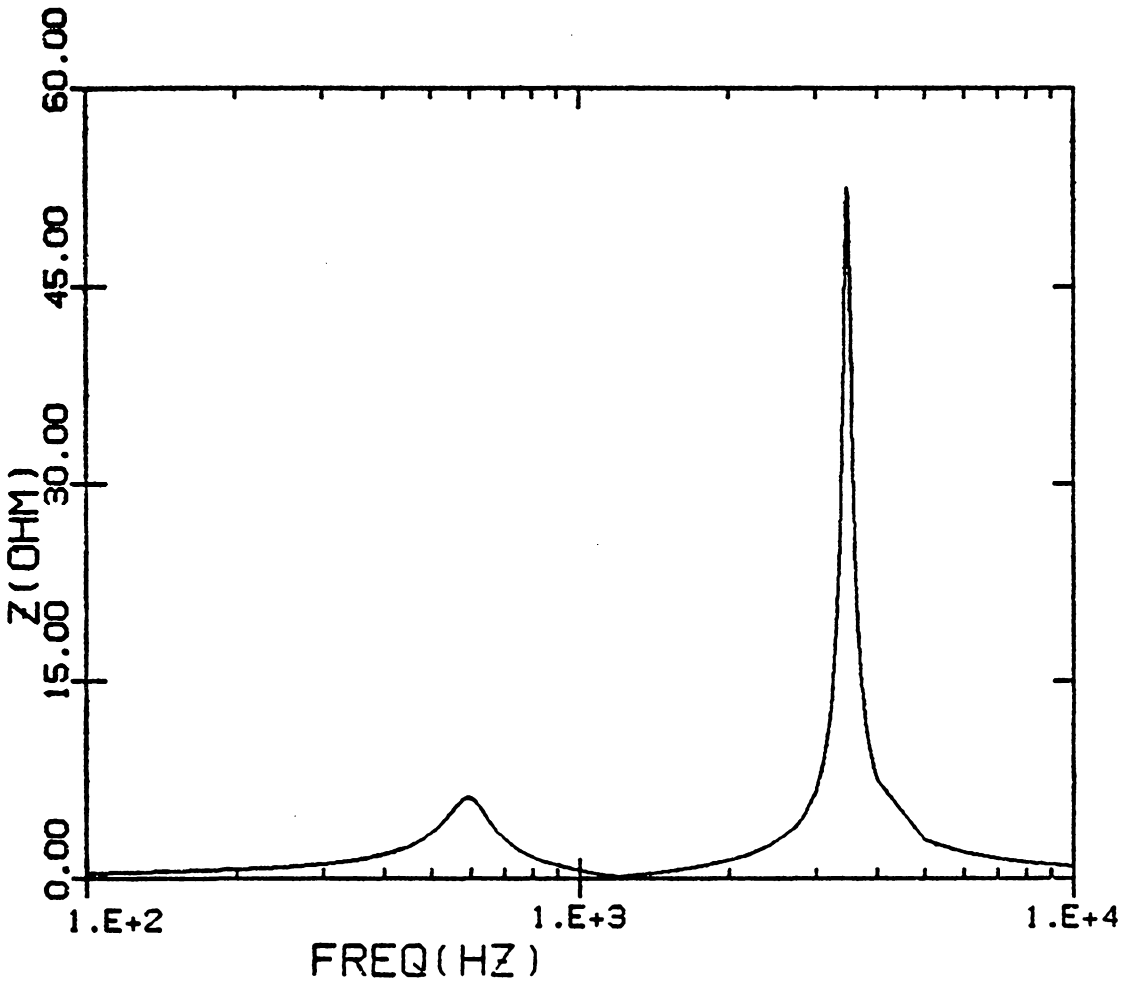


Figure 54: Z of two stage input filter, $R_3$=0.075 ohm

above, this confirms anew the adaptive nature of the feedforward circuit.

## 6.4 MEASUREMENTS OF OUTPUT IMPEDANCE.

The closed-loop output impedance of a switching regulator should be as low as possible in order that the regulator behave as much as an ideal voltage source as possible. However, as pointed out in Chapter 2, the peaking of the output impedance of the input filter increases the closed-loop output impedance of the regulator.

Measurements of the regulator output impedance with and without feedforward were made, using the two-stage input filter of Figure 36 with $R_3$ = 0.075 ohm (ESR of $C_2$). Measurements were made by injecting a small signal sinusoidal disturbance at the output in parallel with the load of the regulator, and then using a HP network analyser to measure the corresponding voltage and current [8,9]. The feedforward circuit used was the adaptive feedforward circuit of Figure 33 . Figures 55 - 58 show the measured values of output impedance with and without feedforward at four values of supply voltage $V_I$ = 25v, 30v, 35v and 40v using the same feedforward circuit in all cases.

It can be seen clearly from the figures that the output impedance is increased at the two resonant frequencies of

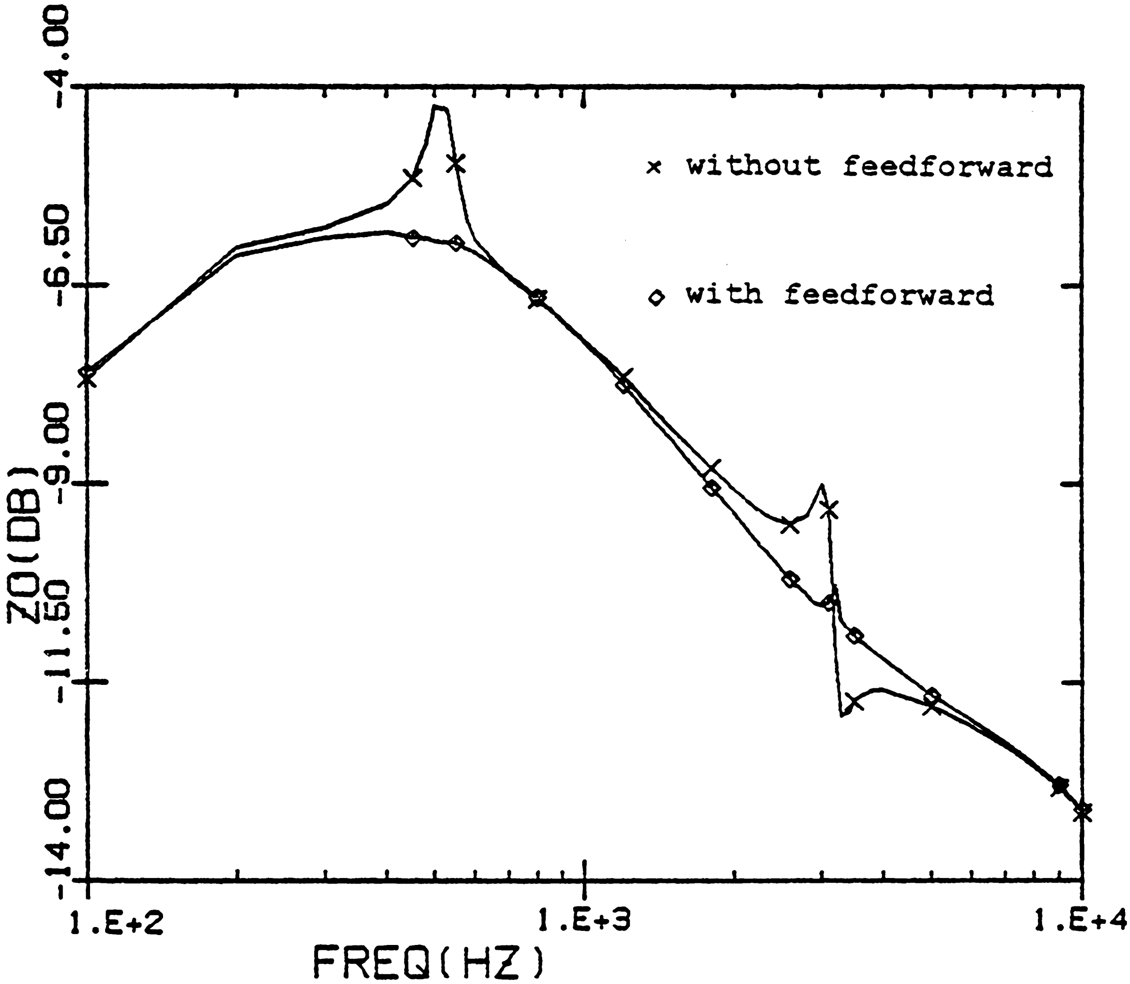


Figure 55: Output impedance with and without feedforward (×) at $V_I$=25v

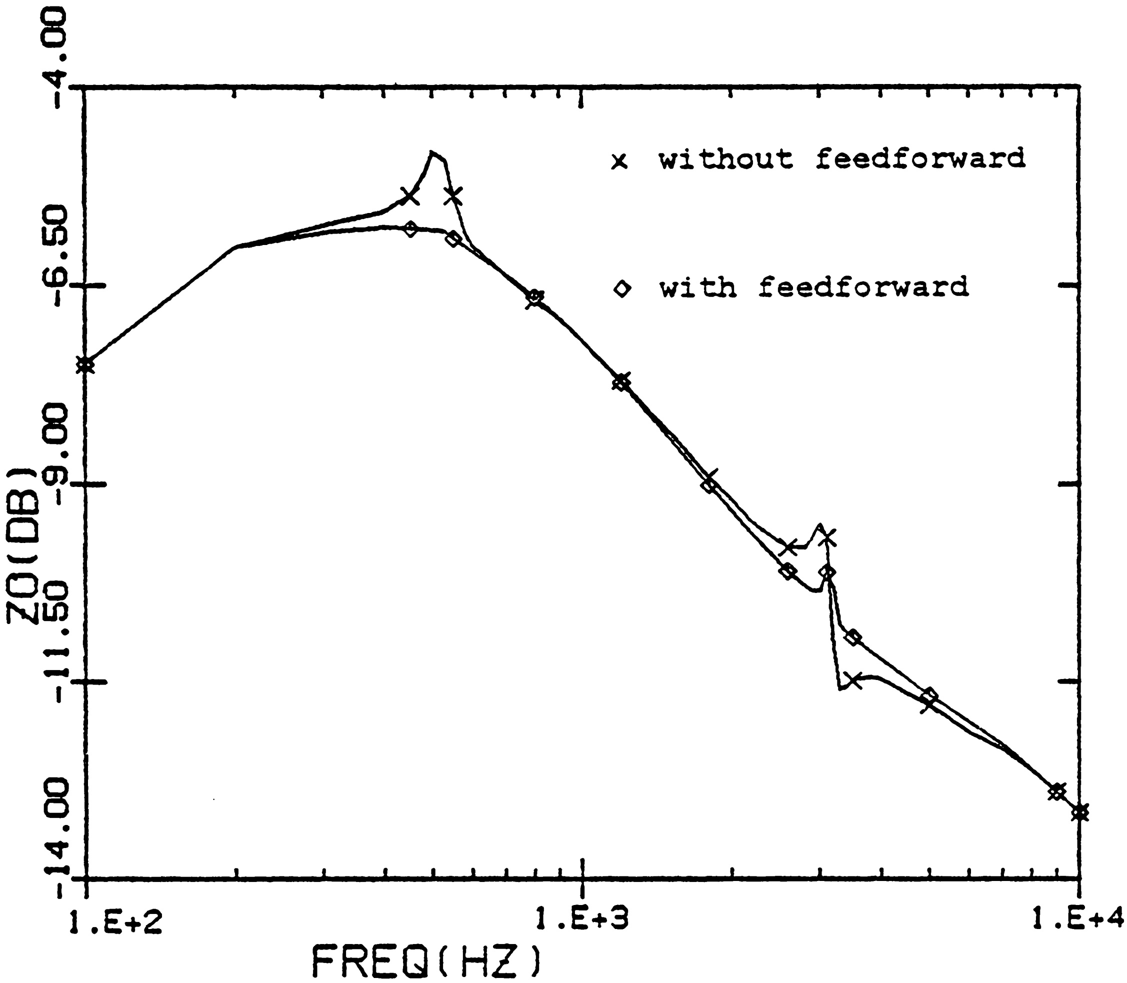


Figure 56: Output impedance with and without feedforward (X) at $V_I$=30v

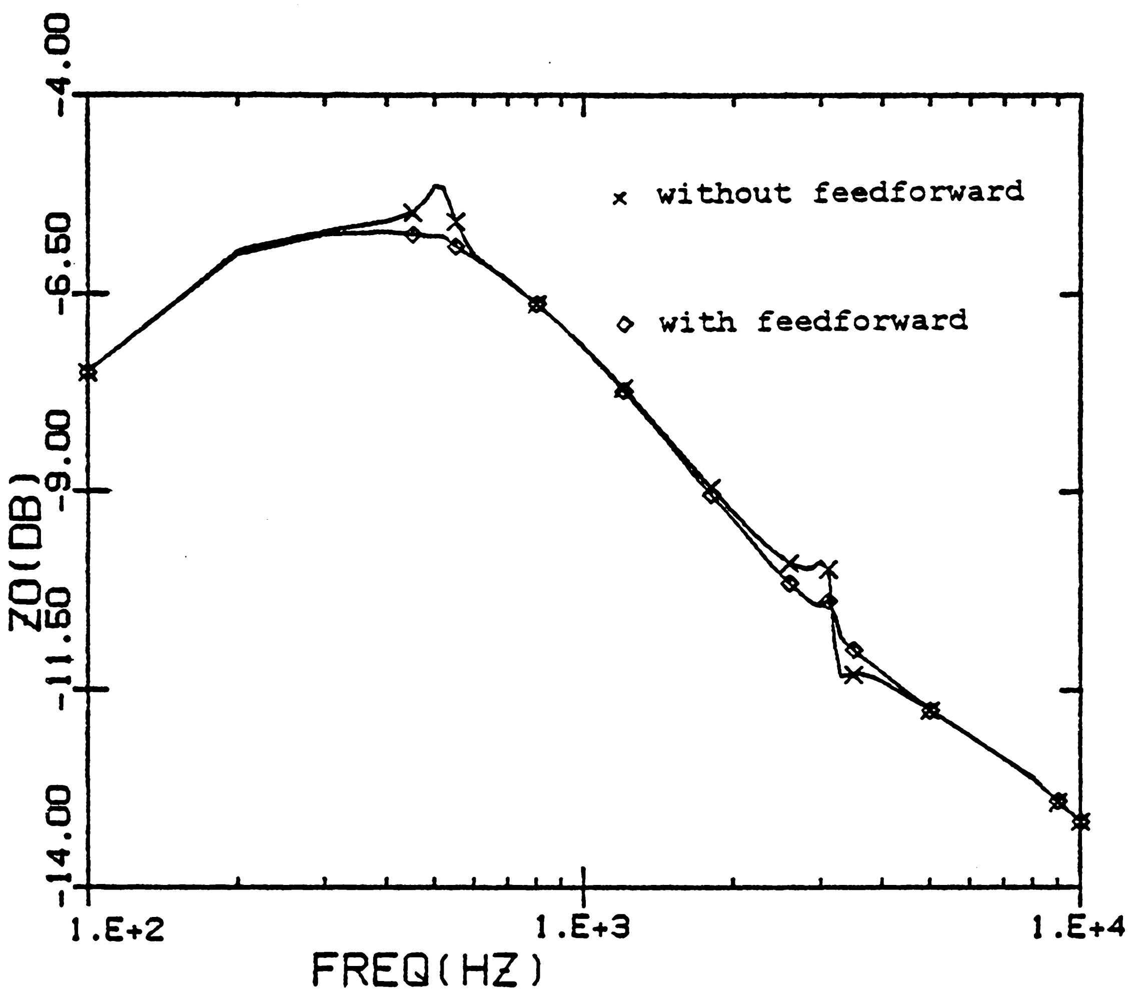


Figure 57: Output impedance with and without feedforward (x) at $V_I$=35v

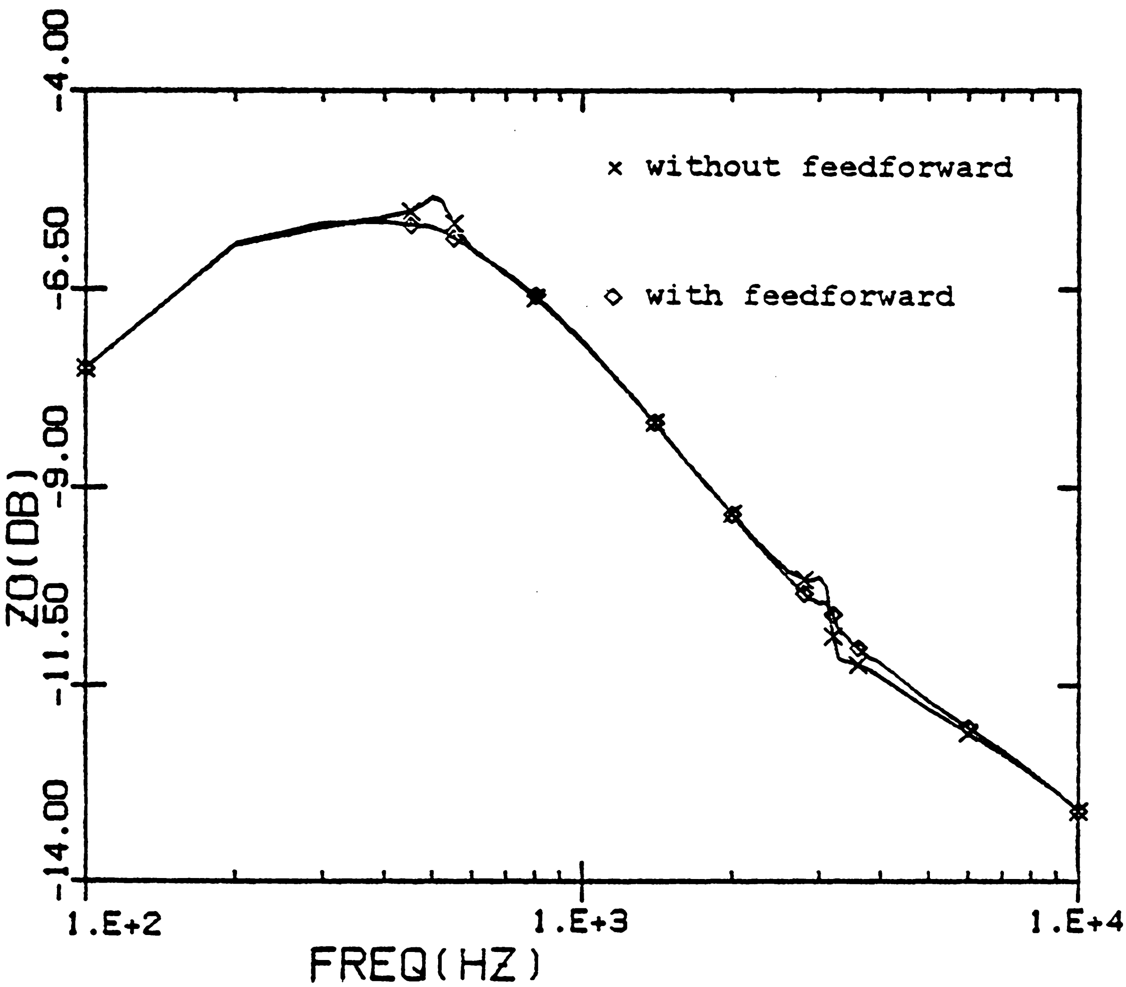


Figure 58: Output impedance with and without feedforward (X) at $V_I$ =40v

the two-stage input filter. This is a consequence of the disturbances in the loop gain produced at those frequencies by the peaking of the input filter output impedance Z(s). As was seen earlier in sections 6.1 and 6.2 the effect of Z(s) on the open loop gain depends on the duty cycle D, at higher values of D i.e. lower supply voltages, the effect of Z(s) on the open loop gain is higher. Thus the effect of Z(s) on the output impedance would be greater at lower supply voltages, and this is experimentally confirmed as can be seen from Figures 55 - 58 .

The addition of feedforward almost totally eliminates the undesirable perturbations in the output impedance characteristic at all supply voltages.

## 6.5 MEASUREMENT OF TRANSIENT RESPONSE AND STARTING OF THE REGULATOR.

In this section measurements of output voltage and other parameters for a step change in input voltage or load are presented with and without feedforward.

### 6.5.1 Small Amplitude Transient Response Measurements.

Photographs of the output voltage ripple and other parameters are presented with and without feedforward for two cases:

(1) Step change in supply voltage.

(2) Step change in load.

The step changes mentioned above are small enough so that the output voltage remains in regulation throughout the transient response period.

6.5.1.1 Step Change in Input Voltage.

The buck regulator used is shown in Figure 34 with the parameters as specified in section 6.1. The input filter used was a single-stage input filter with the following parameters:

$R_{L1}$ = 0.2 ohm  L1 = 325 micro H  C1 = 220 micro F

The adaptive feedforward circuit of Figure 33 was used in making the measurements.

The input voltage was abruptly switched from $V_I$ = 30v to 40v and photographs of output voltage ac ripple, input filter capacitor voltage, output filter inductor current and control voltage without using a feedforward loop were taken as shown in Figures 59 (a) and (b) , 60 (a) and (b), respectively. The control voltage is the input to the pulse modulator; without feedforward it is the output at the integrator in the feedback loop while with feedforward it is the sum of the above signal and the feedforward signal. Figures 61 (a) and (b) , 62 (a) and (b) show the photographs of the same variables with feedforward control. Comparing, for example, the photographs of the output voltage ripple with and without feedforward, Figures 59 (a) and 61 (a), it can be clearly seen that the transient response is improved with the addition of feedforward. The amount of overshoot is less with feedforward. The magnitude of the oscillations in the output voltage caused by the interaction between the input filter and the regulator control are also lessened with the addition of feedforward.

Comparison of the photographs of input filter capacitor voltage, output filter inductor current and control voltage do not reveal much difference between the two cases (with and without feedforward). This may be explained by noting that the gain of the feedforward loop is fairly small ( 0.03 for $V_I$ = 30v ) and thus the feedforward signal would be fairly small in amplitude. The addition of such a small amplitude signal to the fairly large amplitude waveforms recorded on the photographs will not show very clearly. The output voltage ripple, however, is small in magnitude and the effect of adding feedforward shows clearly. A computer program was written to simulate the step change in voltage; results from the program are presented in the next chapter and show close agreement with the measurements.

Thus it is concluded that feedforward improves transient response for the case where the supply voltage is subjected to a step change.

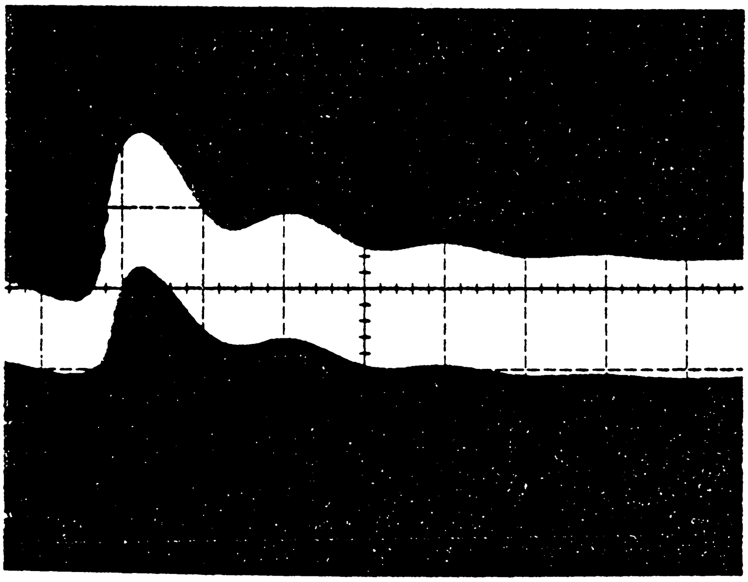

(a)

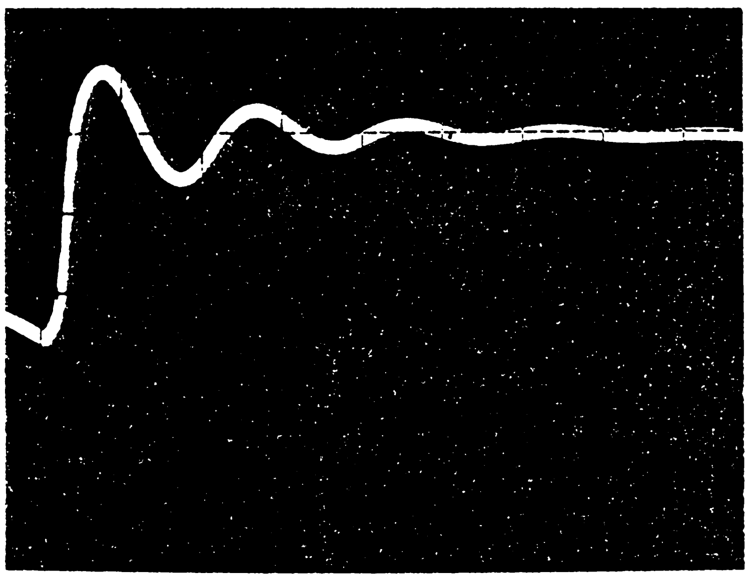

(b)

Figure 59: Output voltage ripple (a) and input filter capacitor voltage (b) without feedforward

(a) Y—0.1v/div X—1 msec/div

(b) Y—5v/div X—1 msec/div

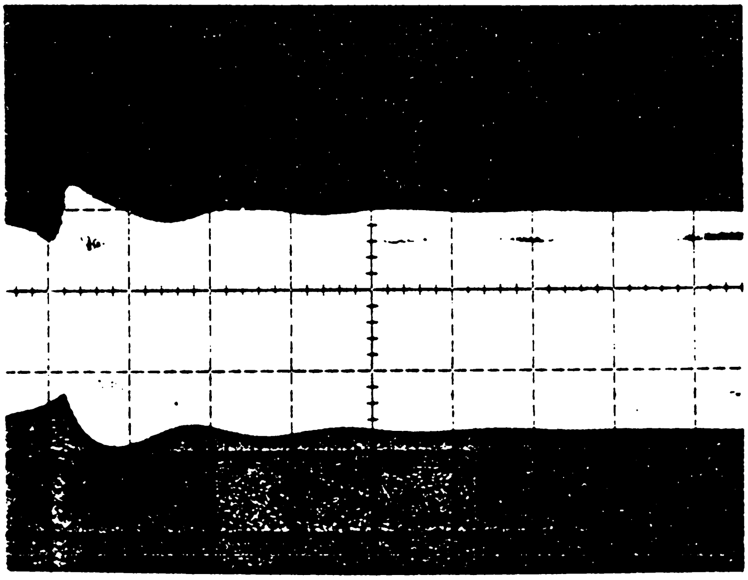

(a)

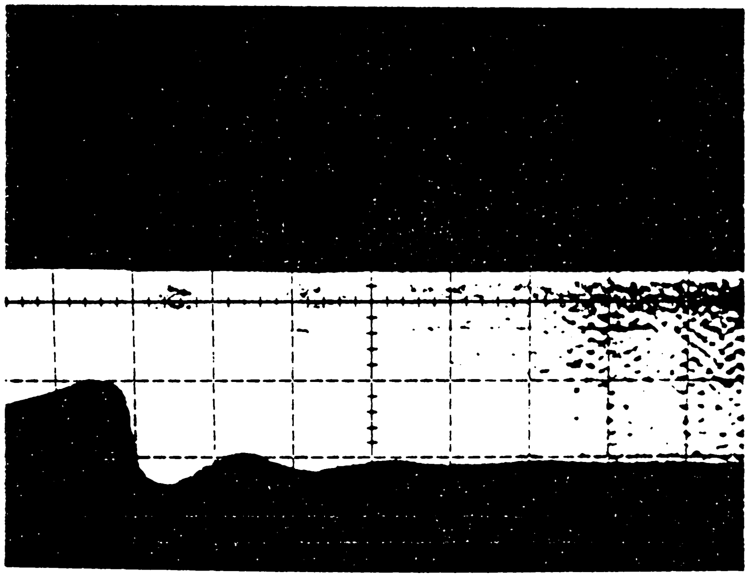

(b)

Figure 60: Output filter inductor current (a) and control voltage (b) without feedforward

(a) Y— 0.5 A/div X—1 msec/div

(b) Y—0.5v/div X—1 msec/div

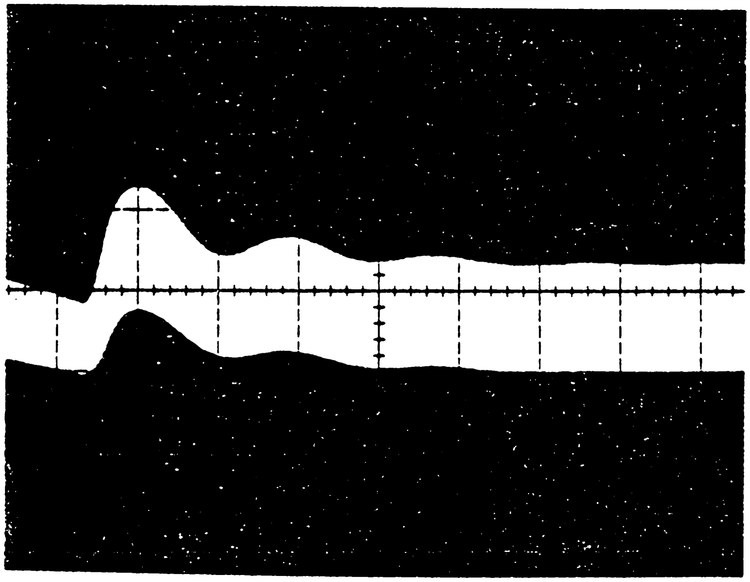

(a)

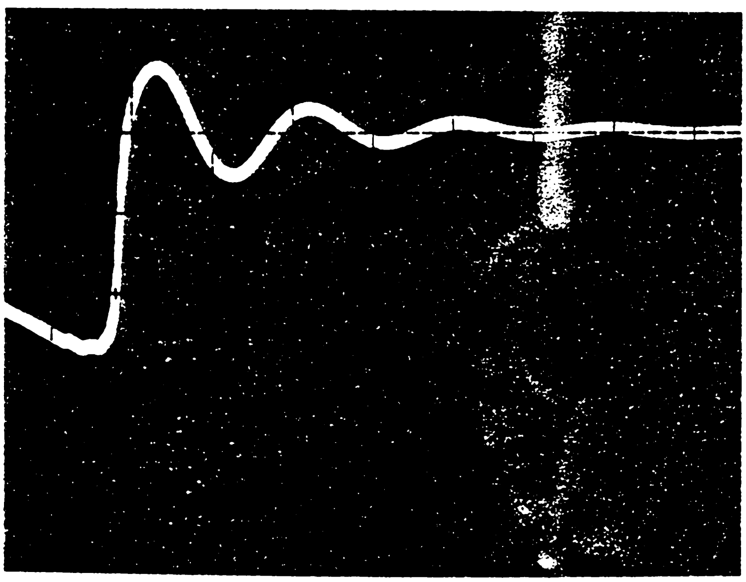

(b)

Figure 61: Output voltage ripple (a) and input filter capacitor voltage (b) with feedforward

(a) Y—0.1v/div X—1 msec/div

(b) Y—5v/div X—1 msec/div

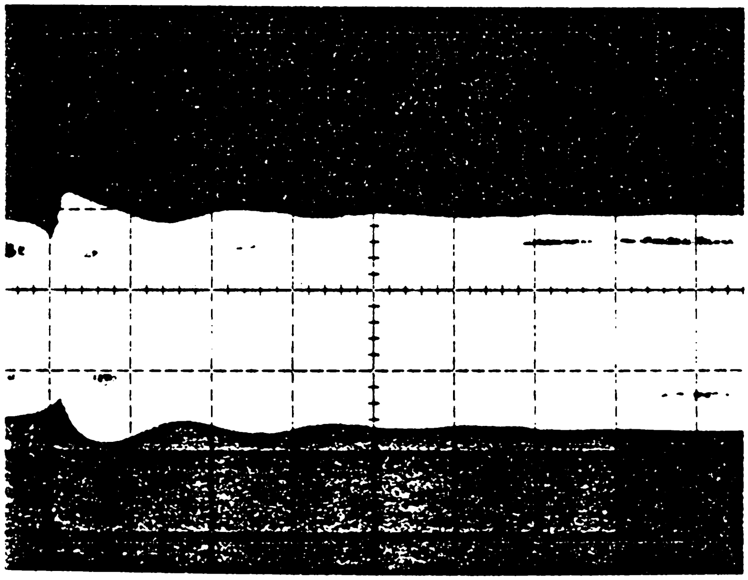

(a)

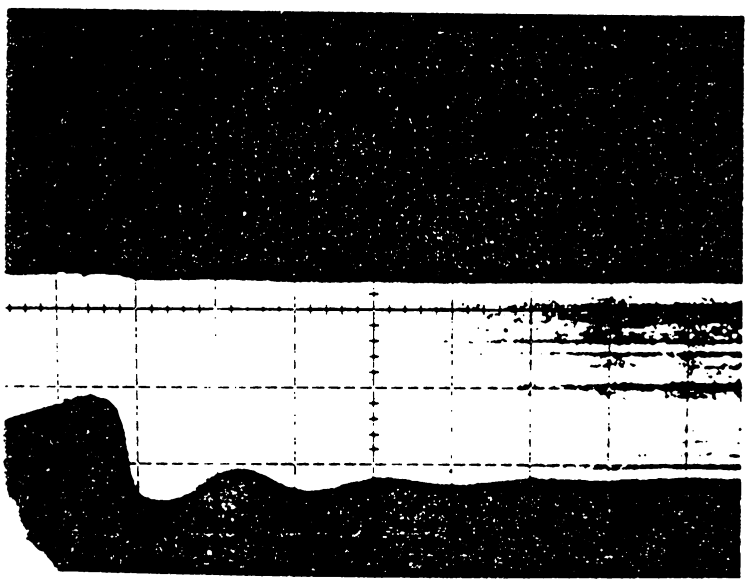

(b)

Figure 62: Output filter inductor current (a) and control voltage (b) with feedforward

(a) Y—0.5 A/div X—1 msec/div

(b) Y—0.5v/div X—1 msec/div

6.5.1.2 Step Change in Load.

The buck regulator used is shown in Figure 34 , with the parameters as specified in section 6.1 with the following changes:

$V_I$ = 25v $R_{14}$ = 3.69 Kilo ohm

A single stage input filter was used with the following parameters:

$R_{L1}$ = 0.2 ohm L1 = 325 micro H C1 = 100 micro F

The adaptive feedforward circuit of Figure 33 was used in making the measurements.

The load was switched repetitively between $R_L$ =10 ohms and $R_L$ = 20 ohms using a transistor switch. Figures 63 (a) and (b) show the photographs of the output voltage ripple without and with feedforward, respectively, as the load is switched. The output voltage ripple without feedforward, Figure 63 , shows distinct oscillations caused by the interaction between the input filter and the regulator control loop. The oscillation frequency coincides with the input filter resonant frequency. These oscillations are eliminated with the addition of feedforward, as is evident from Figure 63 (b).

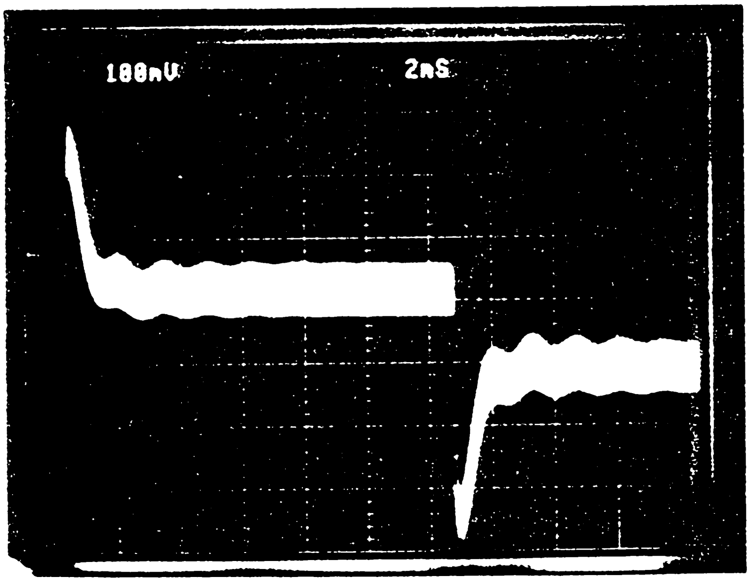


(a)

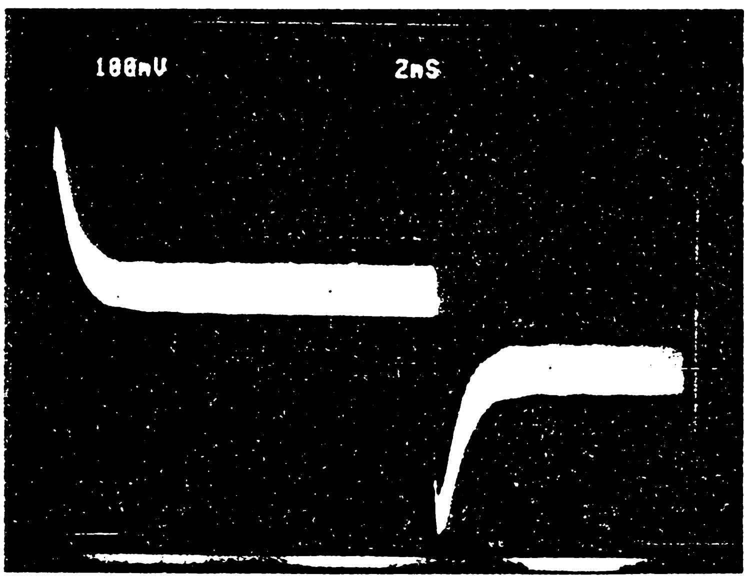


(b)

Figure 63: Output voltage without feedforward (a) and with feedforward (b)

6.5.2 Large Amplitude Transient Response Measurements. Photographs of the output voltage ripple and other parameters are presented with and without feedforward for two cases:

(1) Large step change in supply voltage.

(2) Starting of the converter.

The cases mentioned above are large signal changes so that the voltage regulation is momentarily lost for part of the transient response period.

6.5.2.1 Large Step Change in Supply Voltage.

The buck regulator used is shown in Figure 34 with the parameters as specified in section 6.1. The input filter used was the single-stage input filter of section 6.5.1.1. The adaptive feedforward circuit of Figure 33 was used in making the measurements with feedforward.

The input voltage was abruptly switched from $V_I$ = 40v to 25v and photographs of the output voltage were made with and without feedforward; Figures 64 (a) and (b) show the photographs.

The step change in supply voltage is large enough to cause the regulator to lose regulation -- the output voltage drops by about 1.5v before the regulator recovers. This may be explained by noting that for such a large change in supply voltage the input filter capacitor voltage drops down close to 20v, and since this value is lower than the design range of 25v - 40v for the regulator supply, the regulator loses regulation. Further details are given in the next chapter which presents results from a computer program written to simulate this large step change. The results show close agreement with the measurements presented here.

Figures 64 (a) and (b) show that the behavior of the regulator is similar with and without feedforward for such a large step change in supply voltage. This is expected since the regulator control loop momentarily loses its control function during this transient period. Since the feedforward is designed to compensate for the effects of input filter interaction via a duty cycle modulation scheme it is expected that the feedforward does not contribute anything under these conditions. Computer based simulation results presented in the next chapter confirm the measurement results. It is also to be noted that the feedforward does not have any detrimental effect on the transient response.

#### 6.5.2.2 Measurements of the Start Up Behavior of the Regulator

This section investigates the start-up behavior of the switching regulator. The regulator used is shown in Figure

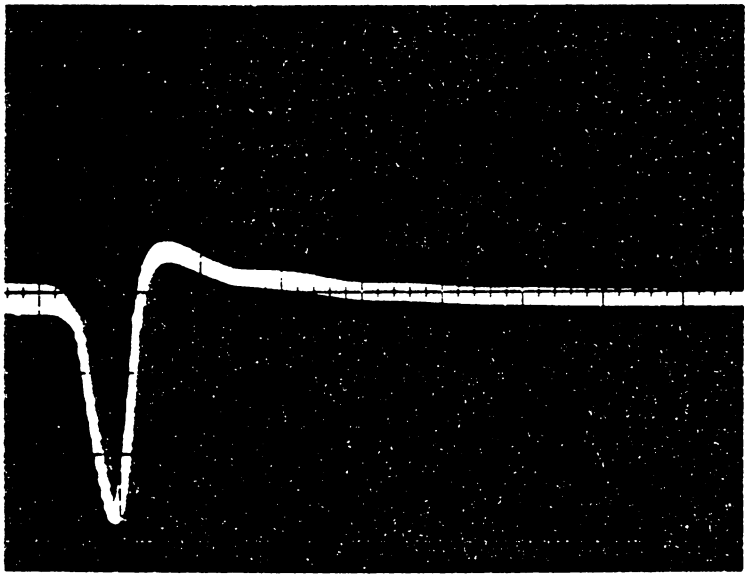

(a)

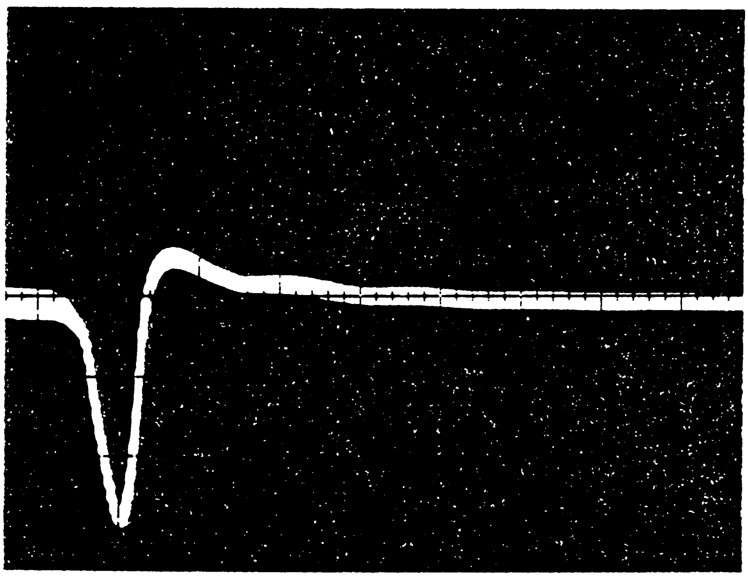

(b)

Figure 64: Output voltage without feedforward (a) and with feedforward (b)

(a) Y—0.5v/div X—0.5 msec/div

(b) Y—0.5v/div X—0.5 msec/div

34 with the parameters as specified in section 6.1. The single stage input filter of section 6.5.1.1 was used with the supply voltage set at 30v. The adaptive feedforward circuit of Figure 33 was used in making the measurements with feedforward.

Prior to starting, the output voltage and the output filter inductor current were both zero. Photographs of the output voltage and output filter inductor current were made with and without feedforward and are shown in Figures 65 (a) and (b) 66 (a) and (b). The output voltage without feedforward builds up from zero to 20v (regulated output) in about 3 msec. The inductor current rises sharply at starting but is limited to about 6.0A by the peak current protection circuit built in with the regulator. It settles down to its steady state value in about 4 msec.

The photographs with feedforward show similar behavior - thus the feedforward does not contribute significantly to this transient period nor does it present any detrimental effects.

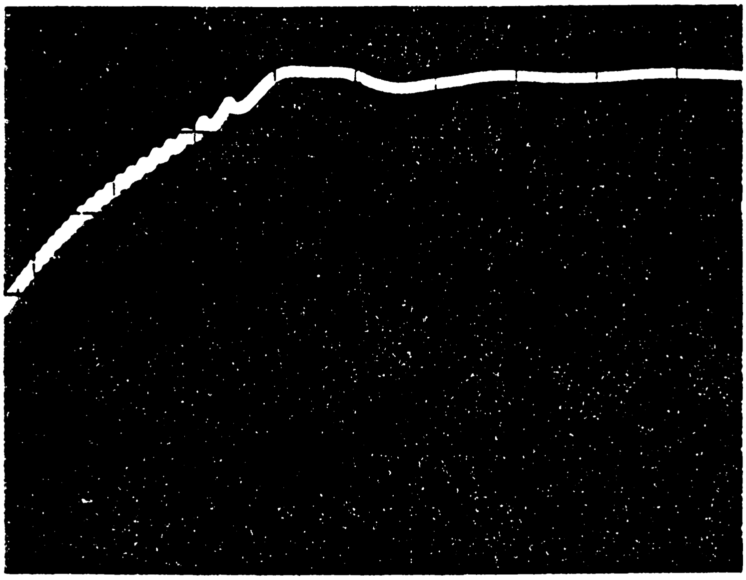

(a)

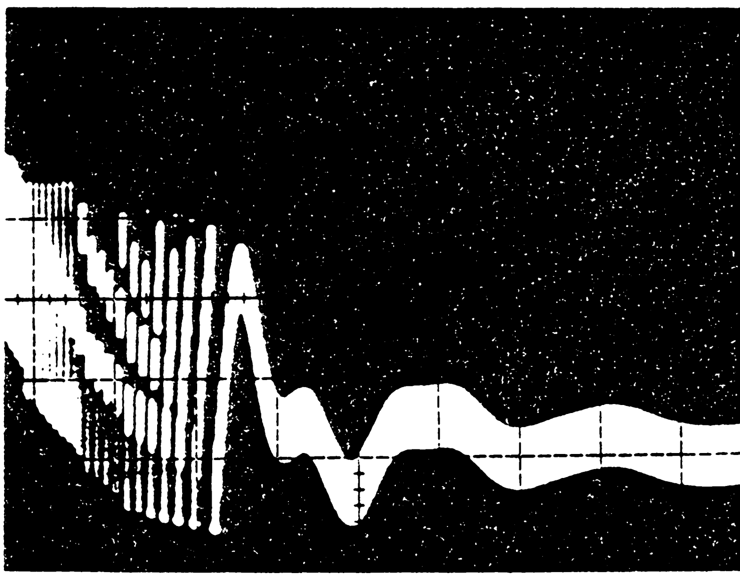

(b)

Figure 65: Output voltage (a) and output filter inductor current (b) without feedforward

(a) Y—5v/div X—0.5 msec/div

(b) Y—1 A/div X—0.5 msec/div

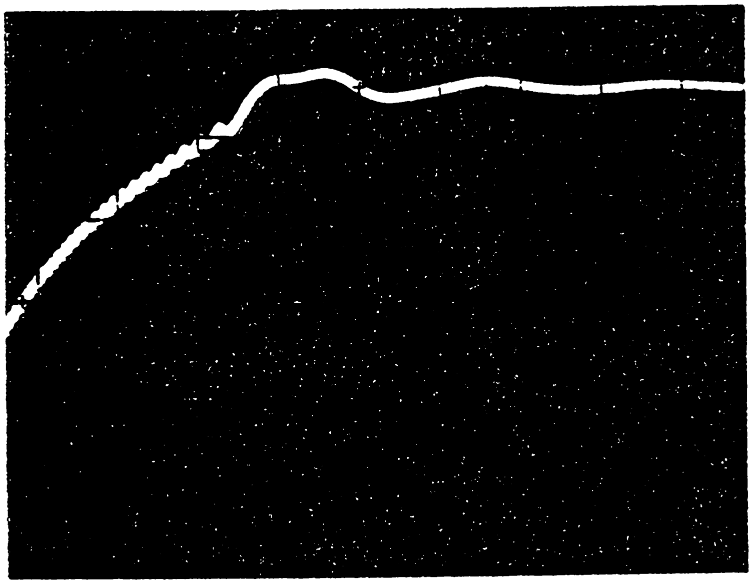

(a)

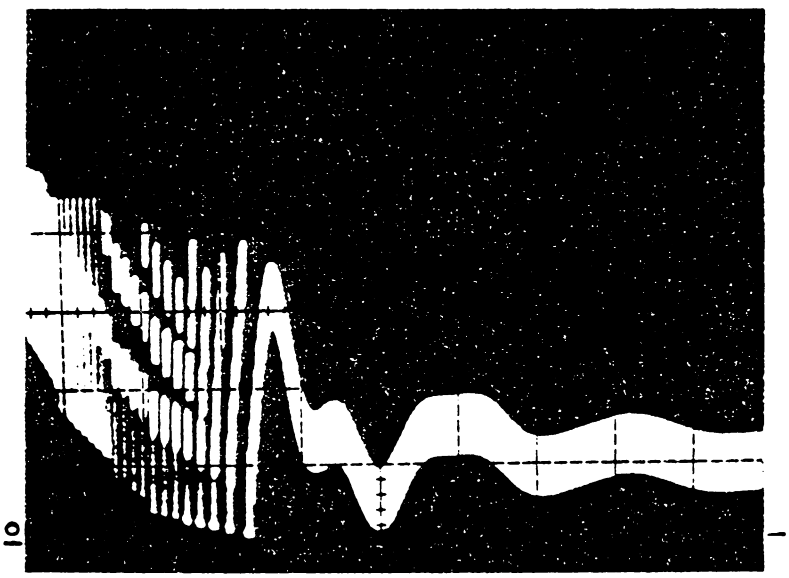

(b)

Figure 66: Output voltage (a) and output filter inductor current (b) with feedforward

(a) Y—5v/div X—0.5 msec/div

(b) Y—1 A/div X—0.5 msec/div

## 6.6 CONCLUSIONS

Extensive measurements made to verify experimentally the feedforward design are presented in this chapter. Measurements of the open loop gain and phase margin, closed loop gain, output impedance and transient response confirm the effectiveness of the feedforward in improving performance, as predicted in the analysis. The following points are noteworthy:

1. The feedforward eliminates the detrimental effect on open loop gain and phase margin of the output impedance of the input filter.
2. The feedforward circuit is shown to be independent of input filter parameters and also independent of input filter configuration.
3. The feedforward effectively eliminates the interaction between an unknown dynamic source impedance and the regulator control loop.
4. The closed loop input-to-output transfer function (audiosusceptibility) and output impedance are both improved significantly by the addition of feedforward.
5. The addition of feedforward improves transient response in those cases where the interaction between the input filter and the control loop degrades the

response. Examples of the above are small step changes in supply voltage and load, and results for these cases are included. For large signal transient behavior the feedforward does not in any way degrade the performance -- examples of these are a large step change in supply voltage and the start up behavior of the regulator.

6. No detrimental effects have been observed due to the use of the proposed feedforward compensation scheme through the course of study and through extensive experiments when the system was subjected to different forms of small and large signal disturbances.